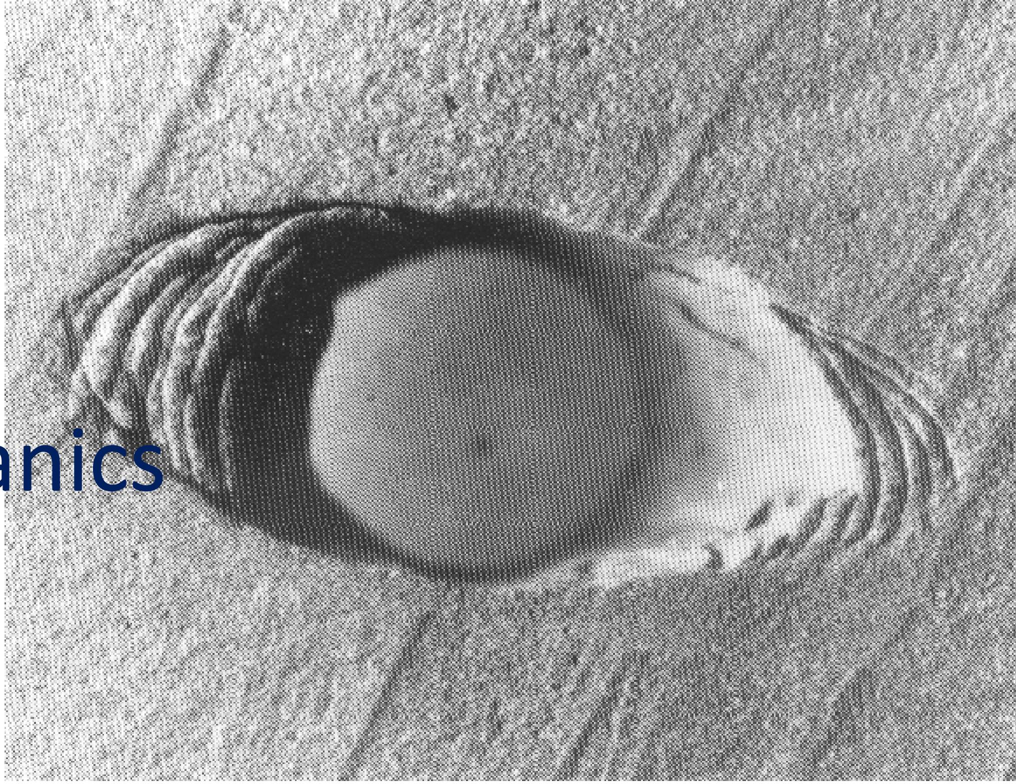

30th ALERT Doctoral School, The legacy of Ioannis Vardoulakis to Geomechanics
Aussois FR, 02-04 October 2019

Petroleum Geomechanics

BOREHOLE STABILITY DURING DRILLING

SOLIDS PRODUCTION

Prof. Euripides Papamichos

Aristotle University of Thessaloniki, Greece, epapamic@civil.auth.gr

SINTEF Petroleum Research, Trondheim, Norway, euripides.papamichos@sintef.no

ALERT School 2006:
Geomechanical and Structural Issues in Energy Production

Sand-production and sand internal erosion: Continuum modeling

Ioannis Vardoulakis NTUA

Recommended textbook

Fjær et al (2008). Petroleum related rock mechanics. Developments in petroleum science 53, 2nd ed, Elsevier.

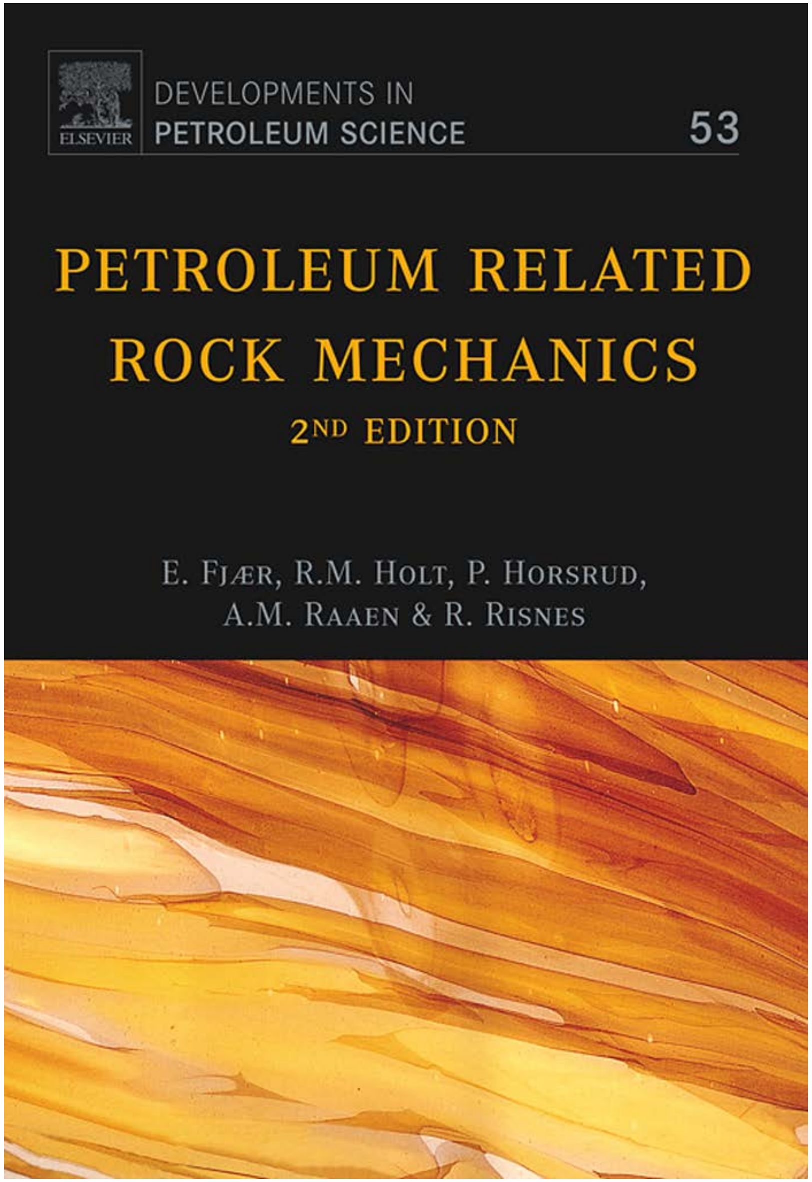

Register at:
https://11alertozcourse.sciencesconf.org/

Green….

- EGS –Enhanced geothermal systems
- CCS – Carbon Capture and storage/CO2 geological storage
- Waste disposal through injection into the ground
- Nuclear waste disposal – underground depositories

Drilling, stimulation and production of hydrocarbons

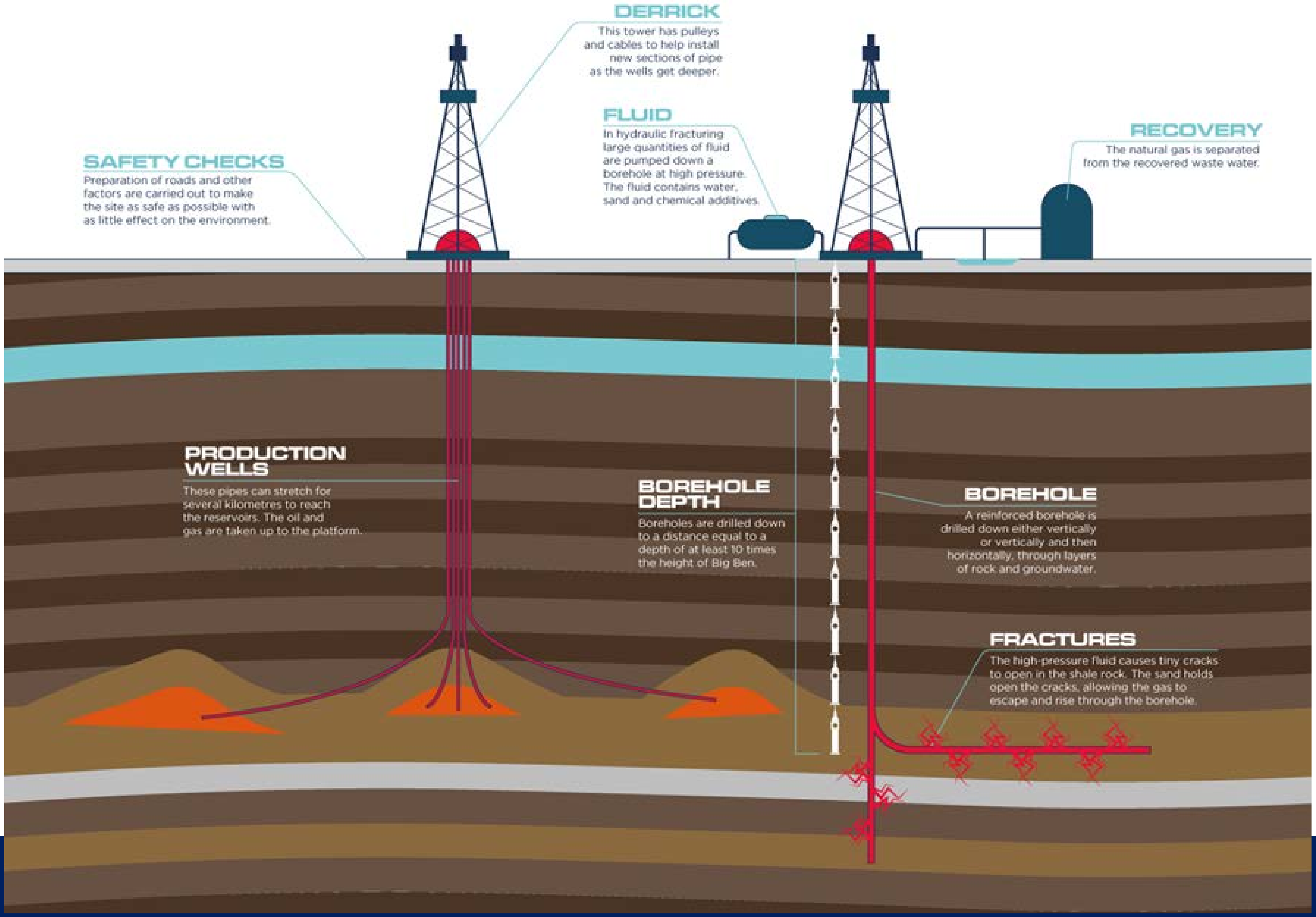

Underground in situ stresses

- **Three principal stresses** and **pore fluid pressure** (pressure of fluid in the pores of the sedimentary rocks)
  - Sedimentary basins: Vertical stress σ_v is major principal stress
  - Areas of tectonic activity: Principal stresses can be rotated and often a horizontal stress is a major principal stress
  - Near surface: Stresses influenced by surface topology

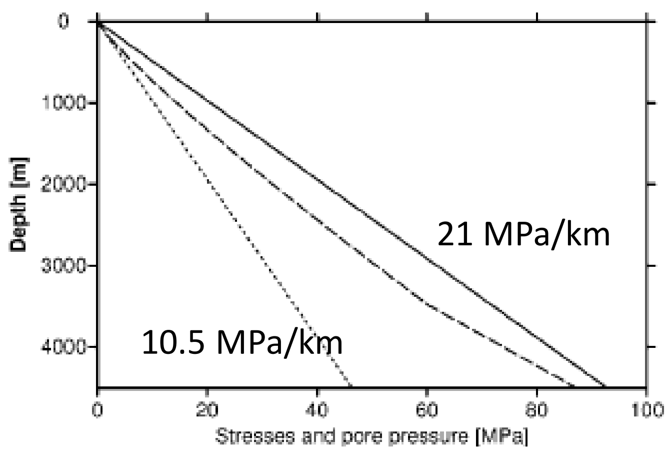

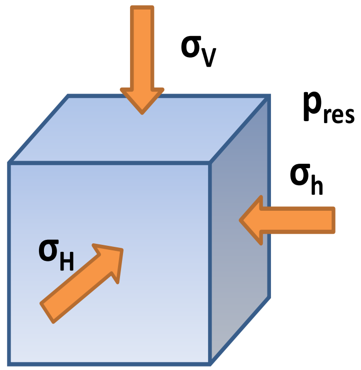

Stresses and faults

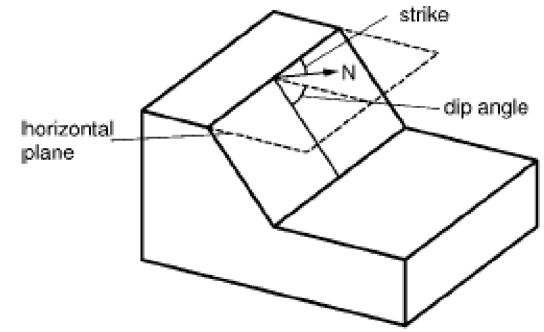

Fig. 3.6. Illustration of dip and strike.

- Normal fault is typical
  - $\sigma_v > \sigma_H \geq \sigma_h \quad \Rightarrow \quad$ dip > 45° (~60°)
- Thrust fault in tectonic areas
  - $\sigma_H \geq \sigma_h > \sigma_v \quad \Rightarrow \quad$ dip < 45°(~30°)
  - E.g. Cuisiana field in Colombia (Andes)
- Strike-slip fault in tectonic areas
  - $\sigma_H > \sigma_v > \sigma_h \quad \Rightarrow \quad$ dip < 10°

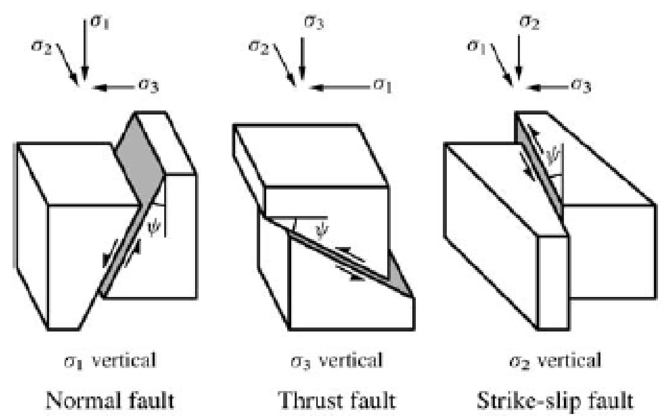

Addis et al 1993

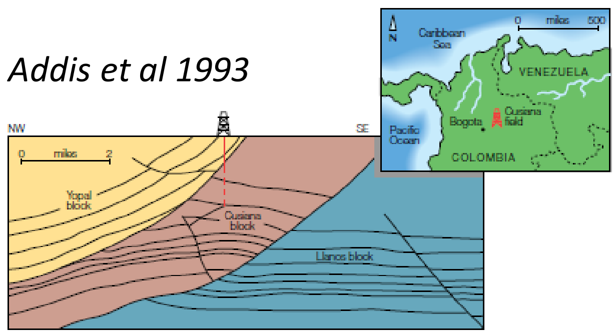

Location, geologic cross section and tectonics of the Cusiana field, eastern Colombia. The active Pacific and Caribbean plates provide ample north-west-southeast compression to the entire area, increasing horizontal stresses significantly above normal levels.

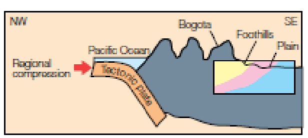

World Stress Map

- Administered GFZ Potsdam
- www.world-stress-map.org
- *Ref: Heidbach, O., Tingay, M., Barth, A., Reinecker, J., Kurfeß, D. and Müller, B., The World Stress Map database release 2008, doi:10.1594/GFZ.WSM.Rel2008, 2008*
- Horizontal stress orientations
  - Hydraulic tests (LOT, XLOT)
  - Earthquake focal mechanisms

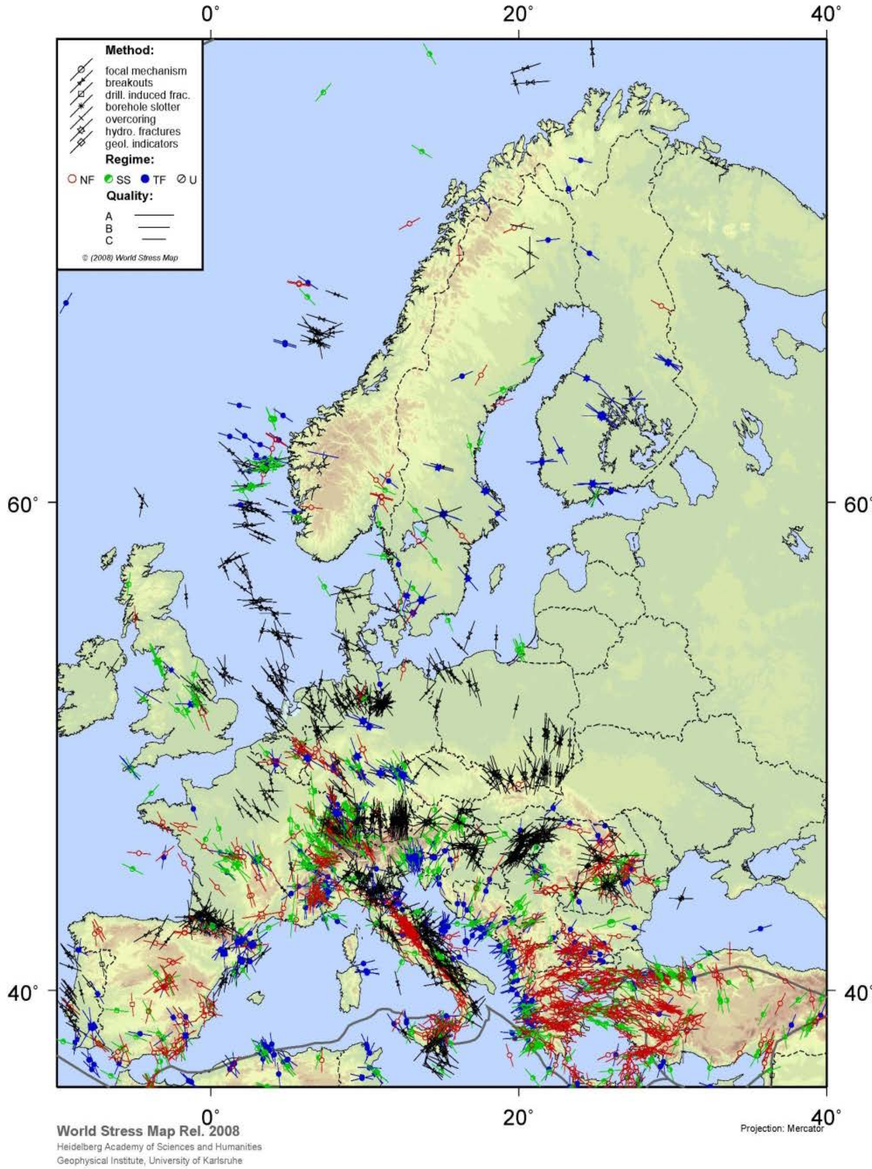

Mechanical collapse of borehole

- Borehole drilled into the ground to reach the reservoir formation is exposed to the underground earth stresses
- During drilling, mud inside the borehole provides the support needed to avoid failure
- Mud is specially designed for each application with a certain specific weight

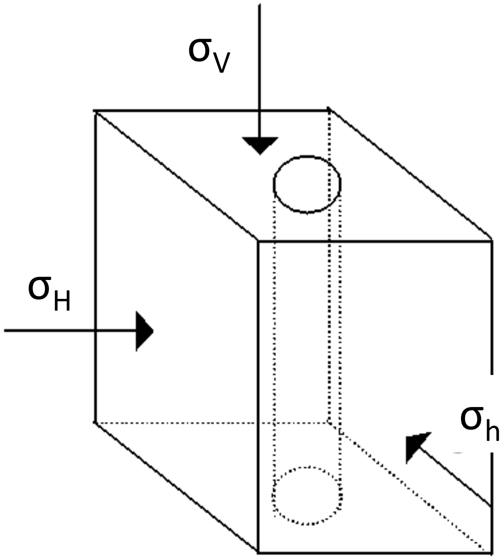

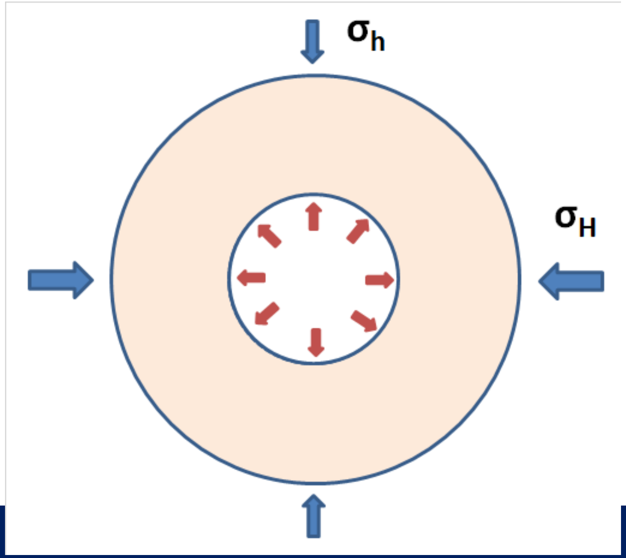

Causes of borehole instability

Causes of Wellbore Instability	
Uncontrollable (Natural) Factors	**Controllable Factors**
Naturally Fractured or Faulted Formations	Bottom Hole Pressure (Mud Density)
Tectonically Stressed Formations	Well Inclination and Azimuth
High In-situ Stresses	Transient Pore Pressures
Mobile Formations	Physico/chemical Rock-Fluid Interaction
Unconsolidated Formations	Drill String Vibrations
Naturally Over-Pressured Shale Collapse	Erosion
Induced Over-Pressured Shale Collapse	Temperature

Pasic et al 2007

Natural factors

- Naturally fractured formations
  - Broken formation plugs the well

- Tectonically stressed formations
- Borehole collapse

- High in situ stresses
  - Near salt domes
  - Near faults

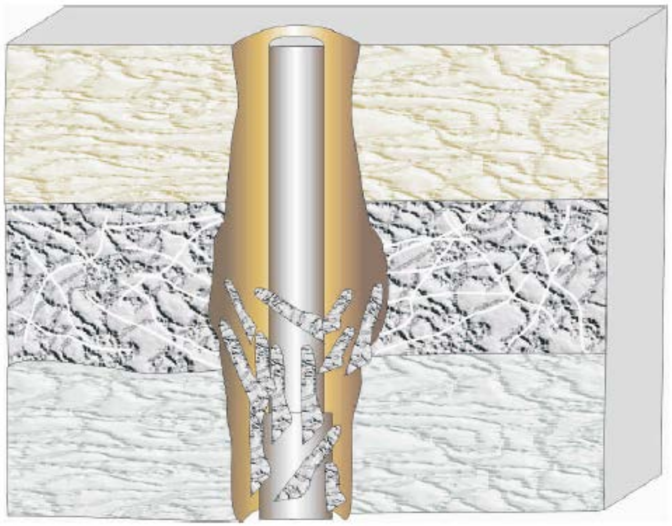

Figure 1 Drilling through naturally fractured or faulted formations

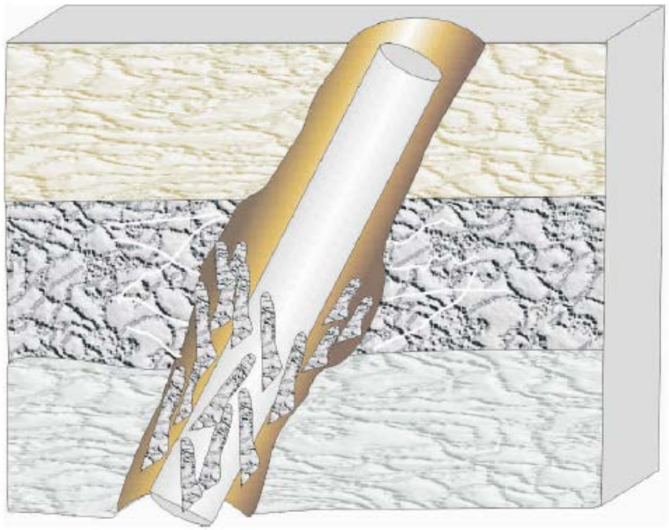

Figure 2 Drilling through tectonically stressed formations

- Mobile formations
    - Formation behaves plastically

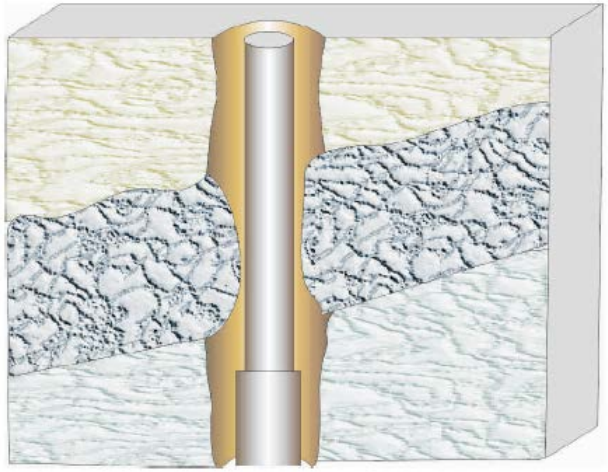

Figure 3 Drilling through mobile formations

- Unconsolidated formations

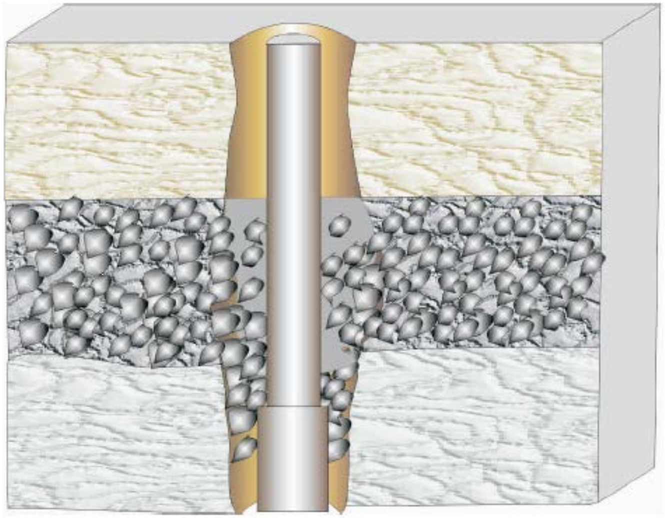

Figure 4 Drilling through unconsolidated formations

- Over-pressured formations
  - Naturally
    - Under compaction
    - Up lift
  - Induced
    - Equilibrium with higher well pressure and lowering of well pressure

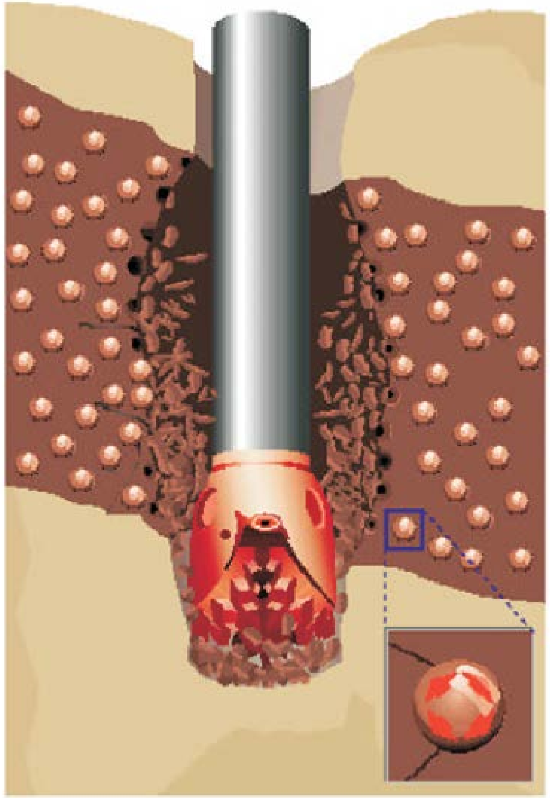

Figure 5 Drilling through a naturally over-pressured shale

Borehole Stability Problems

- Tight hole / Stuck pipe incidents
  - Responsible for 5-10% of drilling time
  - Most frequently occurring in shale
  - Often high pore pressure and in presence of swelling clay minerals (e.g. smectite)
  - Often in deviated wells
- Lost circulation / Mud losses
  - May lead to kick / blow-out
  - Caused by fluid lost into natural fractures or by new generated fractures

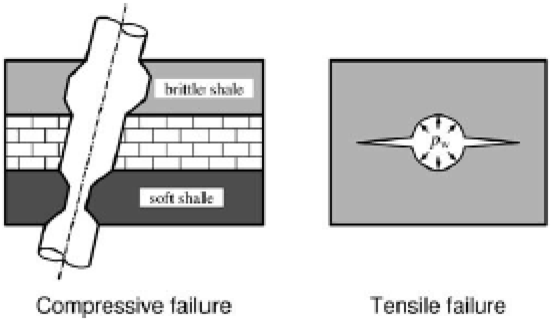

Fig. 9.1. Stability problems during drilling (after Bradley, 1979; with permission from

Lost circulation / Mu

- Consequences
  - Operational problem
    - Costs of mud
    - Limited mud on rig
    - Possible pressure drop i
  - Dangerous situation espe gas, a major safety issue (
  - Risk of life and equipmen
- Solutions
  - Overall well design i.e.
    - Casing program
    - Mud weight
    - Lost circulation material (LCM)

The Lucas Gusher at Spindletop Hill, TX, 1901

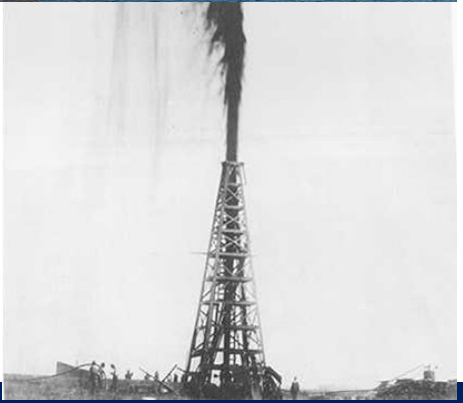

Borehole Stress Analysis

- Stresses from elastic or elastoplastic analysis
- Drilling mud:
  - Prevent flow of pore fluid
  - Prevent hole failure
  - Transport drill cuttings to surface and cool drill-bit
- Mud pressure p_w is controlled by mud density ρ_w
  - $p_w = \rho_w g D$
- Drilling language refers to mud weight in density units ρ_w (SG) and gradients of stress or pressure $\rho_w g$ (MPa/km)
- Equivalent Circulating Density (ECD): Effective mud pressure is 5-10% higher than the static mud pressure (due to friction in the annulus during flow)

- Drilling of borehole
  - Unloading at the hole $\Rightarrow$ Stress redistribution $\Rightarrow$ Failure at the hole?

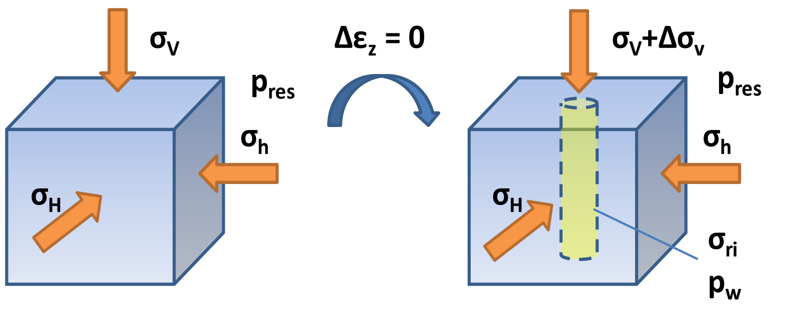

- Stresses around a borehole essential for any borehole related problem
  - Drilling, production, hydraulic fracturing, water injection, waste disposal, CO_2 injection, etc.

Stresses in cylindrical coordinates

- 3 normal stresses: Radial σ_r, tangential σ_θ and axial σ_z
- 3 shear stresses: $\sigma_{r\theta}$ (or $\tau_{r\theta}$), $\sigma_{\theta z}$ (or $\tau_{\theta z}$), σ_{rz} (or τ_{rz})

$$\sigma_r = \frac{1}{2}(\sigma_x + \sigma_y) + \frac{1}{2}(\sigma_x - \sigma_y)\cos 2\theta + \tau_{xy}\sin 2\theta$$

$$\sigma_\theta = \frac{1}{2}(\sigma_x + \sigma_y) - \frac{1}{2}(\sigma_x - \sigma_y)\cos 2\theta - \tau_{xy}\sin 2\theta$$

$$\sigma_z = \sigma_z$$

$$\tau_{r\theta} = \frac{1}{2}(\sigma_y - \sigma_x)\sin 2\theta + \tau_{xy}\cos 2\theta$$

$$\tau_{rz} = \tau_{xz}\cos\theta + \tau_{yz}\sin\theta$$

$$\tau_{\theta z} = \tau_{yz}\cos\theta - \tau_{xz}\sin\theta$$

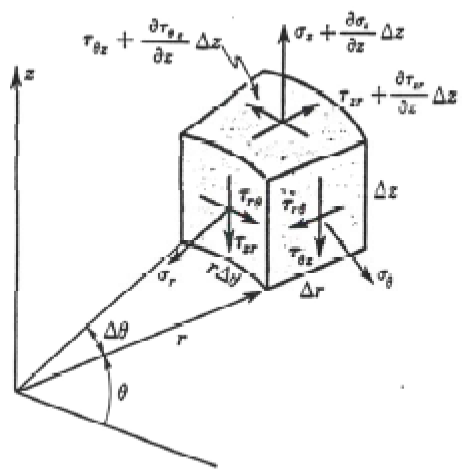

- Compression positive

Strains in cylindrical coordinates

- 3 normal strains: Radial ε_r, tangential ε_θ and axial ε_z
- 3 shear strains: $\varepsilon_{r\theta}$, $\varepsilon_{\theta z}$, ε_{rz}

$$\varepsilon_r = \frac{1}{2}(\varepsilon_x + \varepsilon_y) + \frac{1}{2}(\varepsilon_x - \varepsilon_y)\cos 2\theta + \varepsilon_{xy}\sin 2\theta$$

$$\varepsilon_\theta = \frac{1}{2}(\varepsilon_x + \varepsilon_y) - \frac{1}{2}(\varepsilon_x - \varepsilon_y)\cos 2\theta - \varepsilon_{xy}\sin 2\theta$$

$$\varepsilon_z = \varepsilon_z$$

$$\varepsilon_{r\theta} = \frac{1}{2}\left(\varepsilon_y - \varepsilon_x\right)\sin 2\theta + \varepsilon_{xy}\cos 2\theta$$

$$\varepsilon_{\theta z} = \varepsilon_{yz}\cos\theta - \varepsilon_{zx}\sin\theta$$

$$\varepsilon_{zr} = \varepsilon_{xz}\cos\theta + \varepsilon_{yz}\sin\theta$$

Relations between strains and displacements

- u (or u_r) = radial displacement
- υ (or u_θ) = tangential displacement
- w (or u_z) = axial displacement

$$\varepsilon_r = \frac{\partial u}{\partial r}$$

$$\varepsilon_\theta = \frac{u}{r} + \frac{1}{r}\frac{\partial v}{\partial \theta}$$

$$\varepsilon_z = \frac{\partial w}{\partial z}$$

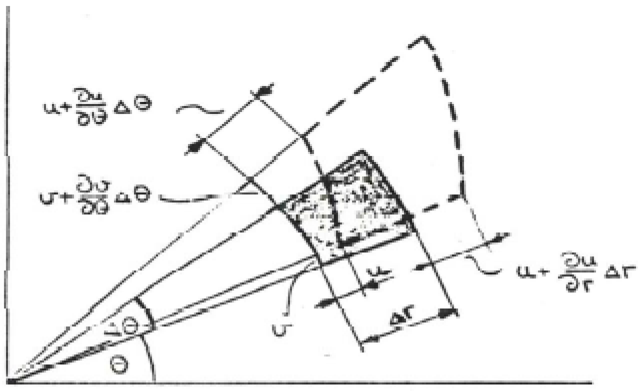

$$\varepsilon_{r\theta} = \frac{1}{2r}\left(\frac{\partial u_r}{\partial \theta} - u_\theta\right) + \frac{1}{2}\frac{\partial u_\theta}{\partial r}$$

$$\varepsilon_{\theta z} = \frac{1}{2}\left(\frac{\partial u_z}{r\partial \theta} + \frac{\partial u_\theta}{\partial z}\right)$$

$$\varepsilon_{zr} = \frac{1}{2}\left(\frac{\partial u_z}{\partial r} + \frac{\partial u_r}{\partial z}\right)$$

Linear thermo-poro-elasticity

- Stress-strain relations
  - For effective stresses $\sigma'_{ij} = \sigma_{ij} - \alpha\, p_f \delta_{ij}$
  - Compression positive

$$\sigma'_r = \frac{E}{(1+\nu)(1-2\nu)}\left[(1-\nu)\varepsilon_r + \nu\left(\varepsilon_\theta + \varepsilon_z\right)\right] + \frac{a_T E}{1-2\nu}\left(T - T_o\right)$$

$$\sigma'_\theta = \frac{E}{(1+\nu)(1-2\nu)}\left[(1-\nu)\varepsilon_\theta + \nu\left(\varepsilon_r + \varepsilon_z\right)\right] + \frac{a_T E}{1-2\nu}\left(T - T_o\right)$$

$$\sigma'_z = \frac{E}{(1+\nu)(1-2\nu)}\left[(1-\nu)\varepsilon_z + \nu\left(\varepsilon_r + \varepsilon_\theta\right)\right] + \frac{a_T E}{1-2\nu}\left(T - T_o\right)$$

$$\sigma_{r\theta} = 2G\varepsilon_{r\theta}$$

$$\sigma_{\theta z} = 2G\varepsilon_{\theta z}$$

$$\sigma_{zr} = 2G\varepsilon_{zr}$$

- Equilibrium equations
  - For total stresses σ_{ij}

$$\frac{\partial \sigma_r}{\partial r} + \frac{1}{r}\frac{\partial \sigma_{\theta r}}{\partial \theta} + \frac{\partial \sigma_{rz}}{\partial z} + \frac{\sigma_r - \sigma_\theta}{r} + f_r = 0$$

$$\frac{\partial \sigma_{r\theta}}{\partial r} + \frac{1}{r}\frac{\partial \sigma_\theta}{\partial \theta} + \frac{\partial \sigma_{\theta z}}{\partial z} + \frac{2\sigma_{r\theta}}{r} + f_\theta = 0$$

$$\frac{\partial \sigma_{rz}}{\partial r} + \frac{1}{r}\frac{\partial \sigma_{\theta z}}{\partial \theta} + \frac{\partial \sigma_z}{\partial z} + \frac{\sigma_{rz}}{r} + f_z = 0$$

Axisymmetric problems

Examples

1. Drilling of a vertical borehole under isotropic in situ horizontal stresses

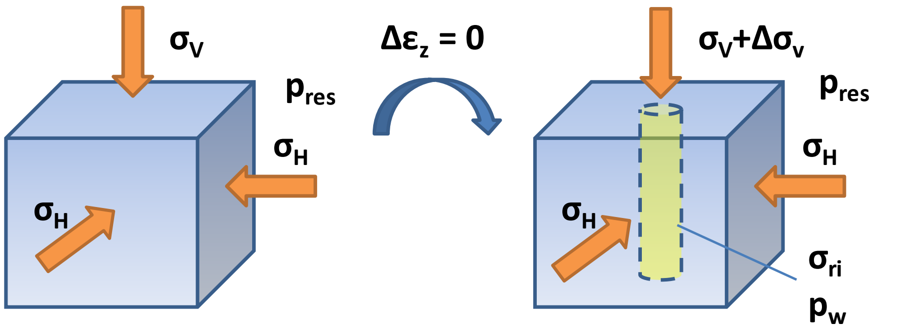

2. Hollow Cylinder (HC) test

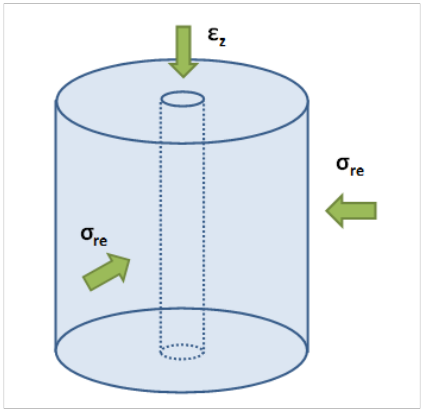

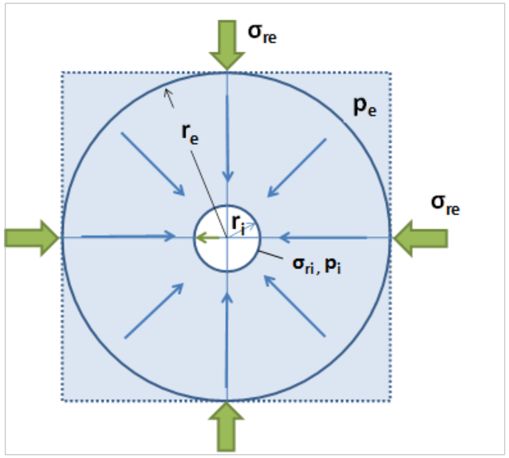

Hollow cylinder test with fluid flow

(Papamichos et al. 2001)

- Typical system
  (SINTEF Industry, Norway)
  - Specimen size:
    o.d. 10/20 cm, i.d. 2/5 cm
  - Isotropic confining stress up to 100 MPa
  - Oil / Water flow up to 4 L/min or 40 MPa fluid pressure
  - Gas flow
  - Temperature up to 80°C
  - Axial, internal and external diametrical deformations
  - Continuous sand production measurements
  - Radial permeability measurements

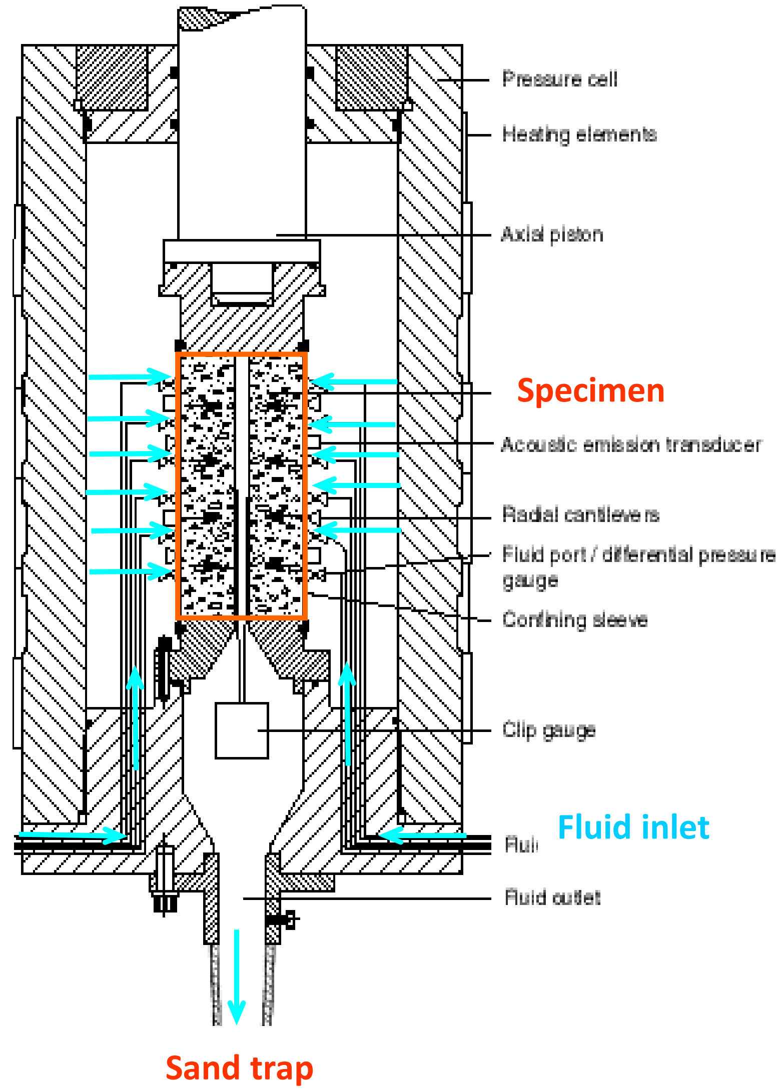

Simplifications due to axisymmetry

- $u_\theta = 0$
- $\sigma_{r\theta} = \sigma_{\theta z} = 0$
- $\varepsilon_{r\theta} = \varepsilon_{\theta z} = 0$

$$\varepsilon_r = \frac{\partial u_r}{\partial r}, \qquad \varepsilon_\theta = \frac{u_r}{r}$$

$$\varepsilon_z = \frac{\partial u_z}{\partial z}, \qquad \varepsilon_{rz} = \frac{1}{2}\left(\frac{\partial u_r}{\partial z} + \frac{\partial u_z}{\partial r}\right)$$

- Equilibrium equations

$$\frac{\partial \sigma_r}{\partial r} + \frac{\partial \sigma_{rz}}{\partial z} + \frac{\sigma_r - \sigma_\theta}{r} + f_r = 0$$

$$\frac{\partial \sigma_{rz}}{\partial r} + \frac{\partial \sigma_z}{\partial z} + \frac{\sigma_{rz}}{r} + f_z = 0$$

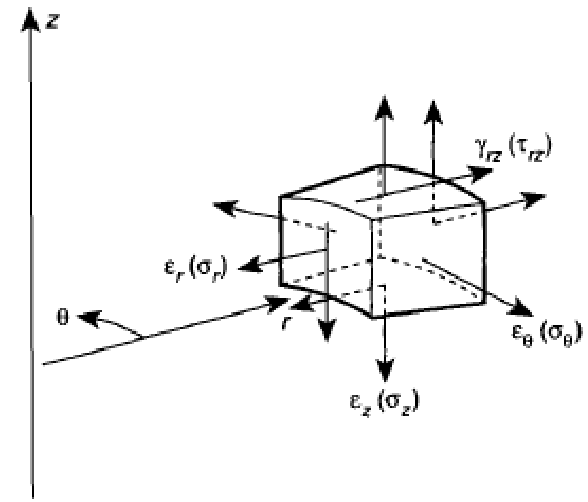

Strains and stresses involved in the analysis of axisymmetric solids.

further…

- Usually in our problems (drilling, HC, HF, ….)
- No shear : $\sigma_{rz} = \varepsilon_{rz} = 0$
- Body forces due to gravity: e.g. in a vertical hole: $f_r = 0$, $f_z = \rho g$
  - $\Rightarrow$ equilibrium equations decouple and can be solved independently

$$
\begin{aligned}
&\frac{\partial \sigma_r}{\partial r} + \cancel{\frac{\partial \sigma_{rz}}{\partial z}} + \frac{\sigma_r - \sigma_\theta}{r} + \cancel{f_r} = 0 \\
&\cancel{\frac{\partial \sigma_{rz}}{\partial r}} + \frac{\partial \sigma_z}{\partial z} + \cancel{\frac{\sigma_{rz}}{r}} + f_z = 0
\end{aligned}
\quad \Rightarrow \quad
\begin{aligned}
&\frac{\partial \sigma_r}{\partial r} + \frac{\sigma_r - \sigma_\theta}{r} = 0 \\
&\frac{\partial \sigma_z}{\partial z} + \rho g = 0
\end{aligned}
$$

Elastic solution for HC problem

- Substitution of σ - ε and $\varepsilon - u_r$ eqs in equilibrium eqs

$$\frac{\partial \sigma_r}{\partial r} + \frac{\sigma_r - \sigma_\theta}{r} = 0 \quad \Rightarrow \quad \frac{d^2 u_r}{dr^2} + \frac{1}{r}\frac{du_r}{dr} - \frac{u_r}{r^2} + \frac{\alpha}{E'}\frac{dp_f}{dr} = 0 \qquad E' = \frac{(1-\nu)E}{(1+\nu)(1-2\nu)}$$

- Two unknowns u_r and p_f
- 1 additional equation is needed

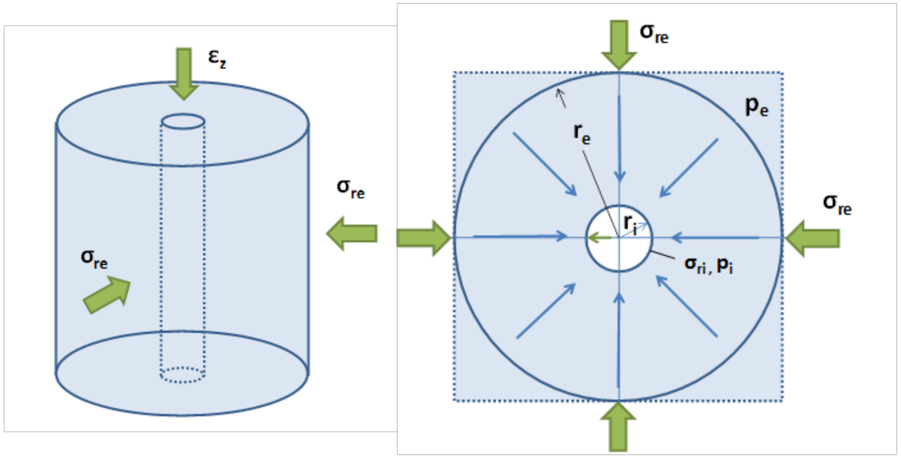

Continuity equation for the fluid in cylindrical coords

- In cylindrical coords $$div q_i = \frac{\partial q_r}{\partial r} + \frac{q_r}{r} + \frac{1}{r}\frac{\partial q_\theta}{\partial \theta} + \frac{\partial q_z}{\partial z} = 0$$

- In axisymmetric problems $q_\theta = 0$
- For radial flow only $q_z = 0$

- Continuity eqn becomes $$\frac{dq_r}{dr} + \frac{q_r}{r} = 0$$

- Direct integration gives $$q_r = \frac{r_e}{r} q_{re}$$
  - B.c. $q_r(r=r_e) = q_{re}$

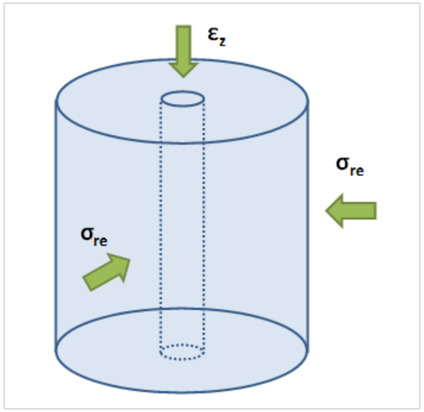

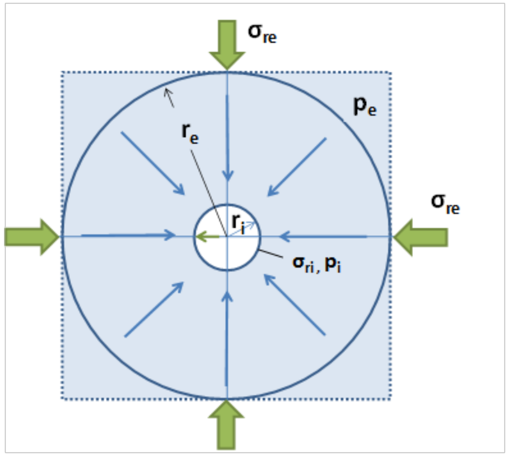

Fluid flux radial profile

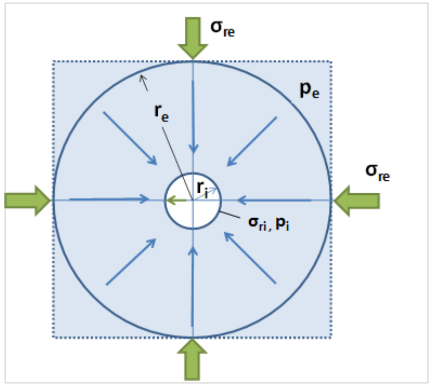

- Normalized fluid flux q_r/q_{re} vs. r/r_i

$$\frac{q_r}{q_{re}} = \frac{r_e}{r}$$

- And $$\frac{q_{ri}}{q_{re}} = \frac{r_e}{r_i}$$

- Because the same volume of fluid has to pass through a smaller cross-section

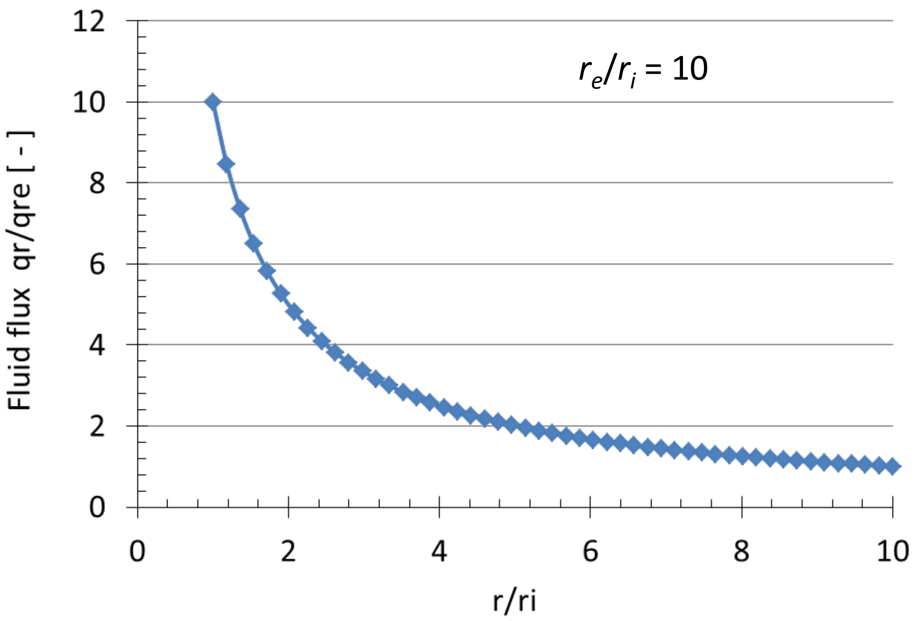

Solution for pore pressure p_f

- Darcy's law for fluid flow
  - k = permeability [D or m^2]
  - η = viscosity [cP or Pa·s]

$$q_r = -\frac{k}{\eta}\frac{dp_f}{dr}$$

1 D = 0.9869233×10^{-12} m^2
1 cP = 10^{-3} Pa·s

- Continuity equation becomes
  - Constant k, η
  - B.c.

$$r\frac{dq_r}{dr} + q_r = 0 \quad \Rightarrow \quad r\frac{d^2 p_f}{dr^2} + \frac{dp_f}{dr} = \frac{d}{dr}\left(r\frac{dp_f}{dr}\right) = 0$$

$$p_f\left(r = r_i\right) = p_{fi}\,, \qquad p_f\left(r = r_e\right) = p_{fe}$$

- With solution

$$p_f = p_{fi} + \left(p_{fe} - p_{fi}\right)\frac{\ln r/r_i}{\ln r_e/r_i} = p_{fe} - \left(p_{fe} - p_{fi}\right)\frac{\ln r/r_e}{\ln r_i/r_e}$$

Pore pressure radial profile

- Normalized pore pressure vs. r/r_i

$$\frac{p_f}{p_{fe}-p_{fi}}=\frac{p_{fi}}{p_{fe}-p_{fi}}+\frac{\ln r/r_i}{\ln r_e/r_i}$$

- Logarithmic profile
- Higher pore pressure drop is necessary to drive the same volume of fluid through a smaller cross-section
- Note: Independent of material properties

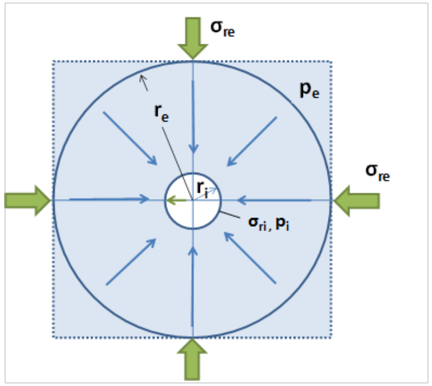

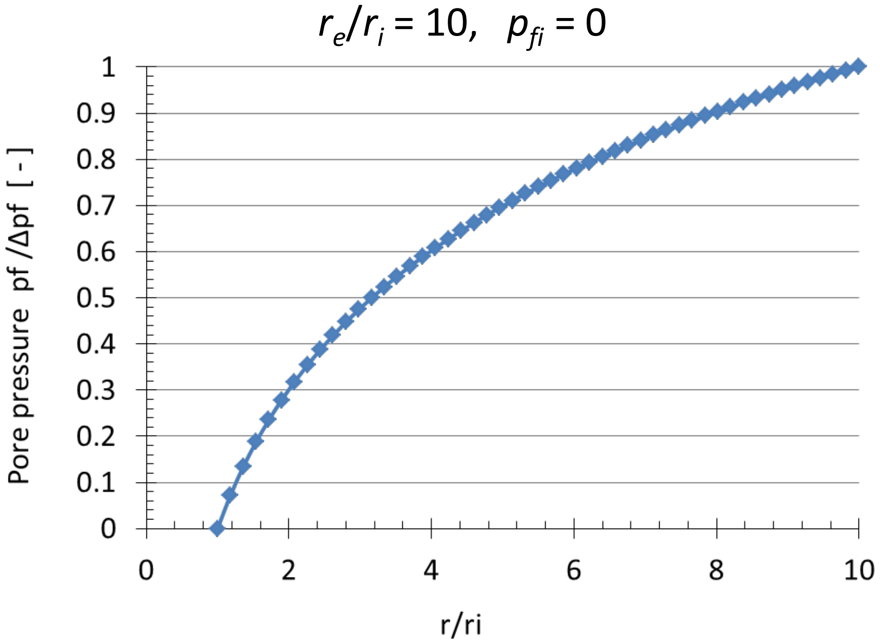

Elastic solution for HC problem

- Equilibrium eqn in terms of displacement u_r

$$\boxed{\frac{d^2u_r}{dr^2}+\frac{1}{r}\frac{du_r}{\partial r}-\frac{u_r}{r^2}+\frac{\alpha}{E'}\frac{dp_f}{dr}=0 \quad\Rightarrow\quad \frac{d}{dr}\left(\frac{du_r}{dr}+\frac{u_r}{r}\right)=\frac{d}{dr}\left[\frac{1}{r}\frac{d}{dr}\left(ru_r\right)\right]=-\frac{\alpha}{E'}\frac{dp_f}{dr}}$$

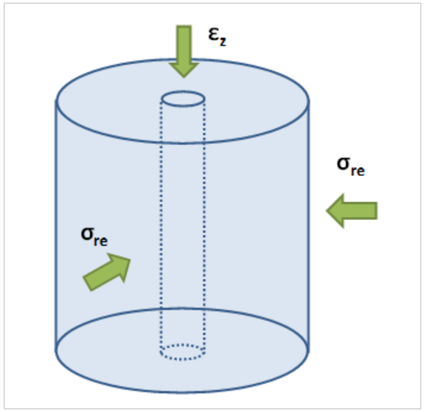

- Direct integration 2 times gives

$$u_r=c_1r+\frac{c_2}{r}-\frac{\alpha}{2E'}\left[p_{fi}+\left(p_{fe}-p_{fi}\right)\frac{1+2\ln r/r_i}{2\ln r_i/r_e}\right]r$$

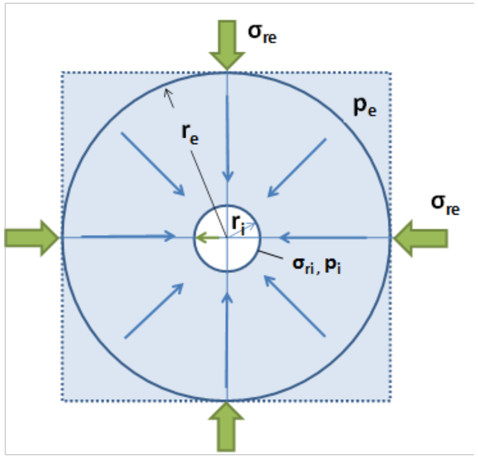

- c_1 and c_2 are integration constants to be solved from the b.c.

$$\sigma_r\left(r=r_i\right)=\sigma_{ri}\ ,\qquad \sigma_r\left(r=r_e\right)=\sigma_{re}$$

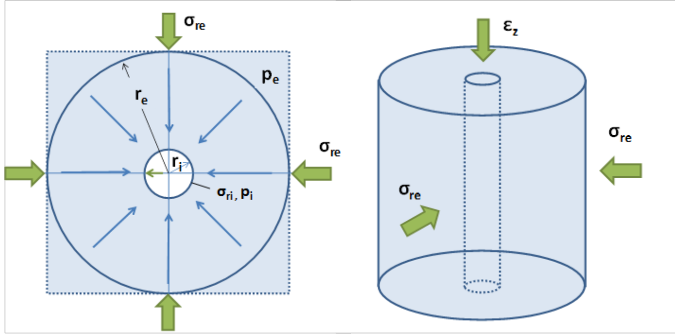

Elastic solution for HC problem

- Displacement u_r and strains ε_r and ε_θ

$$\varepsilon_r = \frac{1-2\nu}{2G}\left(\sigma_{ri} - \alpha p_{fi}\right) + \frac{\sigma_{re}-\sigma_{ri}}{2G}\frac{1-2\nu - r_i^2/r^2}{1-r_i^2/r_e^2} - \frac{p_{fe}-p_{fi}}{2G}\frac{\alpha(1-2\nu)}{2(1-\nu)}\left(\frac{1-2\nu - r_i^2/r^2}{1-r_i^2/r_e^2} + \frac{\ln r_i/r - \nu}{\ln r_i/r_e}\right) - \nu\varepsilon_z$$

$$\varepsilon_\theta = \frac{u_r}{r} = \frac{1-2\nu}{2G}\left(\sigma_{ri} - \alpha p_{fi}\right) + \frac{\sigma_{re}-\sigma_{ri}}{2G}\frac{1-2\nu + r_i^2/r^2}{1-r_i^2/r_e^2} - \frac{p_{fe}-p_{fi}}{2G}\frac{\alpha(1-2\nu)}{2(1-\nu)}\left(\frac{1-2\nu + r_i^2/r^2}{1-r_i^2/r_e^2} + \frac{\ln r_i/r + 1 - \nu}{\ln r_i/r_e}\right) - \nu\varepsilon_z$$

- Stresses σ_r, σ_θ, σ_z

$$\sigma_r = \sigma_{ri} + \left(\sigma_{re}-\sigma_{ri}\right)\frac{1-r_i^2/r^2}{1-r_i^2/r_e^2} - \left(p_{fe}-p_{fi}\right)\frac{\alpha(1-2\nu)}{2(1-\nu)}\left(\frac{1-r_i^2/r^2}{1-r_i^2/r_e^2} - \frac{\ln r_i/r}{\ln r_i/r_e}\right)$$

$$\sigma_\theta = \sigma_{ri} + \left(\sigma_{re}-\sigma_{ri}\right)\frac{1+r_i^2/r^2}{1-r_i^2/r_e^2} - \left(p_{fe}-p_{fi}\right)\frac{\alpha(1-2\nu)}{2(1-\nu)}\left(\frac{1+r_i^2/r^2}{1-r_i^2/r_e^2} + \frac{1-\ln r_i/r}{\ln r_i/r_e}\right)$$

$$\sigma_z = \nu\left(\sigma_r + \sigma_\theta\right) + \alpha(1-2\nu)p_f + E\varepsilon_z =$$

$$= 2\nu\sigma_{ri} + \alpha(1-2\nu)p_{fi} + \left(\sigma_{re}-\sigma_{ri}\right)\frac{2\nu}{1-r_i^2/r_e^2} - \left(p_{fe}-p_{fi}\right)\frac{\alpha(1-2\nu)}{2(1-\nu)}\left(\frac{2\nu}{1-r_i^2/r_e^2} + \frac{\nu - 2\ln r_i/r}{\ln r_i/r_e}\right) + E\varepsilon_z$$

Borehole problem (drilling in balance)

- Example: Vertical well, reservoir section, drilling in balance ($p_w = p_{fm}$)
- INITIAL STATE = In situ stresses σ_v, $\sigma_H = \sigma_h$ and formation pressure p_{fm}
  - $\sigma_z = \sigma_v$
  - $\sigma_{re} = \sigma_{ri} = \sigma_H = \sigma_h$
  - $p_{fe} = p_{fi} = p_{fm}$

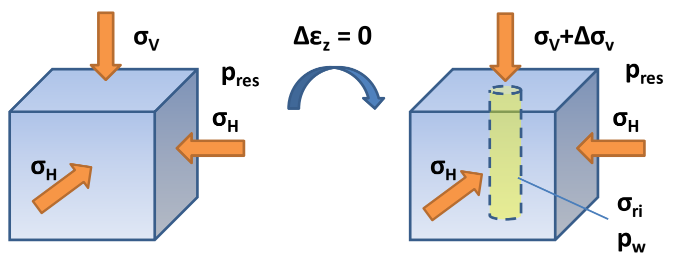

- After DRILLING
  - $\varepsilon_z = 0 \quad \Rightarrow \quad \Delta\varepsilon_z = 0$
  - $\sigma_{re} = \sigma_H = \sigma_h \quad \Rightarrow \quad \Delta\sigma_{re} = 0$
  - $p_{fe} = p_{fm} \quad \Rightarrow \quad \Delta p_{fe} = 0$
  - $\sigma_{ri} = p_w = p_{fm} \quad \Rightarrow \quad \Delta\sigma_{ri} = p_{fm} - \sigma_H < 0$
  - $p_{fi} = p_w = p_{fm} \quad \Rightarrow \quad \Delta p_{fi} = 0$

Borehole problem (production)

- During PRODUCTION
  - $\varepsilon_z = 0 \quad \Rightarrow \quad \Delta\varepsilon_z = 0$
  - $\sigma_{re} = \sigma_H = \sigma_h \quad \Rightarrow \quad \Delta\sigma_{re} = 0$
  - $\sigma_{ri} = p_w \quad \Rightarrow \quad \Delta\sigma_{ri} = p_w - p_{fm} < 0$
  - $p_{fe} = p_{fm} \quad \Rightarrow \quad \Delta p_{fe} = 0$
  - $p_{fi} = p_w \quad \Rightarrow \quad \Delta p_{fi} = p_w - p_{fm} < 0$

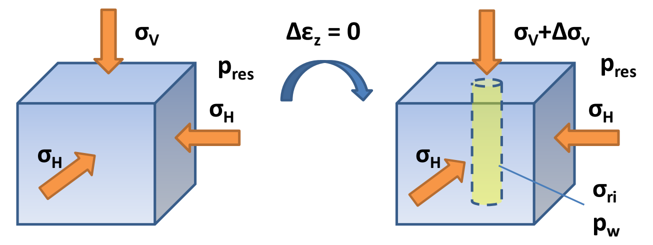

- NOTE on b.c. at well:
  - Permeable wall : $\sigma_{ri} = p_{fi} = p_w$
  - Impermeable wall: $\sigma_{ri} = p_w$, $p_{fi} = p_{fm}$

- Equations for HC are still valid for stress and pore pressure changes
  - FINAL stresses are found by adding:
    - Initial stresses + Stress changes (drilling) + Stress changes (production) + Etc.
- Super-position principle applies

In situ stresses and pore pressure

- Total vertical stress gradient = 20.3 MPa/km
  - From integration of density log
- Total horizontal stress gradient = 17.6 MPa/km
  - From closure stress of initial part of fracturing stimulations
- Pore pressure gradient = 16.1 MPa/km

Table 1: Valhall Field, pertinent data sheet

Discovery	1975
First Production	October 1982
Water depth, (m)	69
Reservoir depth, (m)	2400-2600
Initial Reservoir Pressure (psi)	6550
Reservoir Temperature (deg C)	90
Oil gravity, (API)	36
Oil viscosity, (cp)	0.40
Original oil-in-place, (MM stb)	2600
Cumulative oil production jan 2003, MM stb)	472
Average thickness, (m)	25
Matrix Permeability range, (mD)	1-10
Total Permeability range, (mD)	1-300
Connate water saturation, (%)	5
Porosity, (%)	35-50
Bubble point pressure, (psi)	3000-4000
Solution GOR (scf/stb)	800-1400
Rock Compressibility (10^{-6} psi^{-1})	10-100

Teufell 1996

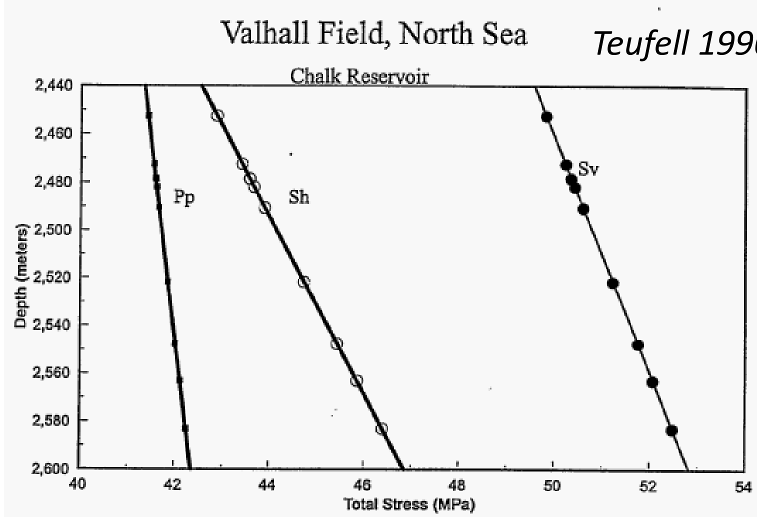

Figure 8. Plot of total vertical stress, total minimum horizontal stress and pore pressure versus depth for chalk reservoirs in the Valhall Field before production.

Final stresses + pore pressure		
Internal radial stress [MPa]	SigRi =	-39.4
External radial stress [MPa]	SigRe =	-43.1
Internal pore pressure [MPa]	pfi =	39.4
External pore pressure [MPa]	pfe =	39.4

Final stresses + pore pressure		
Internal radial stress [MPa]	SigRi =	-29.4
External radial stress [MPa]	SigRe =	-43.1
Internal pore pressure [MPa]	pfi =	29.4
External pore pressure [MPa]	pfe =	39.4

Valhall field North Sea

Material properties		
Young's modulus [MPa]	E =	5500
Poisson's ratio [-]	nu =	0.15
Biot's eff. stress coeff. [-]	alfa =	1
Geometry		
Internal radius [m]	ri =	**0.1**
External radius [m]	re =	**100**
Initial stresses + pore pressure		
Radial stress [MPa]	SigRo =	-43.1
Axial stress [MPa]	SigZo =	-49.7
Pore pressure [MPa]	pfo =	39.4

Drilling (no flow)

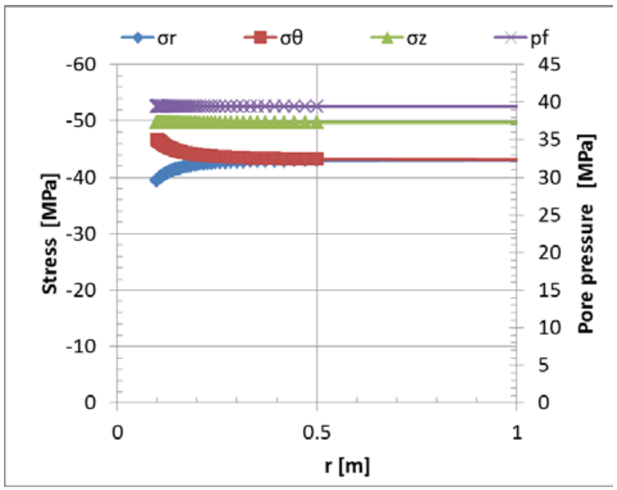

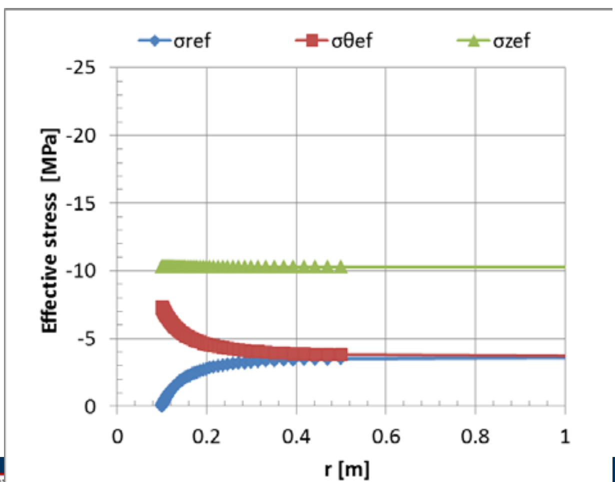

Production

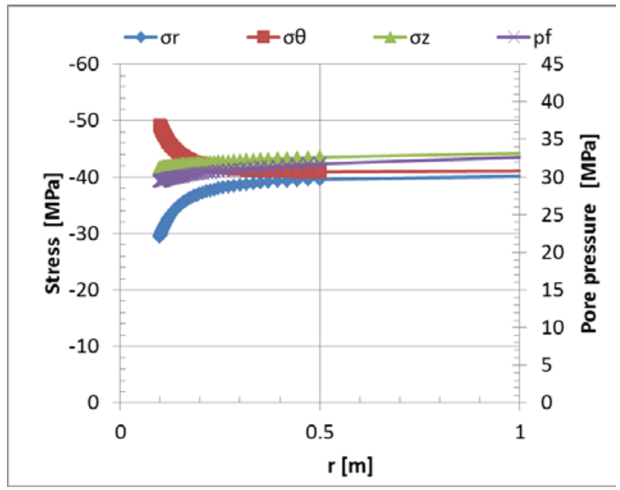

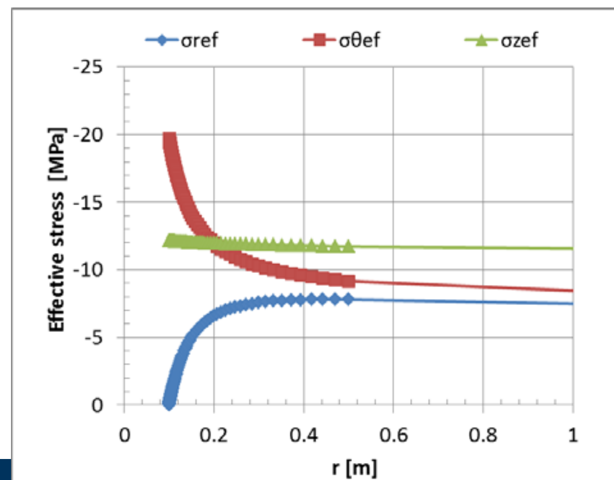

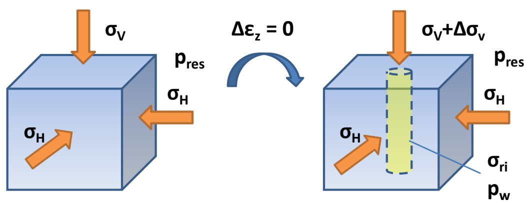

Effects of temperature changes

- Temperatures at the well may differ from formation temperatures, e.g. during
  - Drilling: Drilling mud may be cooler than formation
  - Hydraulic fracturing: Injected fluid is cooler
  - Water injection for pressure maintenance: Injected fluid is cooler
  - CO_2 or waste injection: Injected fluid is cooler
- Cooling causes shrinkage of the formation and lower compressive stresses
- Heat flows through
  - Conduction
  - Convection (heat carried by the flowing fluid)

Anisotropic lateral loading

Superposition of

1. Isotropic loading σ_{re}, σ_{ri} + pore pressure p_{fe}, p_{fi} + axial strain ε_z
2. Anisotropic loading σ_{Re} - σ_{re} , σ_{ri} = p_{fe} = p_{fi} = ε_z = 0
3. (Eventually temperature loading ΔT_e, ΔT_i w/ again boundary stresses and pore pressures and vertical strain = 0)

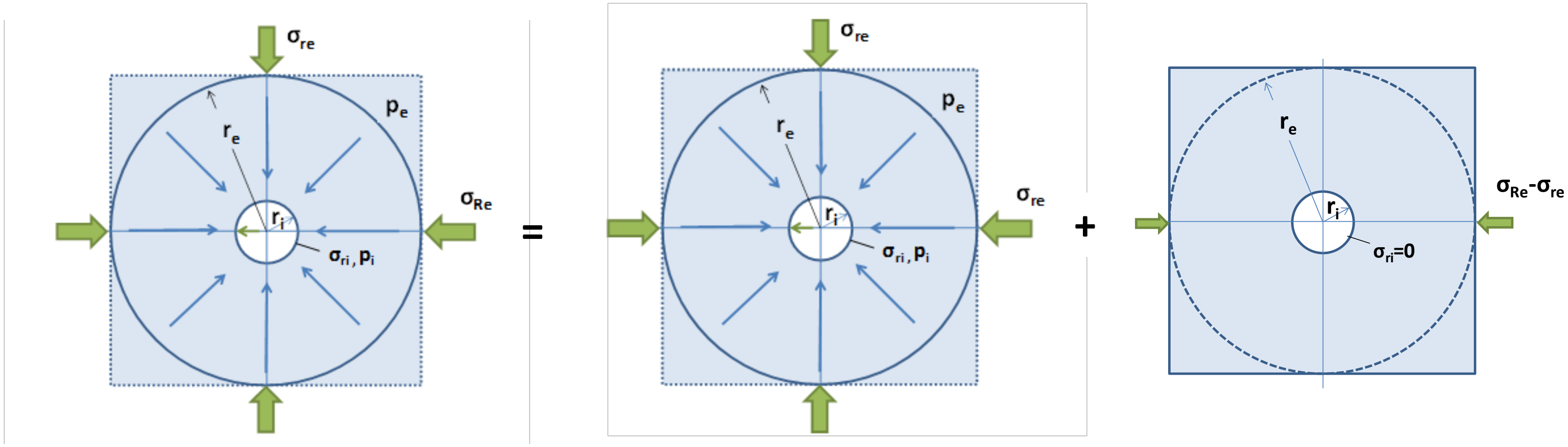

Coordinate systems for deviated (inclined) wells

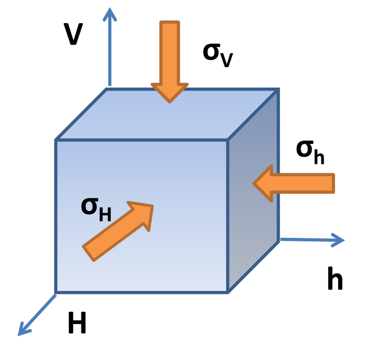

1. *H*-, *h*-, *v*-axes Cartesian coordinate system of in situ stresses

2. *x*-, *y*-, *z*-axes Cartesian coordinate system of a deviated wellbore

- *z*-axis points along the axis of the hole
- *x*-axis points towards the lowermost radial direction of the hole
- *y*-axis is horizontal
- For vertical hole: *x*-axis points towards the direction of the major horizontal stress σ_H

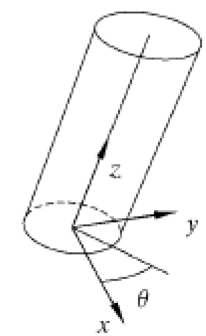

3. Polar coordinate system (r, θ, z) associated with the wellbore
   - *z*-axis along the axis of the hole
   - *r*-axis along the *x*-axis
   - Angle θ is measured anticlockwise from the *r*-axis

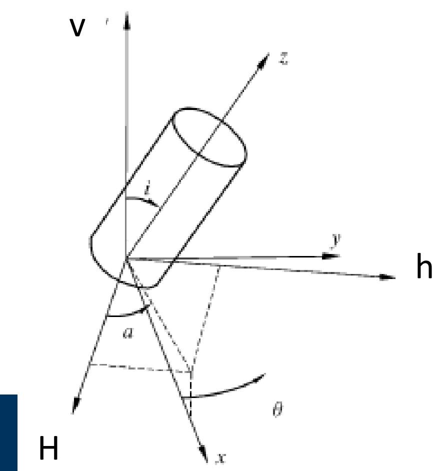

Deviated wellbore

Drilling and production =
= coordinate transform +
+ superposition of 2 plane strain loadings

1. Coordinate transform to well coordinate system
2. Make radial and shear stresses at wellbore = 0 (solution by *Hiramatsu and Oka* 1962, 1968)
3. Make radial stress at wellbore = $\sigma_{ri} = p_w$
4. If permeable wellbore, make pore pressure at well $p_{fi} = p_w$ (else p_f remains p_{fm})
5. (Eventually cooling of the wellbore)

Hiramatsu Y, Oka Y (1962). Stress around a shaft or level excavated in ground with a three-dimensional stress state. Mem. Fac. Eng. Kyotu Univ. 24, 56–76.

Hiramatsu Y, Oka Y (1968). Determination of the stress in rock unaffected by boreholes or drifts, from measured strains or deformations. Intl J Rock Mechanics Mining Science 5, 337–353.

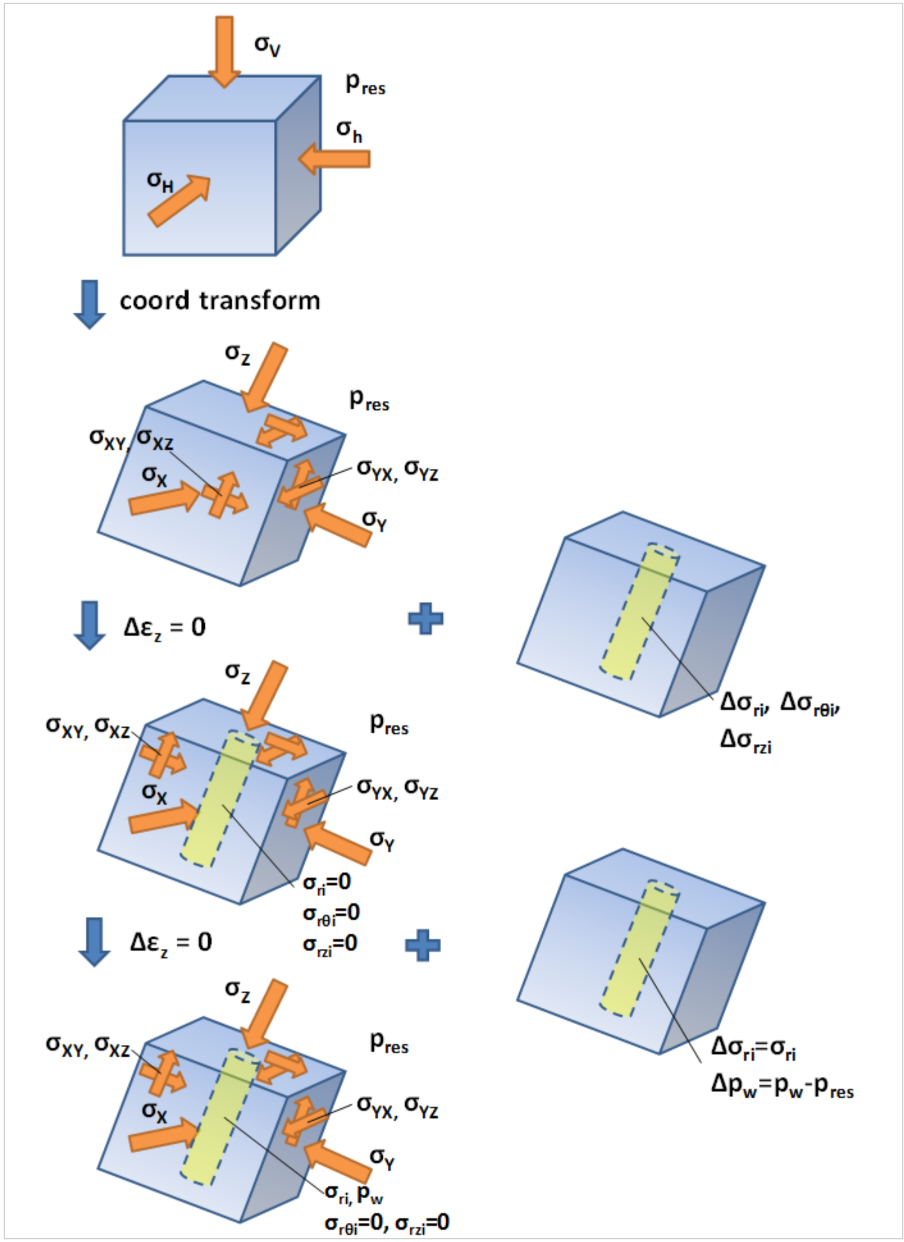

Poro-elastic time dependent effects

- Time effects because pore pressure changes are transient, i.e. not immediate but take time to reach steady-state conditions
  - Relevant for low permeability formations
    - Shales, Chalks
- Poro-elastic time dependent effects
  - Pore pressure change due to production or invasion of wellbore fluid
    - If wellbore is sealed then no pore pressure changes (e.g. filter cake during drilling)
  - Pore pressure change due to volumetric strain as a result of changes in applied stress
    - C.f. Terzaghi's consolidation problem
- *Paper by Detournay E, Cheng AHD (1988). Poroelastic response of a borehole in a non-hydrostatic stress field. Intl J Rock Mechanics Mining Sciences & Geomechanics Abstracts 25, 171–182.*
- *Detournay E, Cheng AHD (1993).Fundamentals of poroelasticity. Chapter 5 in Comprehensive Rock Engineering: Principles, Practice and Projects, Vol. II, Analysis and Design Method, ed. C Fairhurst, Pergamon Press, 113-171.*

Solution of transient problems

- No analytical solutions
  - Numerical methods
  - Laplace transforms

Borehole Stress Analysis

1. Stresses at vertical impermeable borehole wall (based on linearly elastic rock and isotropic horizontal stresses):

Case a: $\boxed{\sigma_\theta > \sigma_z > \sigma_r}$

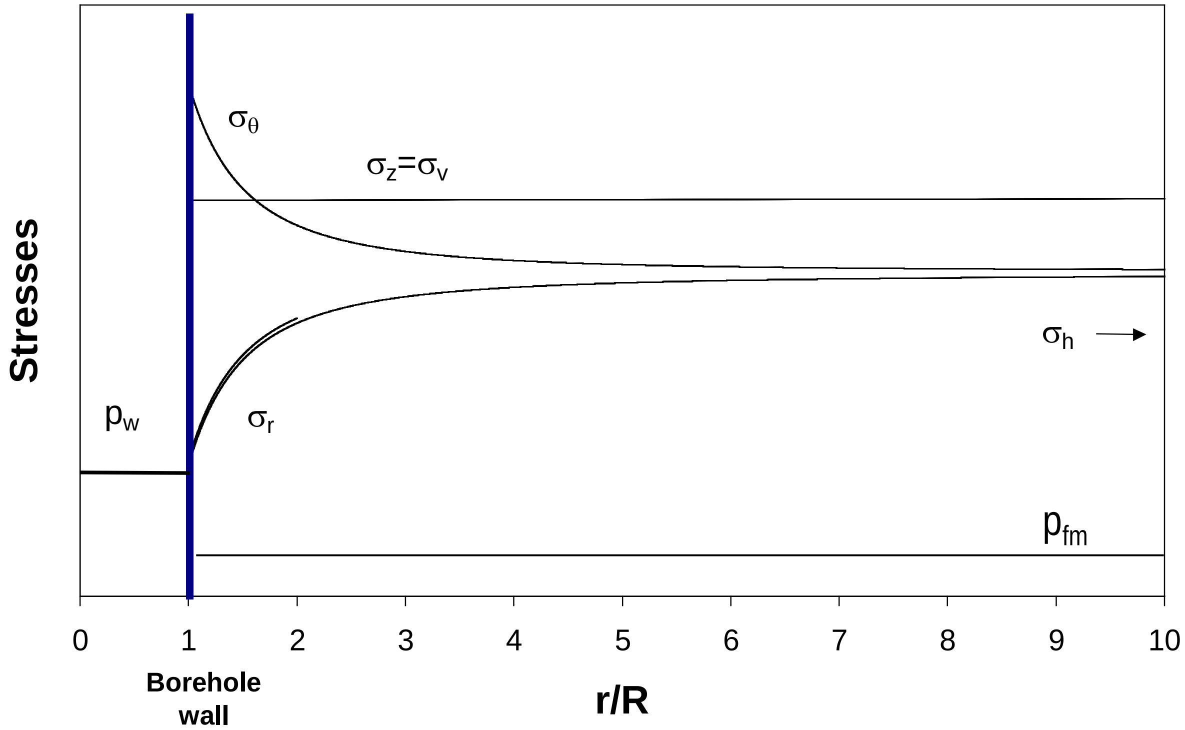

$$\sigma_r = p_w$$
$$\sigma_\theta = 2\sigma_h - p_w$$
$$\sigma_z = \sigma_v$$

Impermeable wall:

- Perfect mud cake
- Drill-out in shale

Borehole Stress Analysis

Case b: $\boxed{\sigma_z > \sigma_\theta > \sigma_r}$

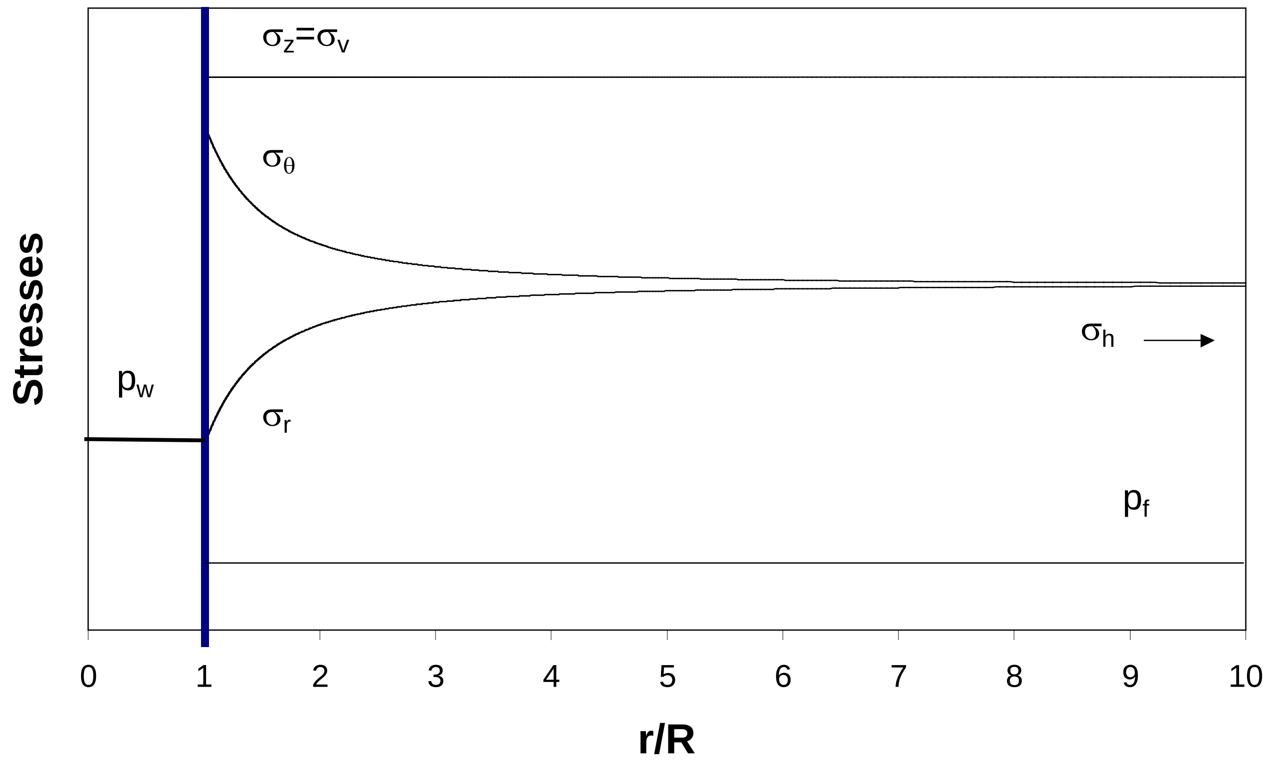

$$\boxed{\begin{aligned} \sigma_r &= p_w \\ \sigma_\theta &= 2\sigma_h - p_w \\ \sigma_z &= \sigma_v \end{aligned}}$$

M-C failure criterion

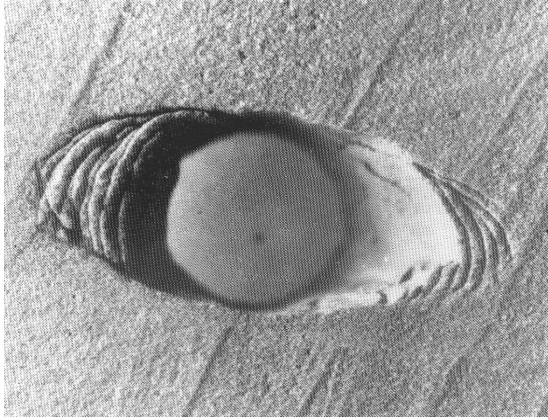

- Borehole stresses + Mohr-Coulomb failure criterion $\Rightarrow$
- Minimum permitted well pressure to prevent shear failure at borehole wall (hole collapse)

$$\sigma_1' = UCS + m\sigma_3' \,, \qquad UCS = \frac{2c\cos\varphi}{1-\sin\varphi}\,, \qquad m = \frac{1+\sin\varphi}{1-\sin\varphi}$$

$$\boxed{p_{w,\min}^{(a)} = \frac{2\sigma_h - UCS + (m-1)\,p_{fm}}{m+1}}$$

or

$$\boxed{p_{w,\min}^{(b)} = \frac{\sigma_v - UCS + (m-1)\,p_{fm}}{m}}$$

$$\Rightarrow \qquad \boxed{\rho_{w,\min} = \frac{p_{w,\min}}{gD}}$$

Minimum mud weight

Borehole shear failure – Complete set of solutions

Case	$\sigma_1 \geq \sigma_2 \geq \sigma_3$	Borehole failure occurs if
a	$\sigma_\theta \geq \sigma_z \geq \sigma_r$	$p_w \leq p_f + \dfrac{2(\sigma_h - p_f) - C_0}{1 + \tan^2 \beta}$
b	$\sigma_z \geq \sigma_\theta \geq \sigma_r$	$p_w \leq p_f + \dfrac{\sigma_v - p_f - C_0}{\tan^2 \beta}$
c	$\sigma_z \geq \sigma_r \geq \sigma_\theta$	$p_w \geq p_f + 2(\sigma_h - p_f) - \dfrac{\sigma_v - p_f - C_0}{\tan^2 \beta}$
d	$\sigma_r \geq \sigma_z \geq \sigma_\theta$	$p_w \geq p_f + \dfrac{2(\sigma_h - p_f)\tan^2 \beta + C_0}{1 + \tan^2 \beta}$
e	$\sigma_r \geq \sigma_\theta \geq \sigma_z$	$p_w \geq p_f + (\sigma_v - p_f)\tan^2 \beta + C_0$
f	$\sigma_\theta \geq \sigma_r \geq \sigma_z$	$p_w \leq p_f + 2(\sigma_h - p_f) - (\sigma_v - p_f)\tan^2 \beta - C_0$

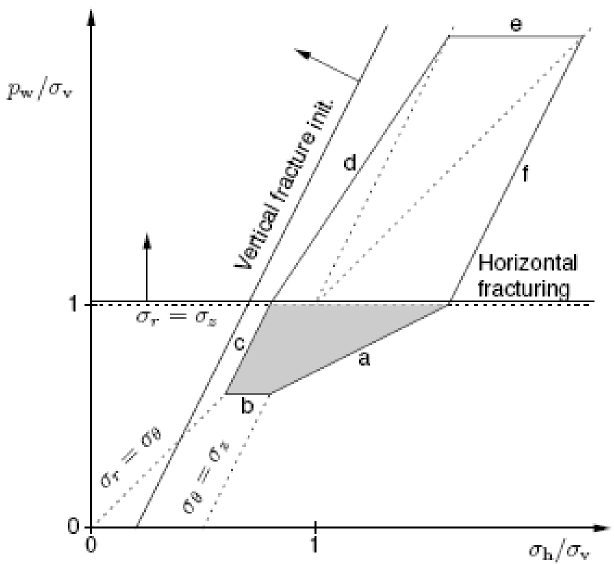

Borehole shear failure modes

- *Maury and Guenot 1987*

May use cavings shape to diagnose failure mechanism

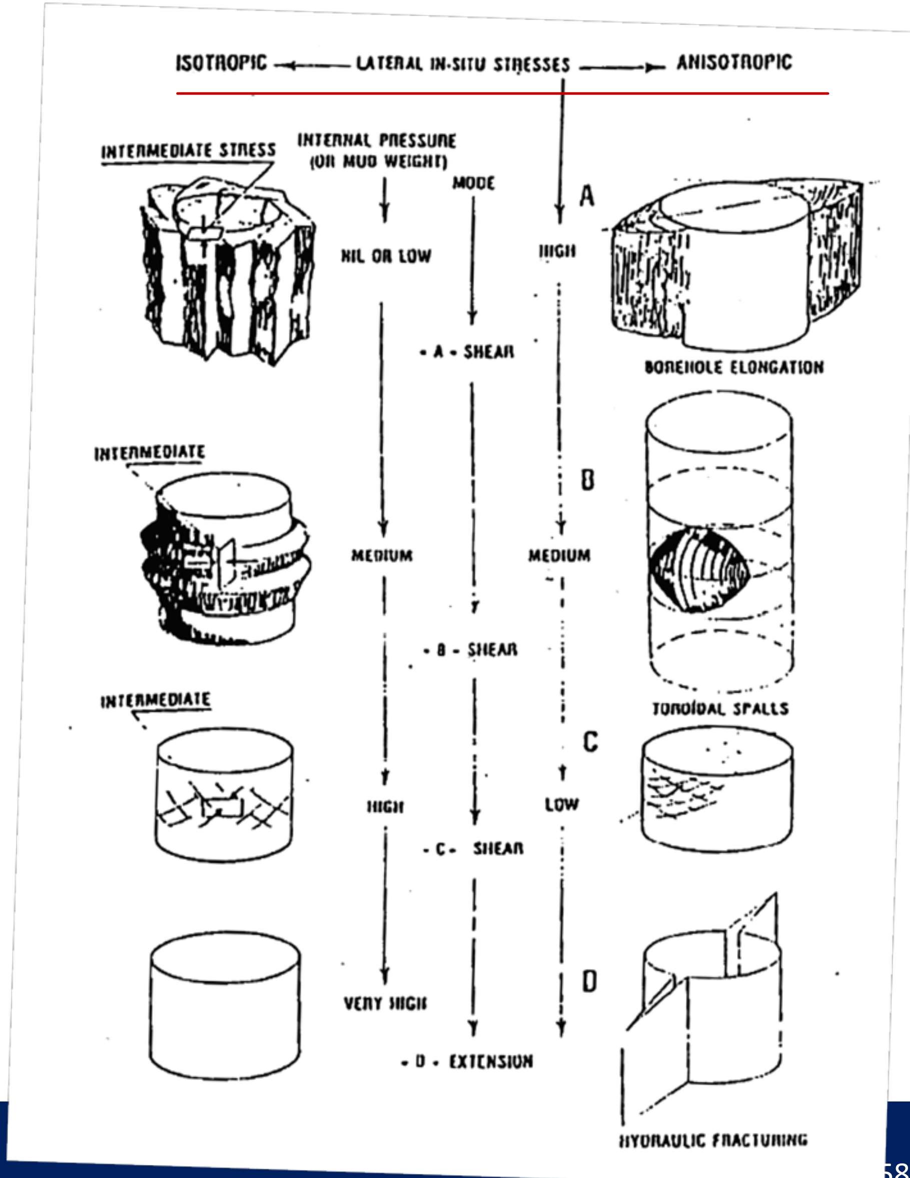

Borehole Failure Analysis – Tensile failure

- May occur at <u>low</u> well pressure (underbalanced drilling $\underline{p_w < p_{fm}}$):

$$\sigma_r' = -T_s \qquad \Rightarrow \qquad \boxed{p_{w,\min}^{rad,tens} = p_{fm} - T_s}$$

Gives sharp, blade-shaped cavings -> Tight hole

- Note: Tensile strength T_s of shale is low

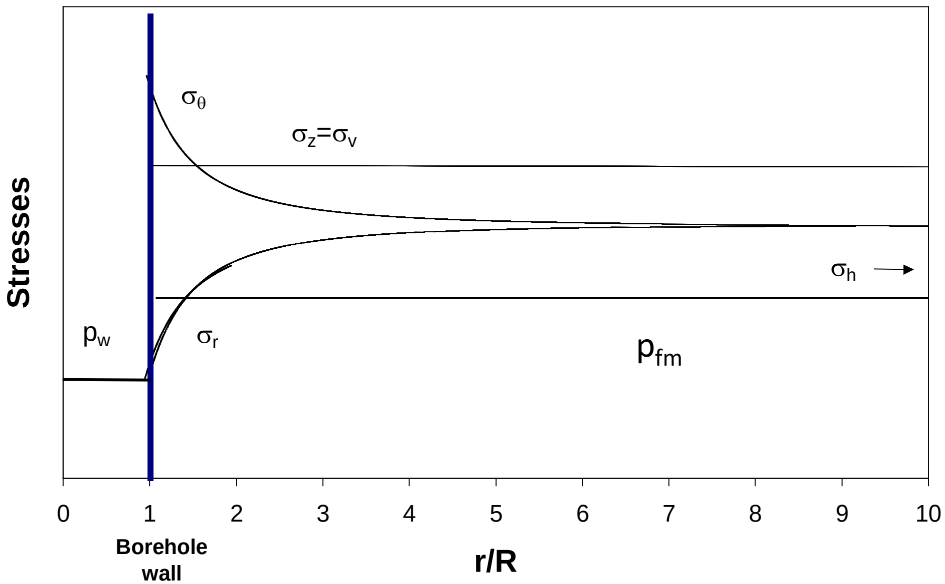

Borehole Failure Analysis – Tensile failure

- May occur at high well pressure (hydraulic fracturing):

$$\sigma'_\theta = -T_s \qquad \Rightarrow \qquad \boxed{p_{w,\max}^{frac} = 2\sigma_h - p_{fm} + T_s}$$

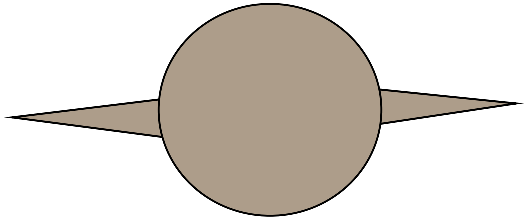

Tensile failure types

Failure type	Geometry and Orientation	Figure
Tensile Failure Cylindrical $\sigma_r \leq -T_o$	This failure is concentric with the borehole. A low mud weight would favor the failure due to the magnitude of σ_r being lower.	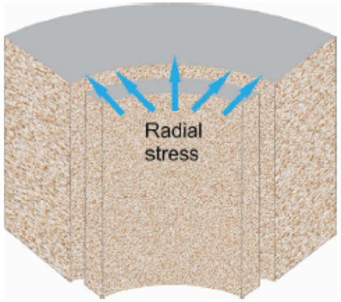
Not likely in vertical wells **Tensile Failure Horizontal** $\sigma_a \leq -T_o$	This failure creates horizontal fractures.	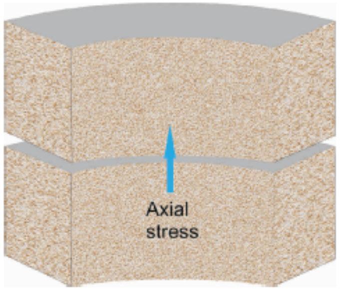
Tensile Failure Vertical $\sigma_t \leq -T_o$	This failure creates a vertical fracture parallel with the maximum horizontal stress direction. This is because, this orientation is the tangential stress has to overcome the smallest formation tensile strength.	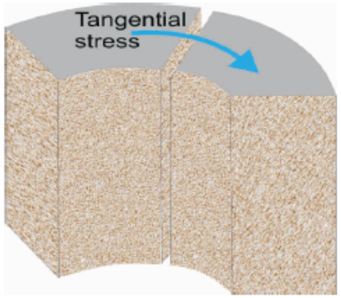

The Mud Weight Window

- Minimum mud weight
  - Hole collapse in shale (shear failure case (a) or (b))
  - Radial tensile failure in shale
  - Pore pressure (in case underbalanced drilling is prohibited)

$$p_{w,\min}^{(a)} = \frac{2\sigma_h - UCS + (m-1)\,p_{fm}}{m+1}$$

or

$$p_{w,\min}^{(b)} = \frac{\sigma_v - UCS + (m-1)\,p_{fm}}{m}$$

$$\boxed{p_{w,\min}^{rad,tens} = p_{fm} - T_s}$$

$$\boxed{p_{w,\min}^{underbal} = p_{fm}}$$

- Maximum mud weight
  - σ_h (minimum horizontal stress) in case of pre-existing natural fractures
  - Fracturing of borehole wall

$$\boxed{p_{w,\max}^{existfrac} = \sigma_h}$$

$$\boxed{p_{w,\max}^{frac} = 2\sigma_h - p_{fm} + T_s}$$

Effect of mud weight and safe mud window

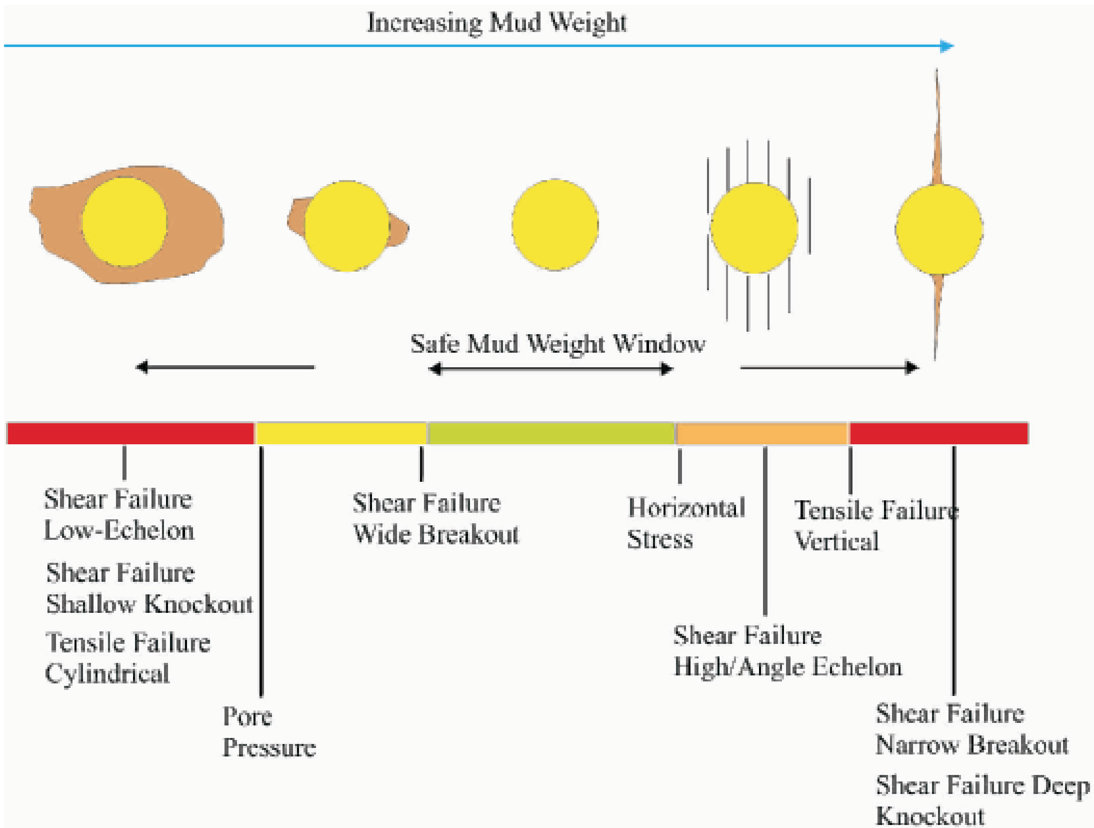

Hawkes and McLellan 1997

Vertical borehole in anisotropic horizontal stress field

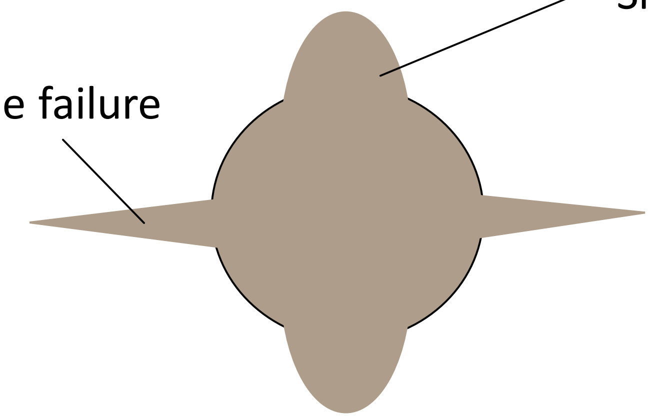

$$\sigma_r = p_w$$
$$\sigma_\theta = \sigma_H + \sigma_h - 2(\sigma_H - \sigma_h)\cos 2\theta - p_w$$
$$\sigma_z = \sigma_v - 2\nu(\sigma_H - \sigma_h)\cos 2\theta$$

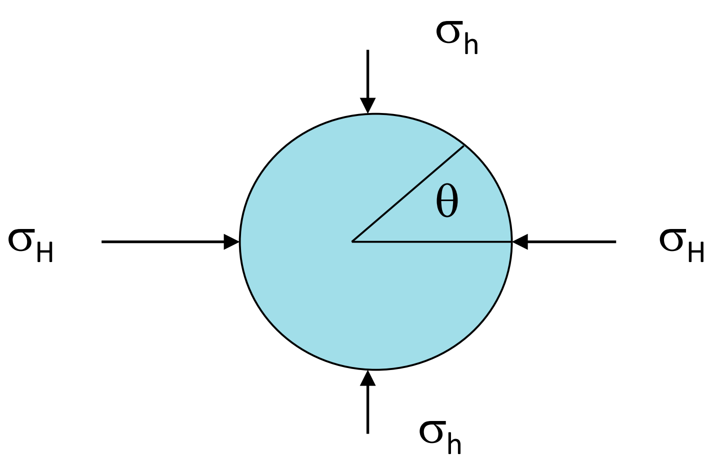

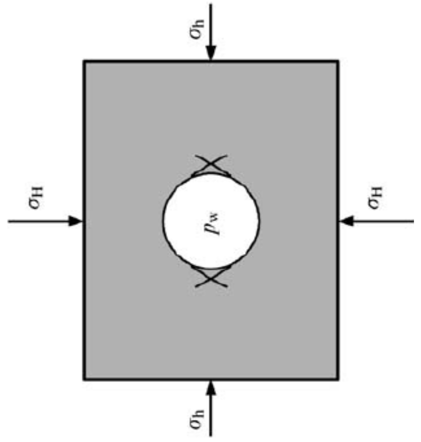

General comments

- If hole axis is parallel to a principal stress, then we can use the borehole stresses for a vertical hole also for horizontal holes, but we need to rotate the coordinate system first

- In general: Holes are most stable towards shear failure initiation when drilled along a direction with low stress anisotropy and with low stress level in the plane perpendicular to it
  - E.g. Drill horizontal well along $\underline{\sigma_h}$ direction
  - Avoid drilling along σ_H direction

- Deviated holes are usually less stable because of shear stresses at the borehole wall

Stability vs. Hole angle

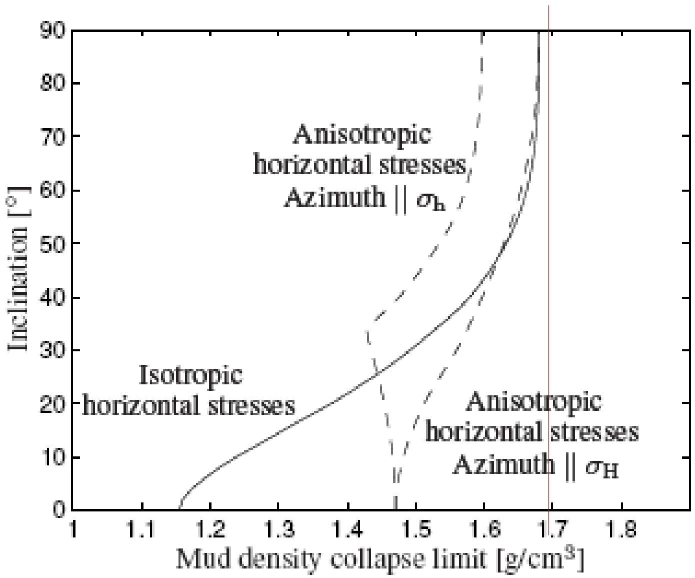

Illustration of stability analysis for a deviated wellbore at 1500 m depth, with vertical stress 30 MPa, isotropic horizontal stresses 25 MPa, and pore pressure 15.5 MPa. The unconfined strength is set to 10 MPa, the friction angle is 30°, the Biot coefficient 1, and Poisson's ratio 0.25. Also included is a case with anisotropic horizontal stresses, where all parameters are kept the same as above, except the maximum horizontal stress 28 MPa.

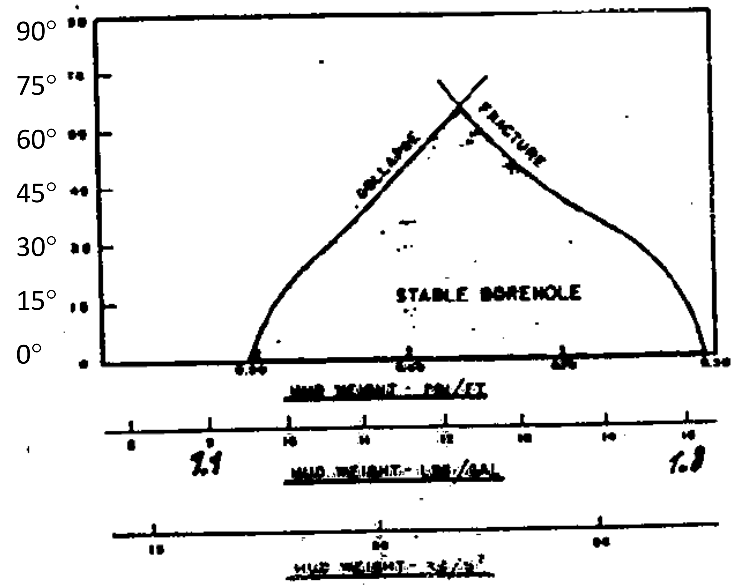

From Bradley 1979: Impossible to pass 60˚?

Maximum mud weight = σ_h = 25 MPa -> ρ_w = 1.7 g/cm^3

Effect of Rock Anisotropy

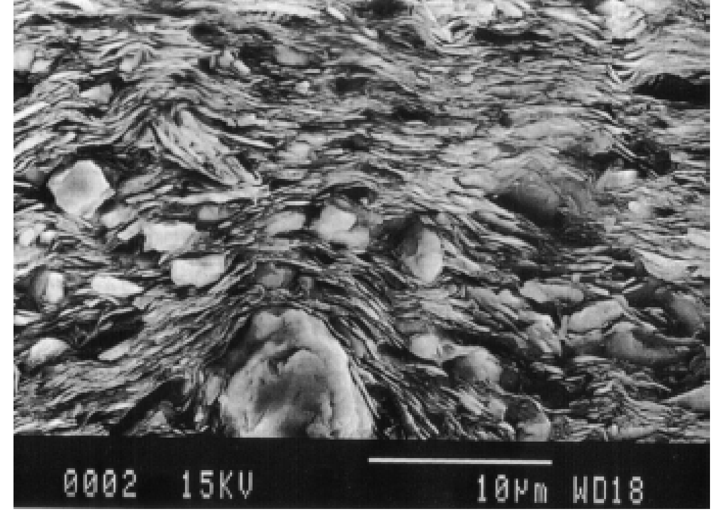

- Shales are anisotropic which leads to strength anisotropy
- The bedding plane is a weak plane

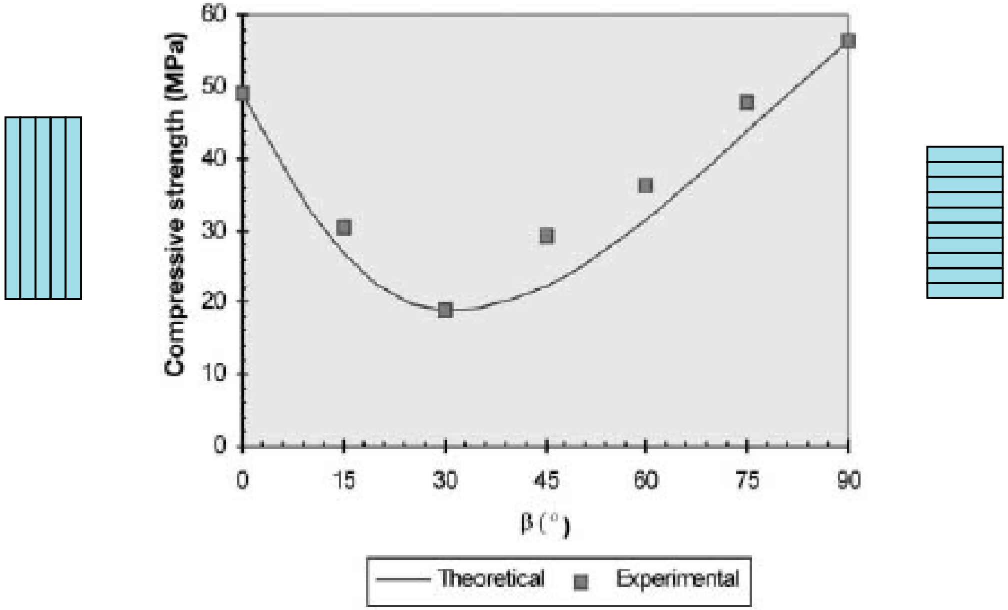

(mudshale)

Borehole Stability

… so far elastic behavior + brittle failure

- But: Note the following field observations:
  - Boreholes are often stronger than predicted by elastic + brittle theory
  - Hole collapse is often time-delayed (~ days) with respect to drill-out
  - Oil-based mud gives better stability than water-based mud
  - Addition of salt (in particular K+) may improve stability

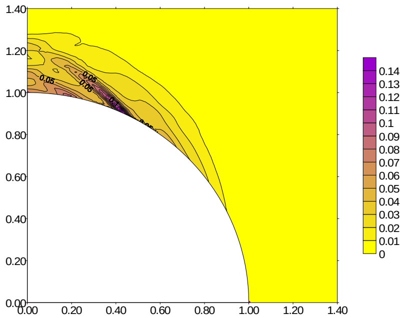

Borehole Stability: Plasticity

- Plastic zone around a borehole
  - Leads to yield/plastified zone around the hole, but may serve as a support to rock behind

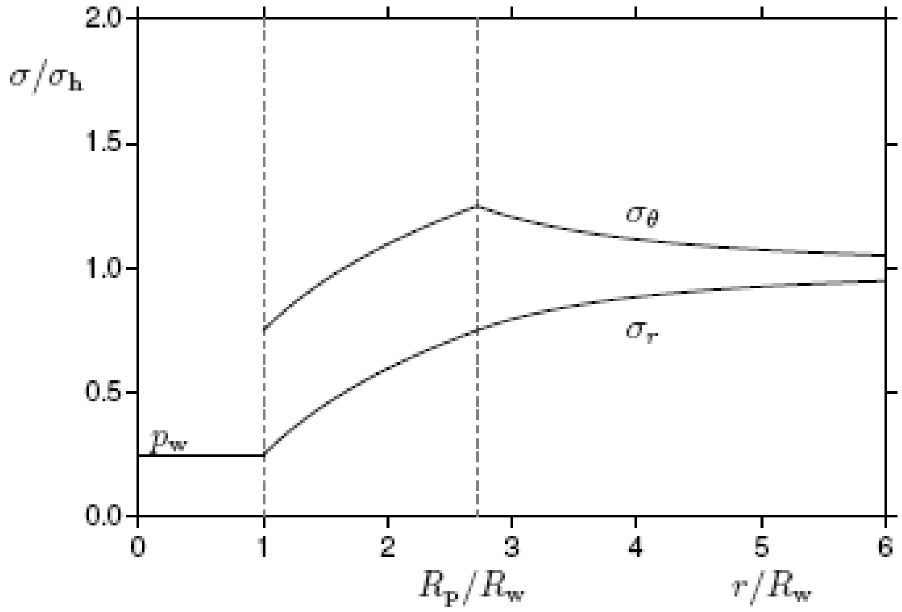

1. Stresses around a borehole with a plastic zone, according to the Tresca model. Parameters are $C_0 = 0.5\sigma_h, p_w = 0.25\sigma_h$.

- Borehole failure criterion can be specified by:
  - A critical amount of plastic strain, or
  - A critical extent of a plastic zone
- Use of the elastic-brittle equations with an up-scaled strength may give acceptable results …

Borehole Stability: Time-delayed borehole failure

- Initial drilling is stable but tight hole/stuck pipe during tripping or running logging tools
- Mechanisms:
  - Creep
  - Consolidation
  - Cooling
  - Chemistry

- **Creep**
  - Thermally activated process on atomic / molecular level
  - Rocks may creep to failure

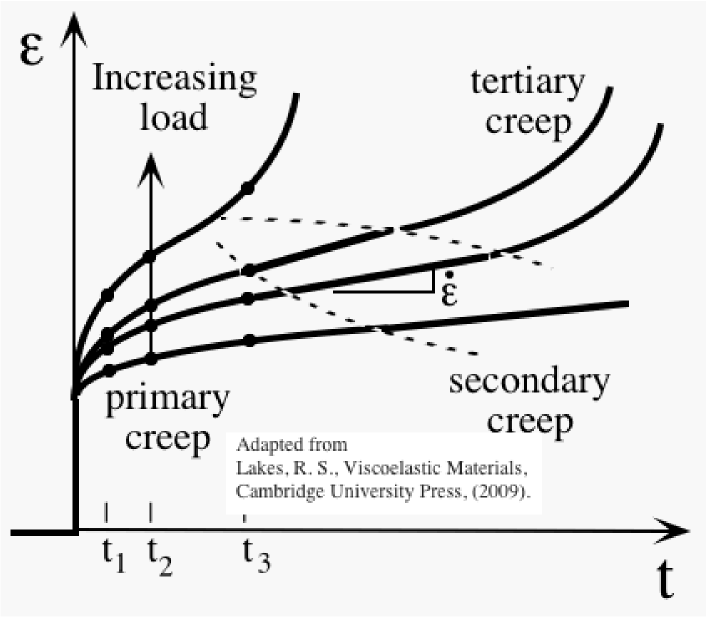

SAND PRODUCTION

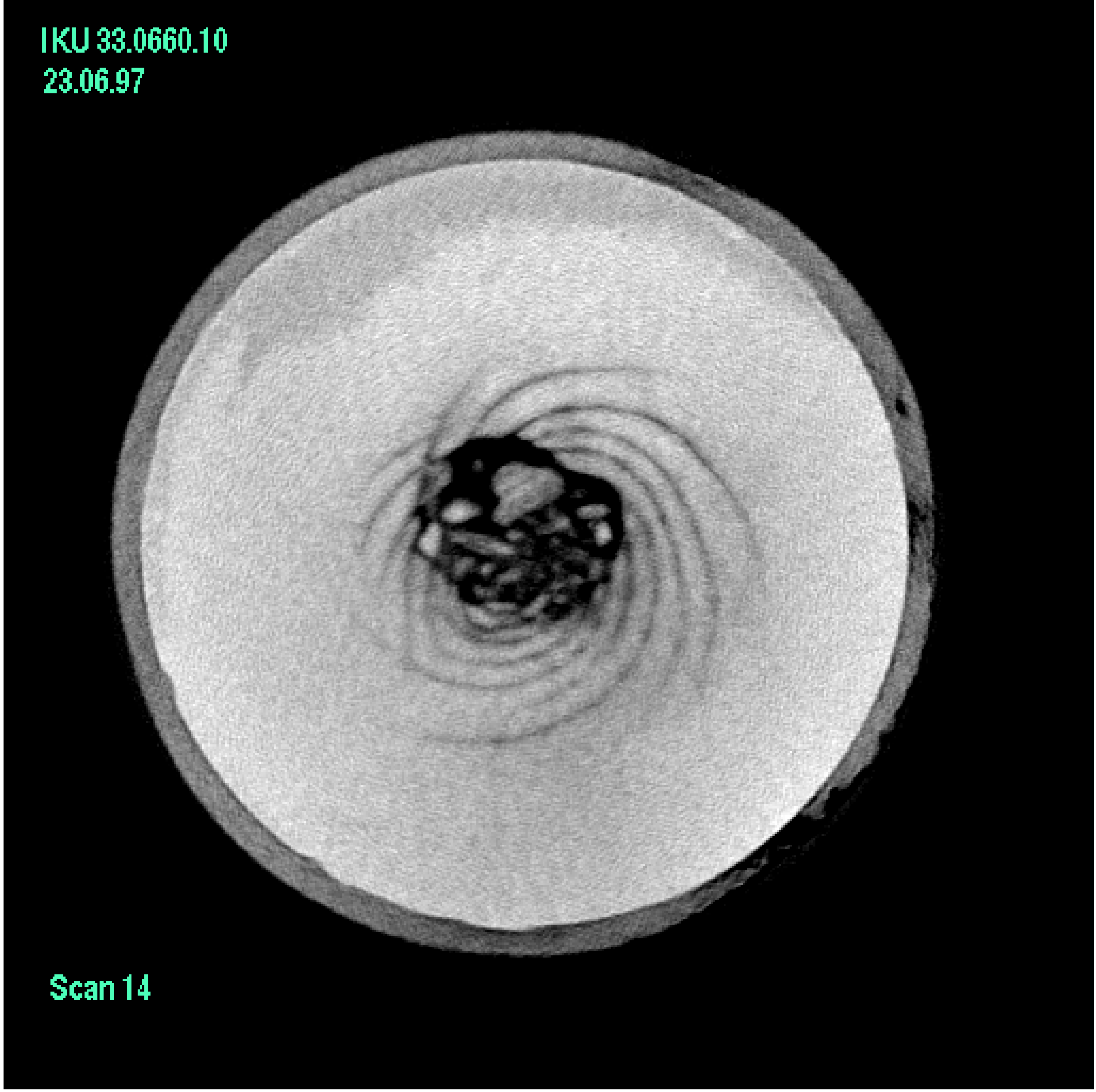

Sand production = An unwanted byproduct of hydrocarbon production

- Why sand production is a problem:

1. Erosion of the production equipment
2. Instability of production cavities and well
3. Large amounts of polluted sand

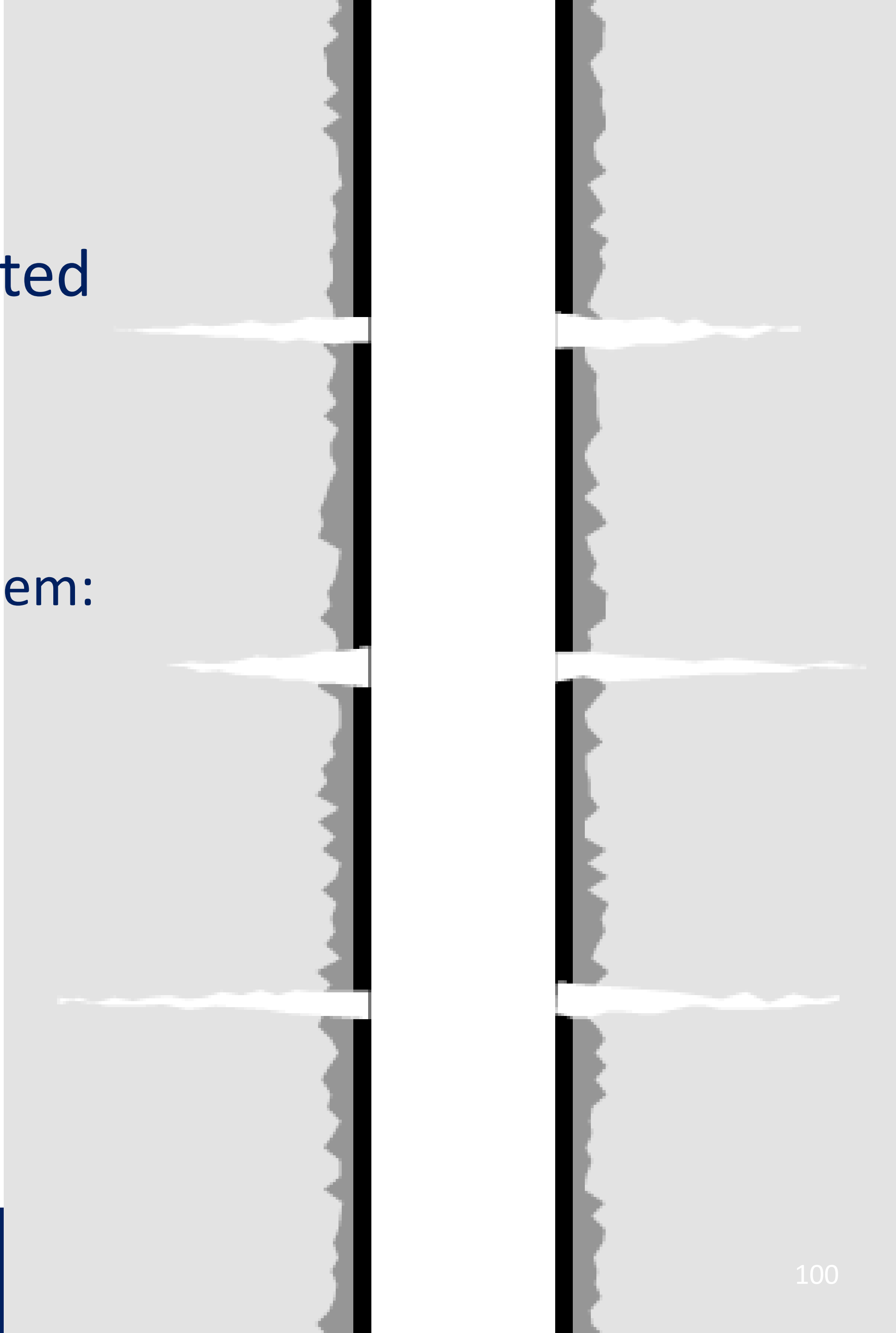

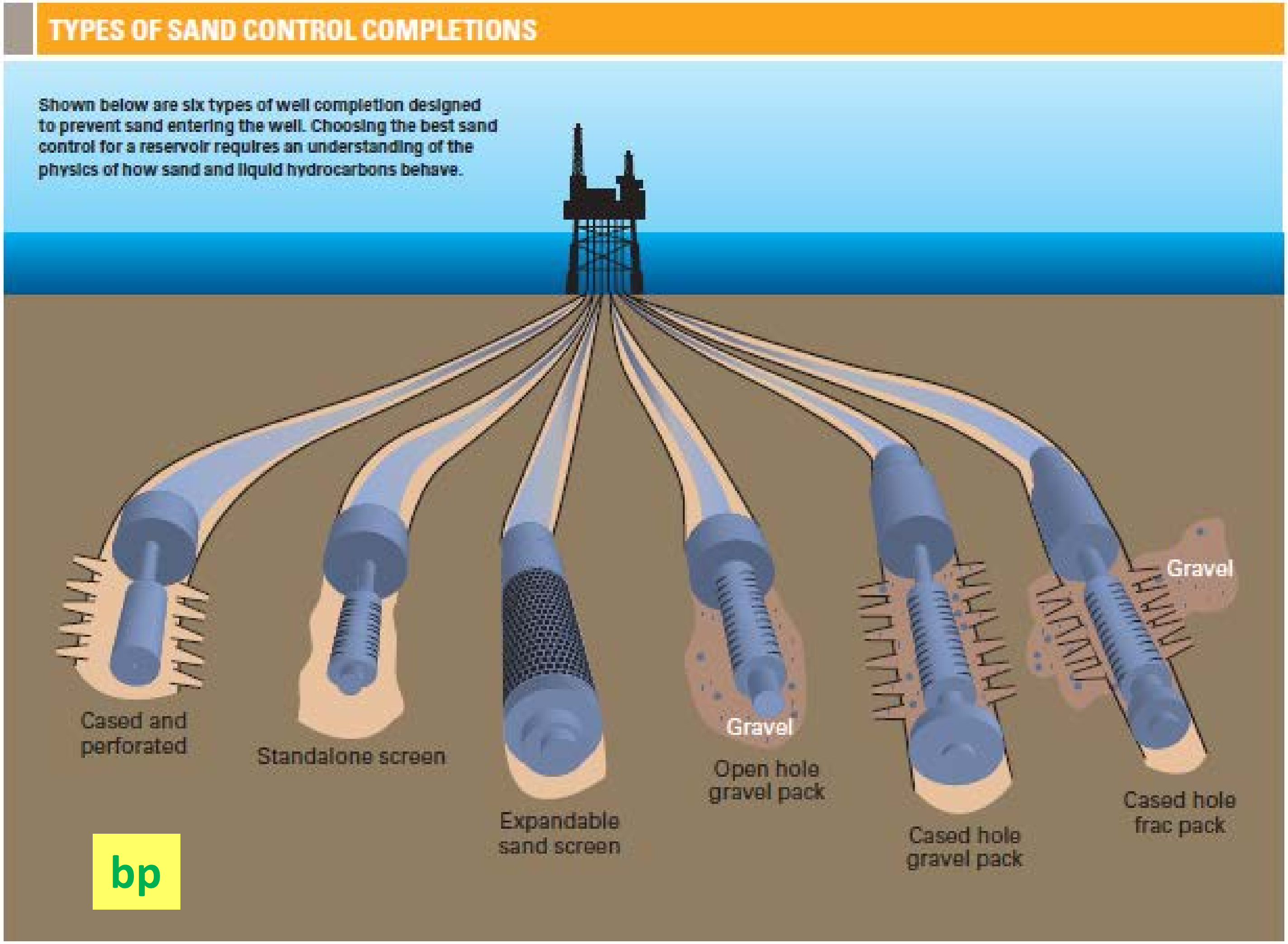
TYPES OF SAND CONTROL COMPLETIONS
Shown below are six types of well completion designed to prevent sand entering the well. Choosing the best sand control for a reservoir requires an understanding of the physics of how sand and liquid hydrocarbons behave.
Cased and perforated
Standalone screen
Expandable sand screen
Gravel
Open hole gravel pack
Cased hole gravel pack
Gravel
Cased hole frac pack
bp

Sand production due to screen failure

North Sea field

Massive sand production in a field in Indonesia

Solids production in chalk

- Chalk fragment
- Chalk influx or l
  - High porosity
    - Pore colla
  - Low permeal
    - Decreases
  - Pore pressur
  - Tensile radial

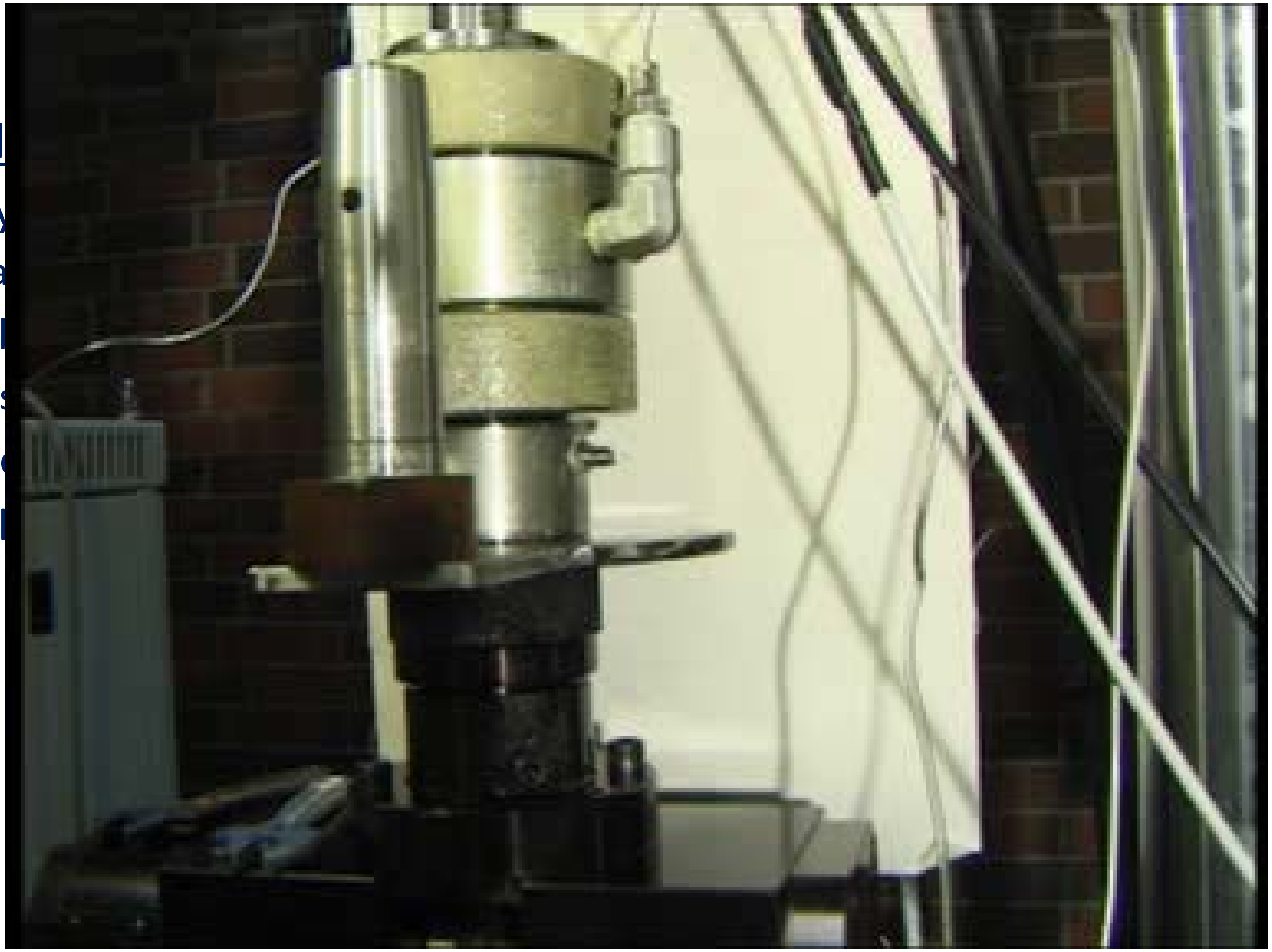

Flatebø (2006)

Sand production regimes

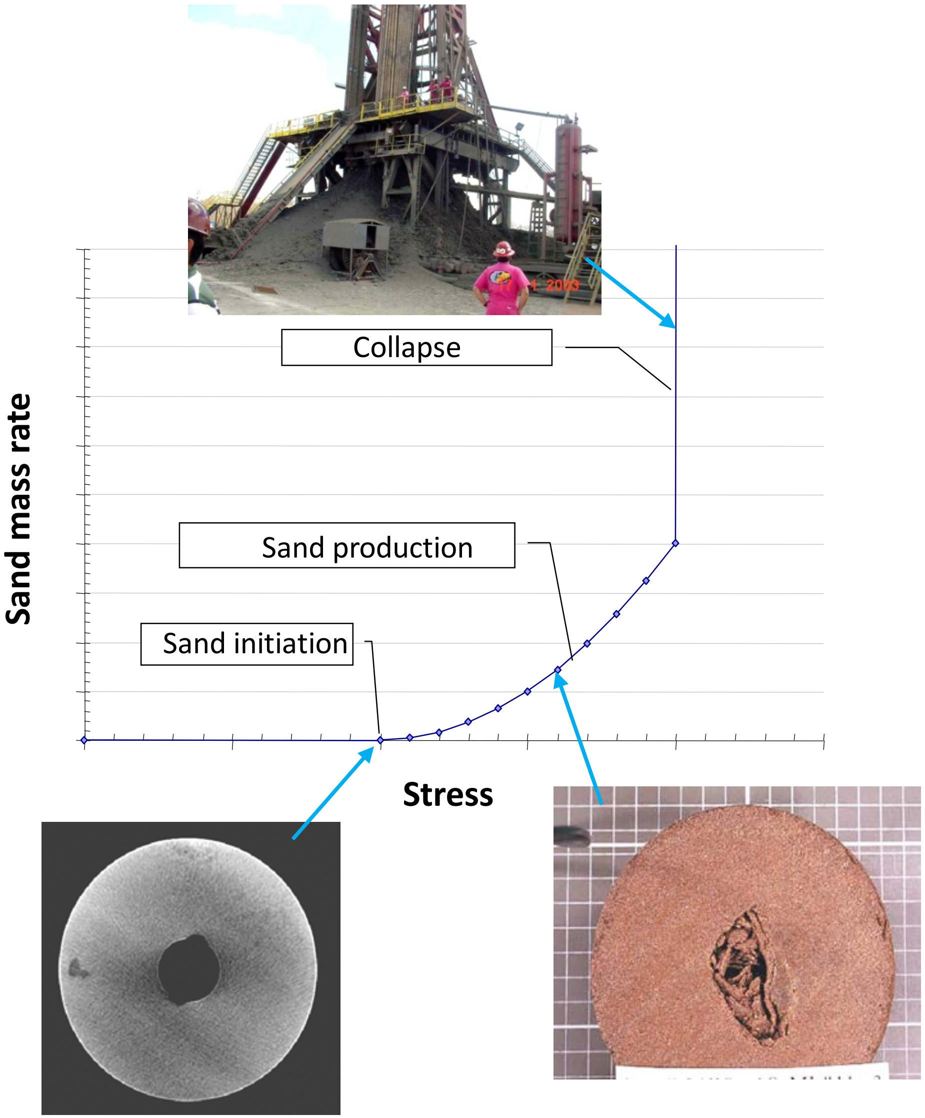

- Initiation
  - When sand will be produced ?
  - Critical stress for failure
- Sand production
  - How much sand will be produced over time ?
  - Sand rate Vs. flow rate, stress, 2 or 3 phase flow (water/gas), etc.
- Collapse
  - What are the critical conditions for massive sand production ?

- Sand production sequence from X-Ray CT scans of tested specimens
  - 1. Applied stresses fail the rock
  - 2. Fluid flow removes / erodes failed rock
  - Hydrodynamic forces too weak to erode intact rock (not the same as in cohesion-less sand). Even capillary cohesion may be sufficient to prevent sand erosion

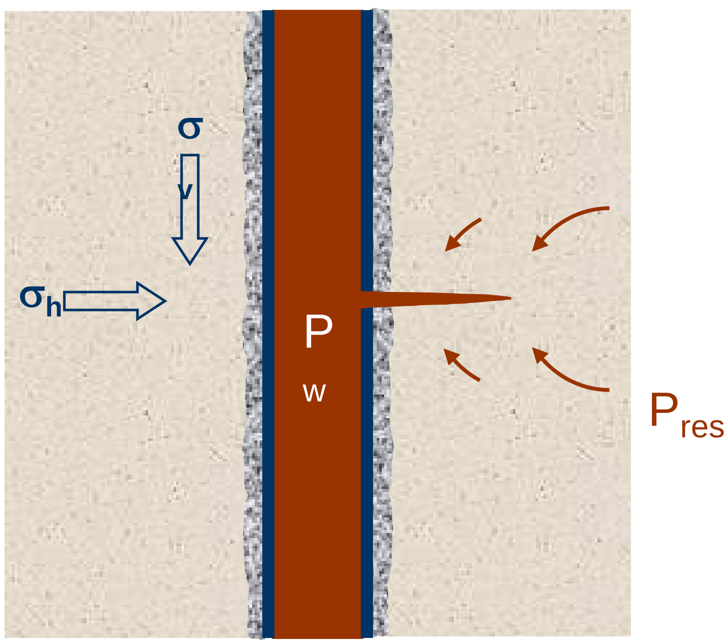

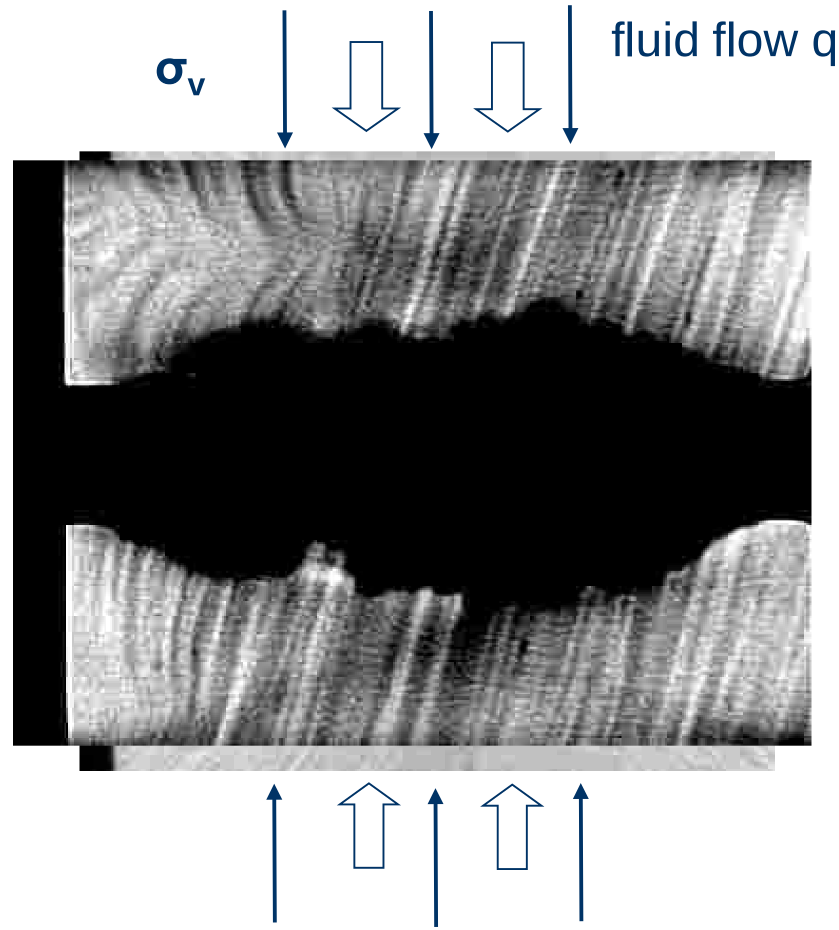

Hollow cylinder test with fluid flow

- Typical test for studying erosion in petroleum engineering

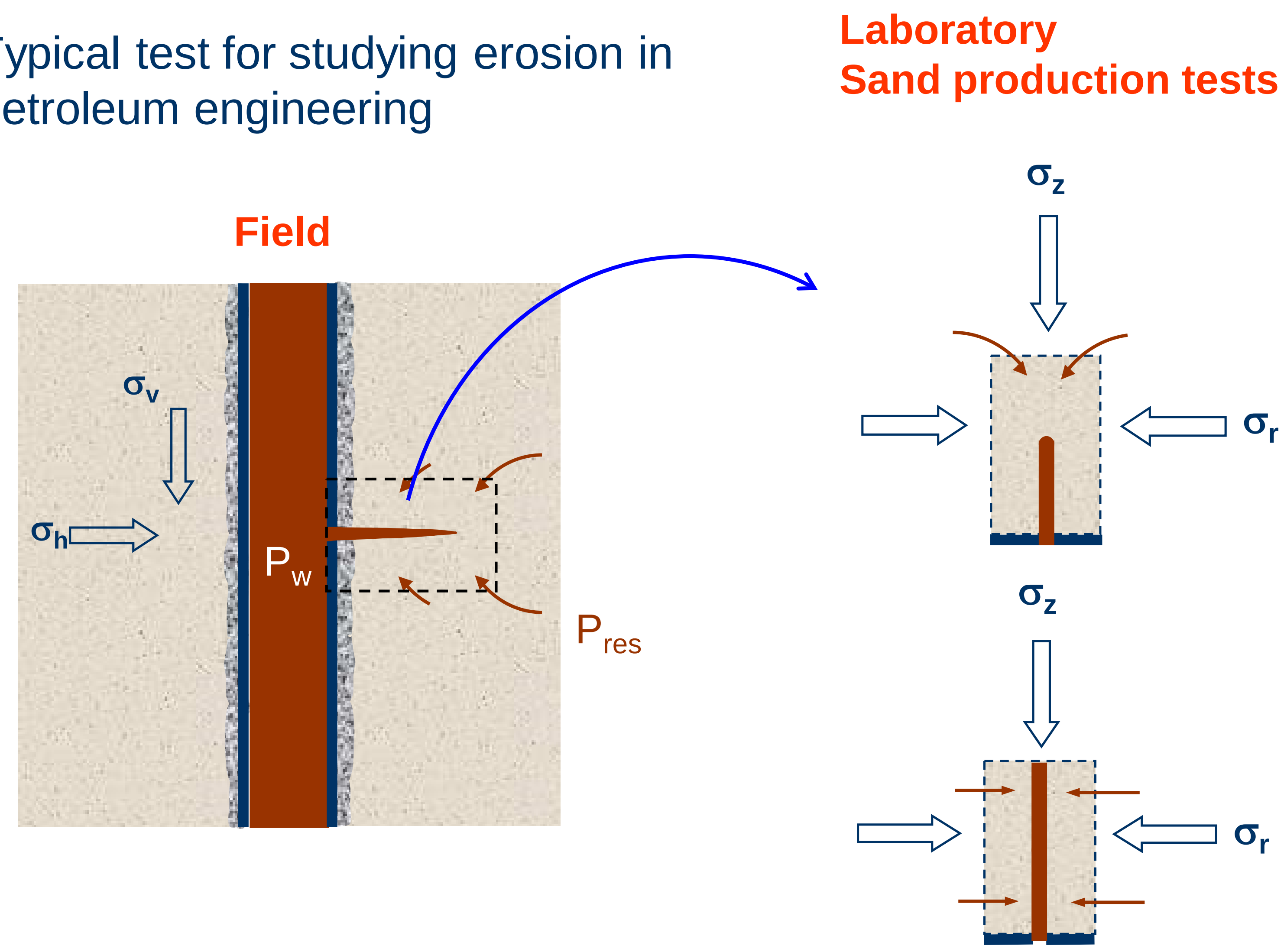

Sand trap

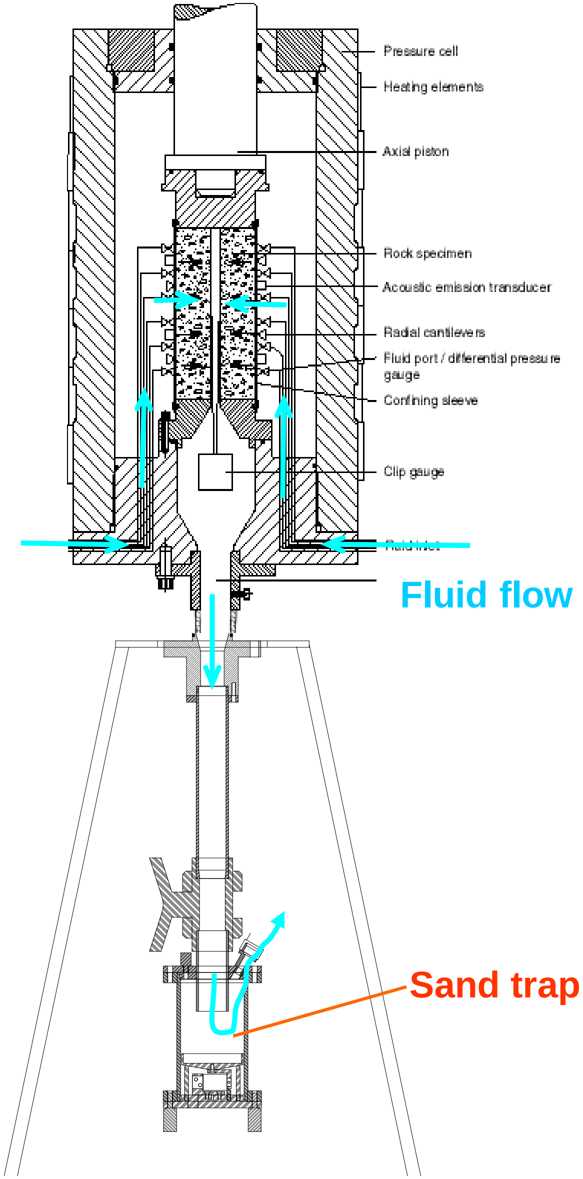

Pressure cell
Heating elements
Axial piston
Rock specimen
Acoustic emission transducer
Radial cantilevers
Fluid port / differential pressure gauge
Confining sleeve
Clip gauge
Fluid flow
Sand trap

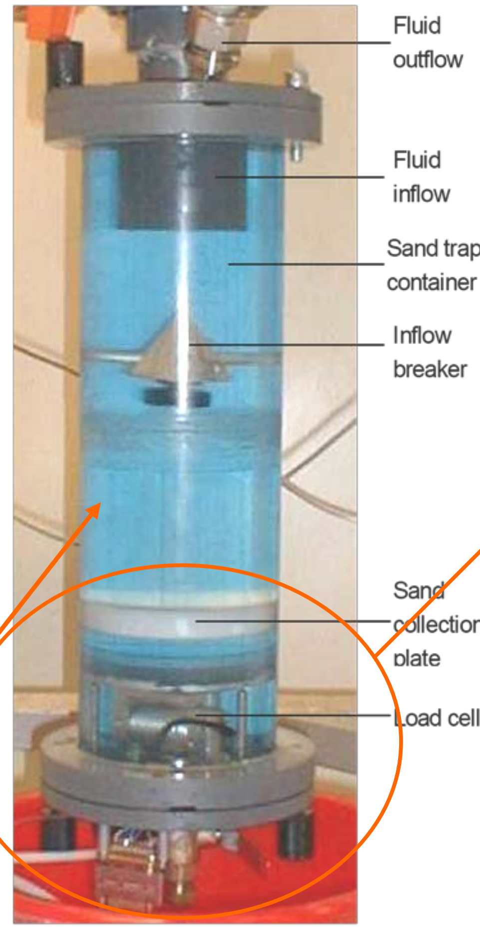

Fluid outflow
Fluid inflow
Sand trap container
Inflow breaker
Sand collection plate
Load cell

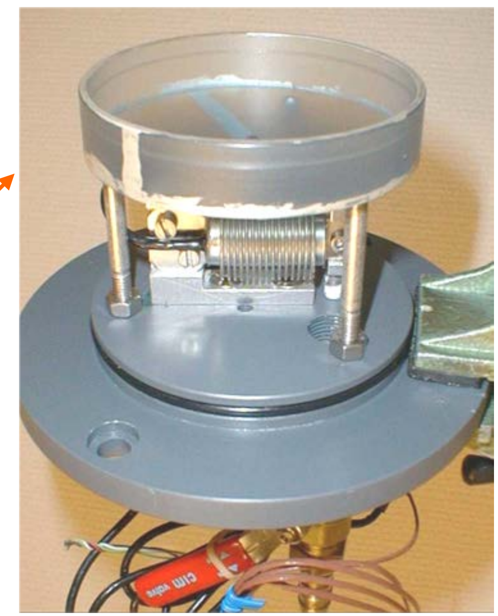

Sand production experiments

Loading cell

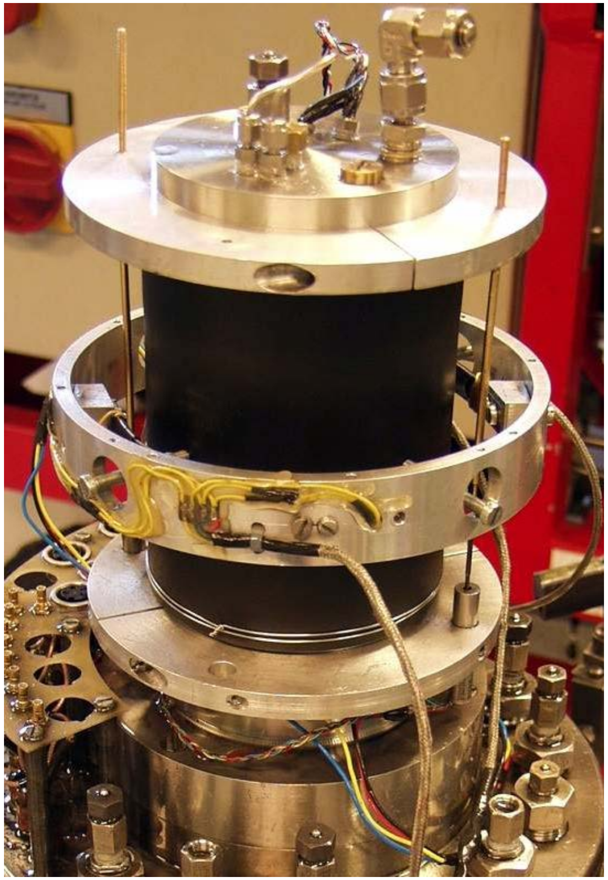

Instrumented jacketed specimen

Photographs SINTEF Petroleum Research, Norway

- Cavity deformations
  - The deviation of the 2 measurements indicates cavity failure
  - AE location and borescope data confirm this

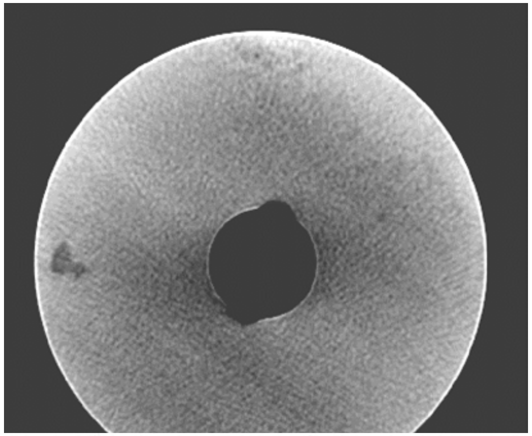

- Initial sand = 42 MPa
- Significant sand = 52 MPa

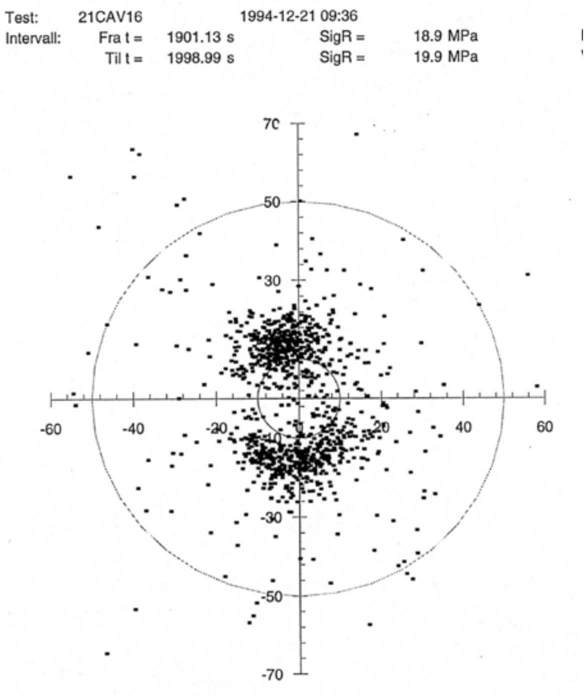

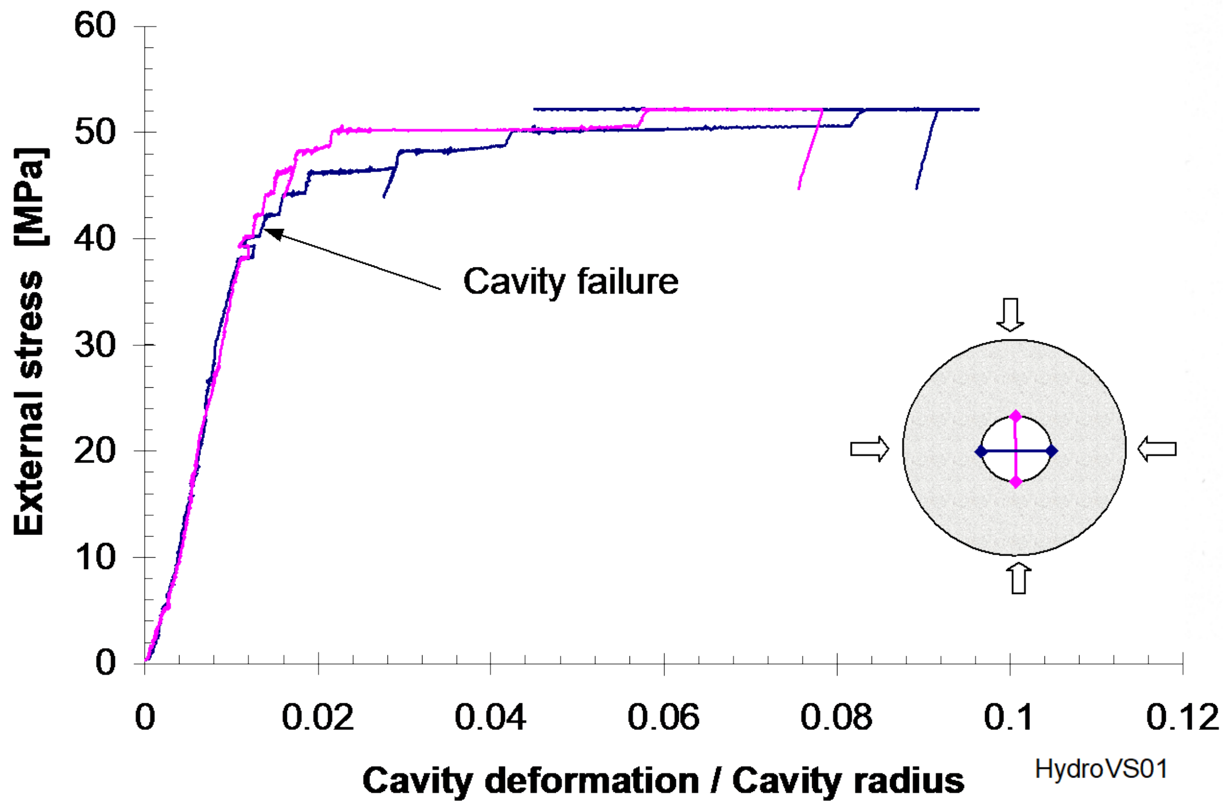

- Various phases of development of
  - (a) Slit failure in Class A brittle sandstones
  - (b) Breakout failure in Class B ductile sandstones
  - (c) Uniform failure in Class C compactive sandstones

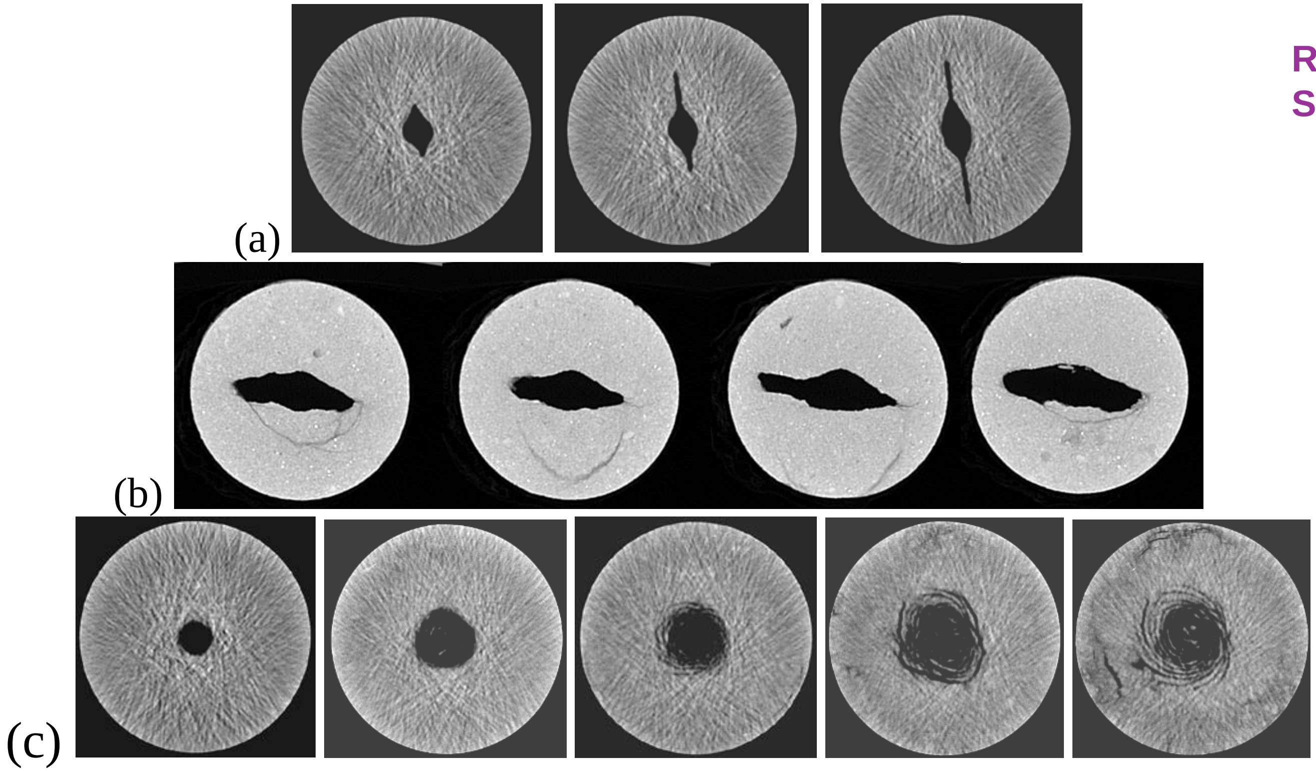

Remember !
Sand production Clip

Sand rate vs. normalized stress

$$\sigma_N = \frac{\sigma - \sigma_S}{\sigma_S}$$

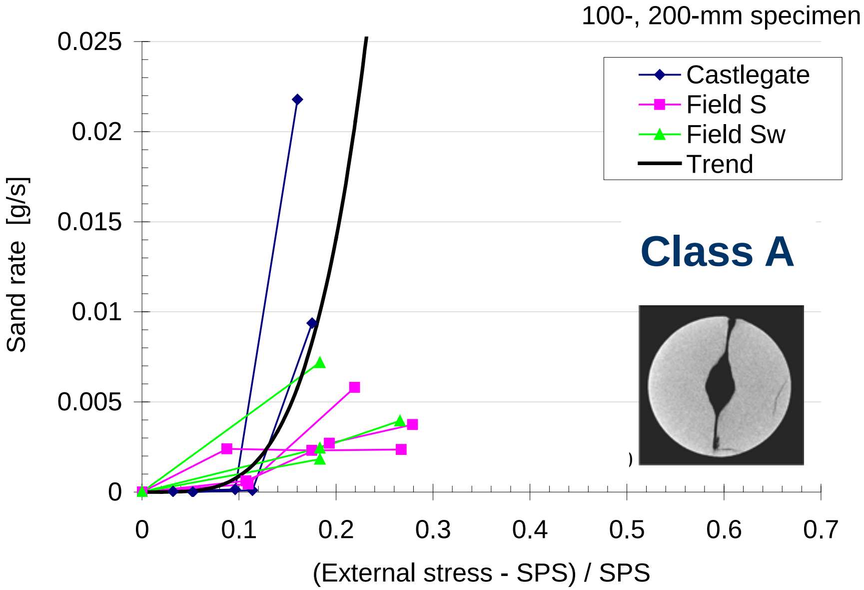

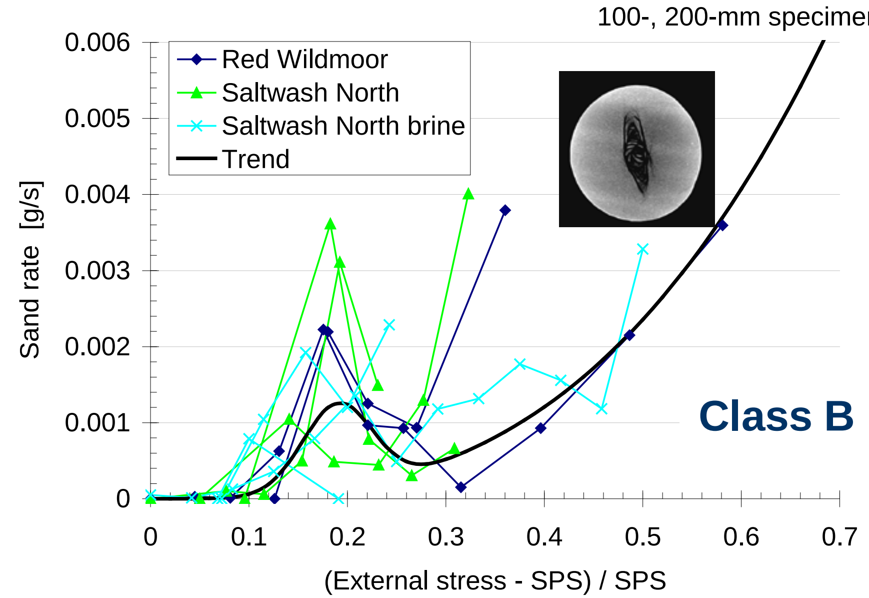

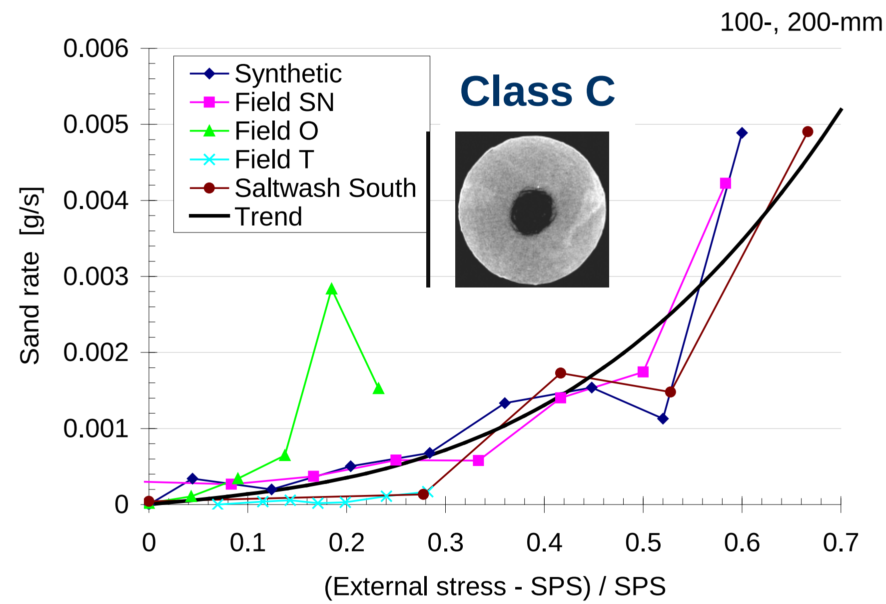

Hydro-mechanical erosion model for rocks

(*Vardoulakis et al. 1996, Papamichos and Stavropoulou 1998, Stavropoulou et al. 1998, Papamichos et al. 2000, Vardoulakis et al. 2001, Papamichos and Malmanger 2001, Vardoulakis and Papamichos 2003, Papamichos and Vardoulakis 2004*)

1. Porous rock as a three-phase medium
2. Mass balance
3. Erosion constitutive law
4. Coupled hydro-mechanical erosion model
5. Finite element implementation

1 Porous rock as a three-phase medium

- Representative Volume Element V:
  - V_s Solid grains s volume
  - V_f Fluid f volume
  - V_{fs} Fluidized grains fs volume
- ϕ Porosity
- c Concentration of fluidized solids in the fluid

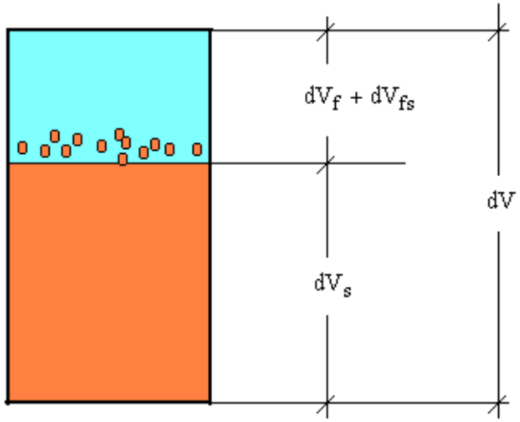

$$\phi = \frac{V_v}{V} = \frac{V_f + V_{fs}}{V} \qquad c = \frac{V_{fs}}{V_v} = \frac{V_{fs}}{V_f + V_{fs}}$$

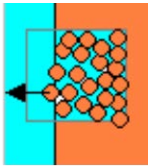

Densities

- Partial densities for the 3 phases (1), (2) and (3)

$$\rho^{(1)} = \frac{m_s}{V} = \rho_s \frac{V_s}{V} = \rho_s \frac{V - V_v}{V} = (1-\phi)\rho_s$$

$$\rho^{(2)} = \frac{m_f}{V} = \rho_f \frac{V_f}{V} = \rho_f \frac{\phi V - V_{fs}}{V} = (1-c)\phi\rho_f$$

$$\rho^{(3)} = \frac{m_{fs}}{V} = \rho_s \frac{V_{fs}}{V} = \rho_s \frac{c\phi V}{V} = c\phi\rho_s$$

- ρ Total density of the mixture

$$\rho = \frac{m}{V} = \frac{m_s + m_f + m_{fs}}{V} = \rho^{(1)} + \rho^{(2)} + \rho^{(3)} = (1-\phi)\rho_s + \phi\rho_f + c\phi\rho_s$$

Fluxes

- Flow rate volumes per unit surface

$$q_i^{(1)} = \frac{dV_s}{dS_i dt},\ v_i^{(1)} = \frac{dV_s}{(1-\phi) dS_i dt} \quad \Rightarrow \quad q_i^{(1)} = (1-\phi) v_i^{(1)} = 0$$

$$q_i^{(2)} = \frac{dV_f}{dS_i dt},\ v_i^{(2)} = \frac{dV_f}{(1-c)\phi dS_i dt} \quad \Rightarrow \quad q_i^{(2)} = (1-c)\phi v_i^{(2)}$$

$$q_i^{(3)} = \frac{dV_{fs}}{dS_i dt},\ v_i^{(3)} = \frac{dV_{fs}}{c\phi dS_i dt} \quad \Rightarrow \quad q_i^{(3)} = c\phi v_i^{(3)} = c\phi v_i^{(2)} = c q_i^{(2)} \big/ (1-c)$$

- Relative (to the solid) specific flux q_i of the fluid-particle mixture

$$q_i = \phi\left(v_i^{(2)} - v_i^{(1)}\right) = \phi v_i^{(2)} = q_i^{(2)} \big/ (1-c)$$

- Summary of 3 mass balance equations for 3-phase medium

$$\frac{\partial \phi}{\partial t} = -\frac{j^{(1)}}{\rho_s}$$

1st mass balance eqn.

$$\frac{\partial (1-c)\phi}{\partial t} = div(c q_i)$$

2nd mass balance eqn.

$$div q_i = 0$$

3rd mass balance eqn.

- 6 unknowns
  - porosity ϕ
  - concentration c
  - rate of produced mass per unit volume $j^{(1)}$
  - 3 fluid fluxes q_i

3 Constitutive laws

- Darcy's law for fluid-particle flow

$$q_i = -\frac{k}{\eta} p_{,i}$$

Physical rock permeability

Pore pressure gradient

Fluid viscosity

Unknowns reduce to 4

- k, η not constant
  - $k = k(\phi)$ e.g. Carman-Kozeny $k = k_c \frac{\phi^3}{(1-\phi)^2}$
  - $\eta = \underline{\rho}(c)\eta_k$ $\underline{\rho} = \rho_f + c\left(\rho_s - \rho_f\right)$

For erosion in rocks c<<1 $\Rightarrow$ $\eta \approx$ constant

Erosion constitutive law

- Laws inspired by theories of filtration of fines through a coarse solid matrix
  (Einstein 1937, Sakthivadivel and Irmay 1966, Iwasaki 1937)

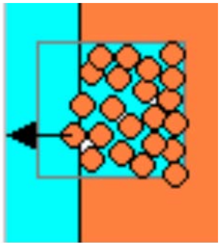

$$\frac{\dot{j}^{(3)}}{\rho_s} = \lambda (1-\phi) c \|q_i\|$$

$$\frac{\dot{j}^{(3)}}{\rho_s} = \lambda (1-\phi) c \left(1 - \frac{c}{c_{cr}}\right) \|q_i\|$$

(Vardoulakis et al. 1996, Papamichos and Stavropoulou 1998, Stavropoulou et al. 1998, Vardoulakis et al. 2001, Wan et al. 2002, Wang et al. 2004)

$$\frac{\dot{j}^{(3)}}{\rho_s} = \lambda \phi c^n \|q_i\|$$

(Vardoulakis and Papamichos 2003)

$$\frac{\dot{j}^{(3)}}{\rho_s} = \lambda (1-\phi) \|q_i\|$$

(Papamichos et al. 2001)

$$\frac{\dot{j}^{(3)}}{\rho_s} = \lambda \frac{\partial^2 \phi}{\partial x_i^2}$$

(Vardoulakis and Papamichos 2003)

- Law with erosion driven by the pore pressure gradient (*Papamichos 2004)*

$$\frac{j^{(3)}}{\rho_s} = \lambda \left\langle \left\| p_{,i} \right\| - p_{gcr} \right\rangle$$

$$\left\langle \left\| p_{,i} \right\| - p_{gcr} \right\rangle = \begin{cases} \left\| p_{,i} \right\| - p_{gcr} & if \quad \left\| p_{,i} \right\| - p_{gcr} > 0 \\ 0 & if \quad \left\| p_{,i} \right\| - p_{gcr} \leq 0 \end{cases}$$

or w/ 1st mass balance eqn.

$$\frac{\partial \phi}{\partial t} = \lambda \left\langle \left\| p_{,i} \right\| - p_{gcr} \right\rangle$$

- Law based on the physics of sand erosion in rocks

Forces on a grain driving erosion

- F_p pressure component $\sim \Delta p$
- F_s shear (drag) component $\sim \eta q$

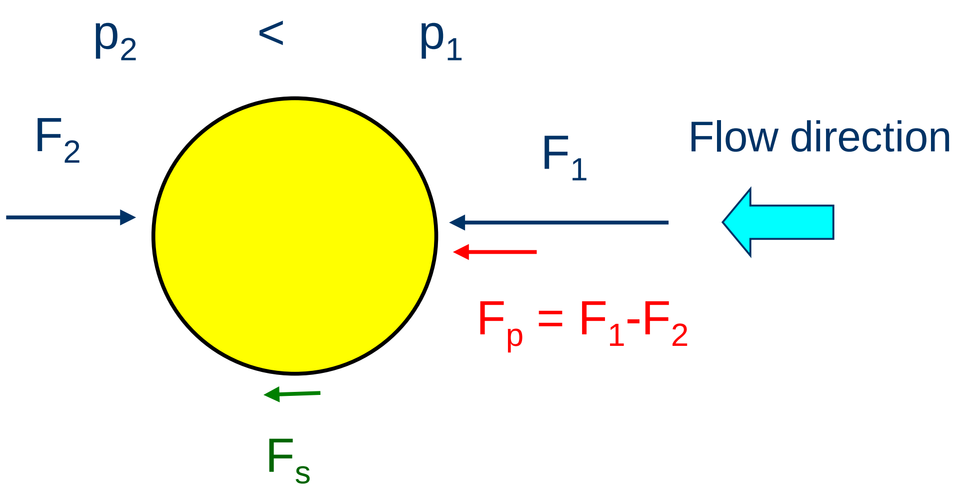

$$F_p = -4\pi r_g^3 p_{,x} / 3$$

$$F_s = C_D A \rho_f v_f^2 / 2$$

In continuum sense the force per unit volume

$$\frac{F_h}{V} = \frac{dp_f}{dr}$$ (Bear 1972)

- Summary of equations for 3-phase medium

$$div q_i = 0$$

3rd mass balance eqn.

$$q_i = -\frac{k}{\eta} p_{,i}$$

Darcy's law

$$\frac{\partial \phi}{\partial t} = \lambda \left\langle \left\| p_{,i} \right\| - p_{gcr} \right\rangle$$

Erosion law + 1st mass balance eqn.

$$\frac{\partial (1-c)\phi}{\partial t} = div\left(c q_i\right)$$

(2nd mass balance eqn.)

- 3 (or 2) independent unknowns
  - porosity ϕ
  - pore pressure p
  - (concentration c)

Summary of equations for 3-phase medium

$$div q_i = 0$$

3rd mass balance eqn.

$$q_i = -\frac{k}{\eta} p_{,i}$$

Darcy's law

$$\frac{\partial \phi}{\partial t} = \lambda \left\langle \left\| p_{,i} \right\| - p_{gcr} \right\rangle$$

Erosion law + 1st mass balance eqn.

$$\frac{\partial (1-c)\phi}{\partial t} = div\left(c q_i\right)$$

(2nd mass balance eqn.)

3 (or 2) independent unknowns

- porosity ϕ
- pore pressure p
- (concentration c)

4 Coupled hydro-mechanical erosion model

- Poro-mechanical behavior of the solid-fluid system
  - Steady-state poro-elastoplasticity
- Erosion of solid matrix
  - Theory of erodable rocks

- 2 additional material parameter
  - Sand coefficient λ [$m^2 s/kg$]
  - Critical pressure gradient p_{gcr} [MPa/m]

$$\sigma_{ij,j} = 0 \qquad T_c = T_c(\phi)$$

Equilibrium eqns.

$$d\sigma_{ij} = C^{ep}_{ijkl} d\varepsilon_{kl} + \alpha dp \delta_{ij} - C^{poro}_{ij} d\phi$$

Constitutive eqns. of elastoplasticity

$$div q_i = 0$$

Continuity eqn. for fluid-particle mixture

$$q_i = -\frac{k}{\eta} p_{,i}$$

Darcy's law

$$\frac{\partial \phi}{\partial t} = \lambda \left\langle \left\| p_{,i} \right\| - p_{gcr} \right\rangle \qquad \lambda = \lambda\left(\gamma^p\right)$$

Erosion law + 1st mass balance eqn.

$$k = k_c \frac{\phi^3}{(1-\phi)^2}$$

Permeability law

- Rock has to fail or weaken before it can be eroded i.e. mechanical behavior influences erosion

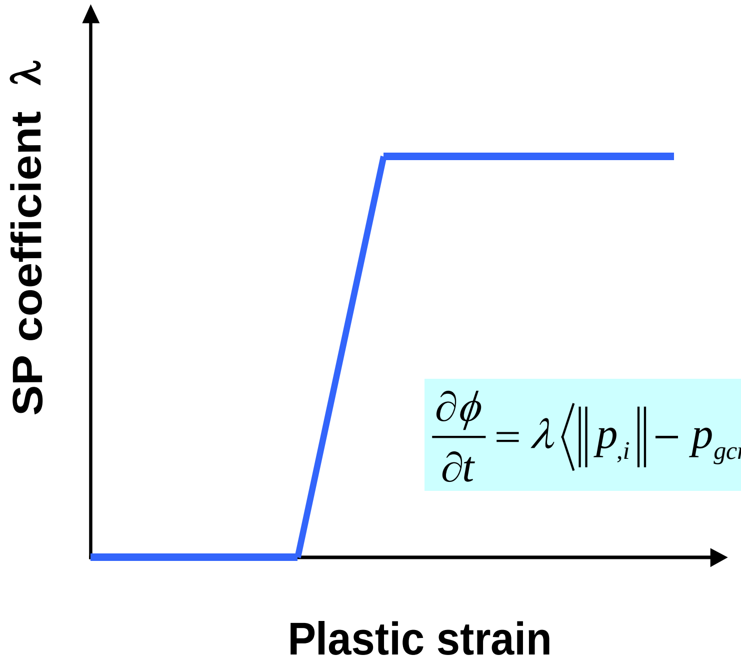

$$\frac{\partial \phi}{\partial t} = \lambda \left\langle \left\| p_{,i} \right\| - p_{gcr} \right\rangle$$

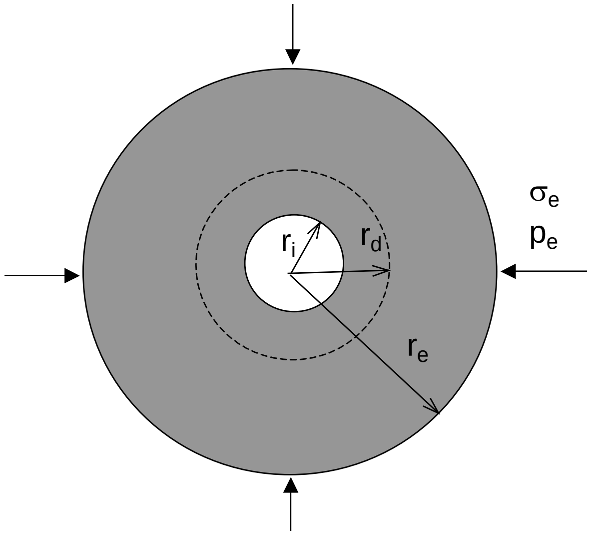

$$\lambda\left(\gamma^p\right) = \begin{cases} 0 & \text{if } \gamma^p \le \gamma^p_{peak} \\ \lambda_1\left(\gamma^p - \gamma^p_{peak}\right) & \text{if } \gamma^p_{peak} \le \gamma^p \le \gamma^p_{peak} + \lambda_2/\lambda_1 \\ \lambda_2 & \text{if } \gamma^p_{peak} + \lambda_2/\lambda_1 \le \gamma^p \end{cases}$$

- Rock weakens when eroded
  i.e. erosion influences mechanical behavior

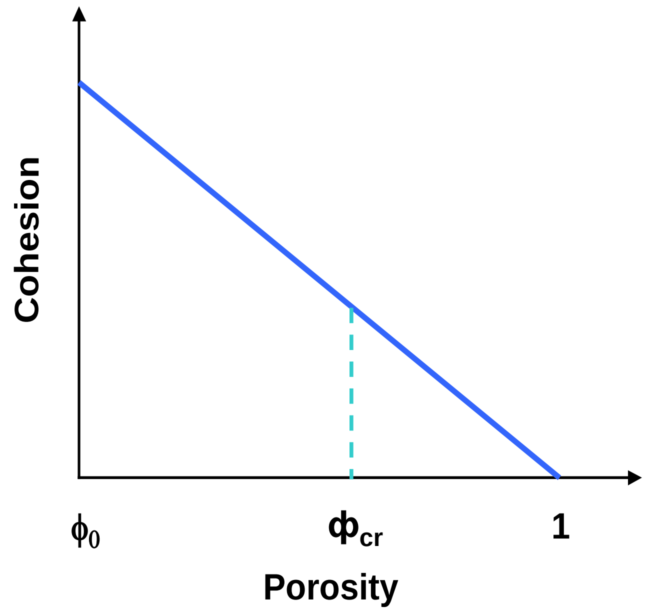

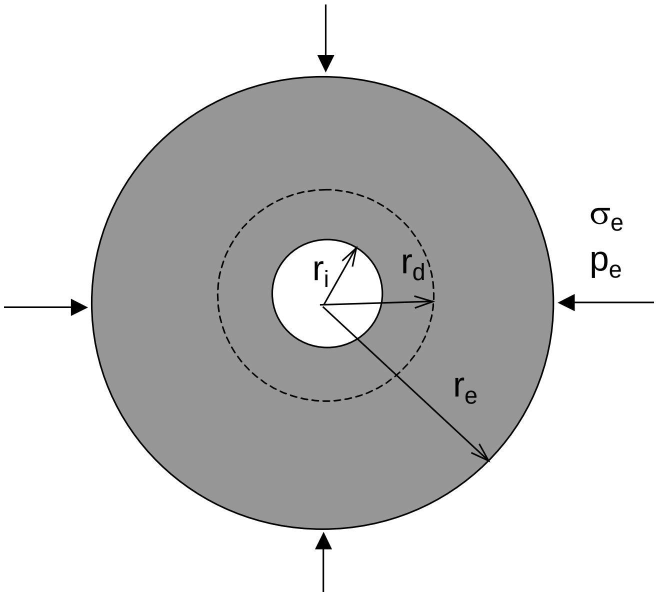

$$T_c\left(\gamma^p,\phi\right)=T_{c\gamma}\left(\gamma^p\right)\frac{1-\phi}{1-\phi_0}$$

Analysis of sand erosion in the hollow cylinder test

Boundary conditions

$$\sigma_r\left(r=r_e\right)=\sigma_{re}=\sigma_e \qquad \sigma_r\left(r=r_i\right)=\sigma_{ri}=\sigma_i=0$$

$$p\left(r=r_e\right)=p_e \qquad p\left(r=r_i\right)=p_i=0$$

$$\phi\left(r=r_e\right)=\phi_o$$

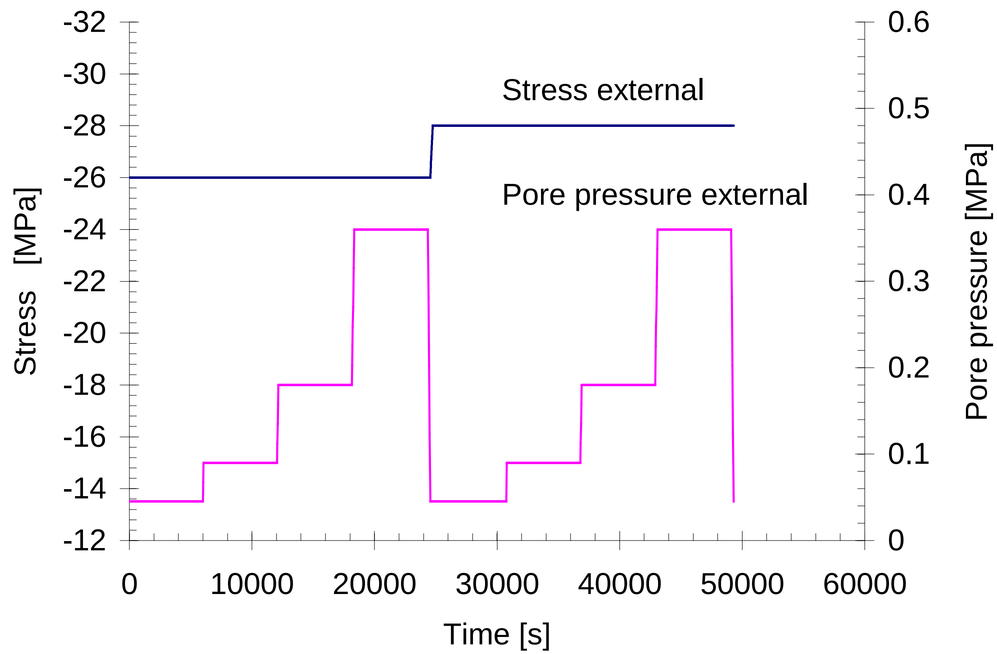

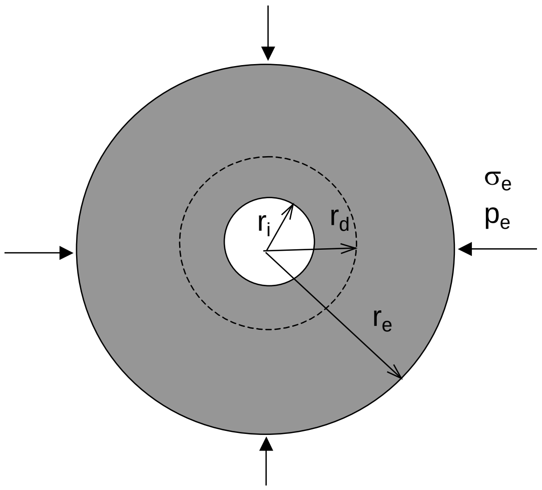

- **Non linear, transient problem**
- **Finite element solution**

$$\int_V \sigma_{ij}\delta\varepsilon_{ij}dV = \int_{\partial V_\sigma} t_i \delta u_i dS$$

$$q_{i,i} = 0$$

$$\frac{\partial \phi}{\partial t} - \lambda \left\langle \left\| \{p_{,i}\} \right\| - p_{gcr} \right\rangle = 0$$

Galerkin space discretization

$$\int_V [B]^T \{\sigma\} dV - \int_{\partial V_\sigma} \{N\}\{t\} dS = 0$$

$$-\int_V [\nabla N]\{q\} dV + \int_{\partial V_q} \{N\} q^b dS = 0$$

$$\int_V \{N\} \left(\frac{\partial \phi}{\partial t} - \lambda \left\langle \left\| \{p_{,i}\} \right\| - p_{gcr} \right\rangle \right) dV = 0$$

$$\Omega = \theta\Omega_{n+1} + (1-\theta)\Omega_n, \qquad \frac{\partial\Omega}{\partial t} = \frac{\Omega_{n+1} - \Omega_n}{\Delta t}$$

Time discretization

$$\Psi^U = \int_V [B]^T \left(\{\sigma\}_{n+1} + \frac{1-\theta}{\theta}\{\sigma\}_n \right) dV - \int_{\partial V_\sigma} \{N\} \left(\{t\}_{n+1} + \frac{1-\theta}{\theta}\{t\}_n \right) dS = 0$$

$$\Psi^P = -\int_V [\nabla N] \left(\{q\}_{n+1} + \frac{1-\theta}{\theta}\{q\}_n \right) dV + \int_{\partial V_q} \{N\} \left(q^b_{n+1} + \frac{1-\theta}{\theta} q^b_n \right) dS = 0$$

$$\Psi^\Phi = \int_V \{N\} \left[\frac{\phi_{n+1} - \phi_n}{\theta\Delta t} - \lambda_{n+1} \left\langle \left\| \{p_{,i}\}_{n+1} \right\| - p_{gcr} \right\rangle - \frac{1-\theta}{\theta} \lambda_n \left\langle \left\| \{p_{,i}\}_n \right\| - p_{gcr} \right\rangle \right] dV = 0$$

Sand mass and rate vs. time

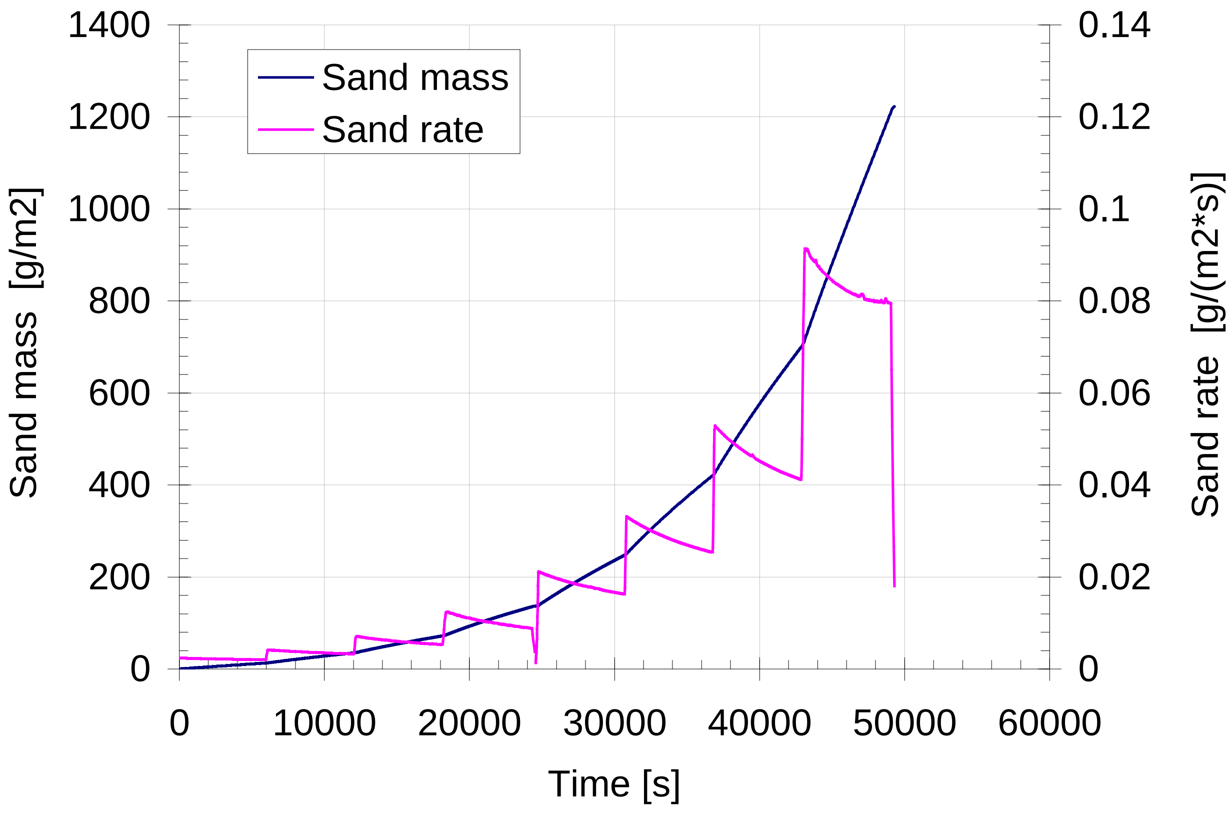

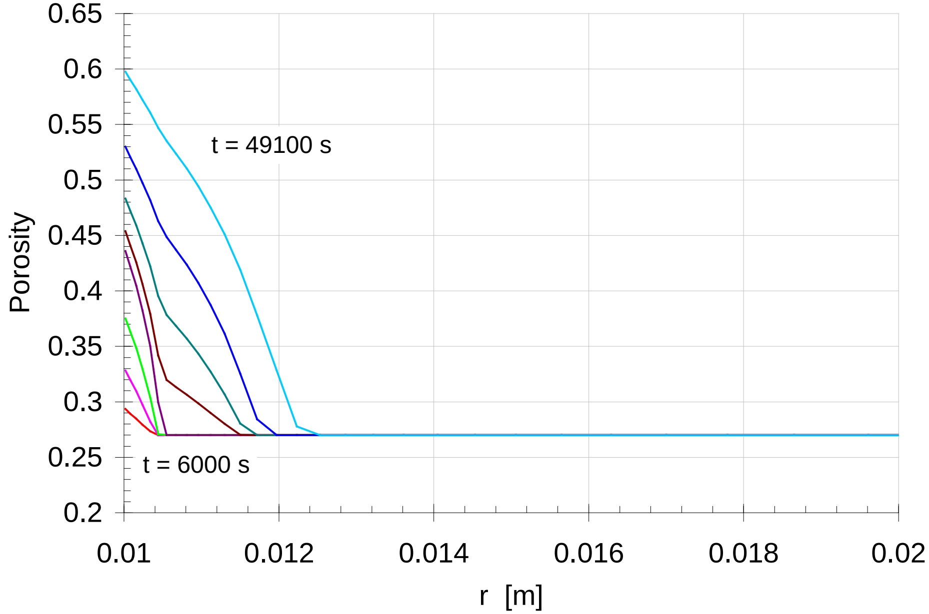

Porosity

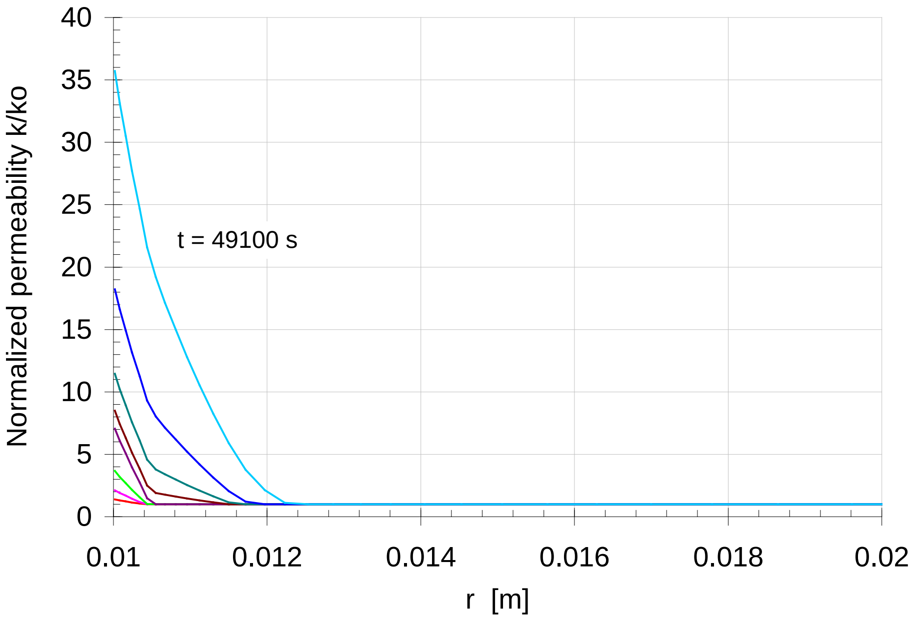

Normalized permeability

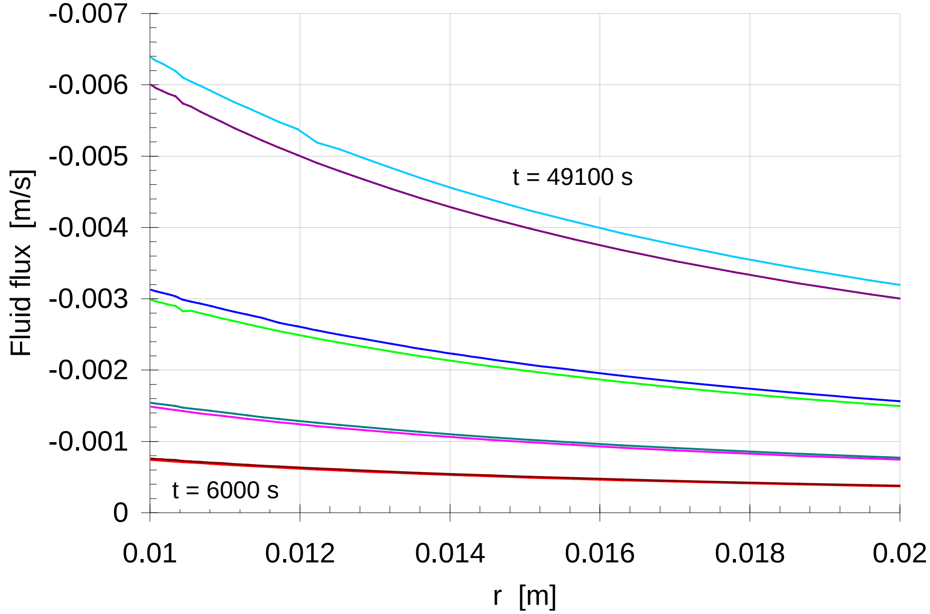

Fluid flux

Pore pressure gradient

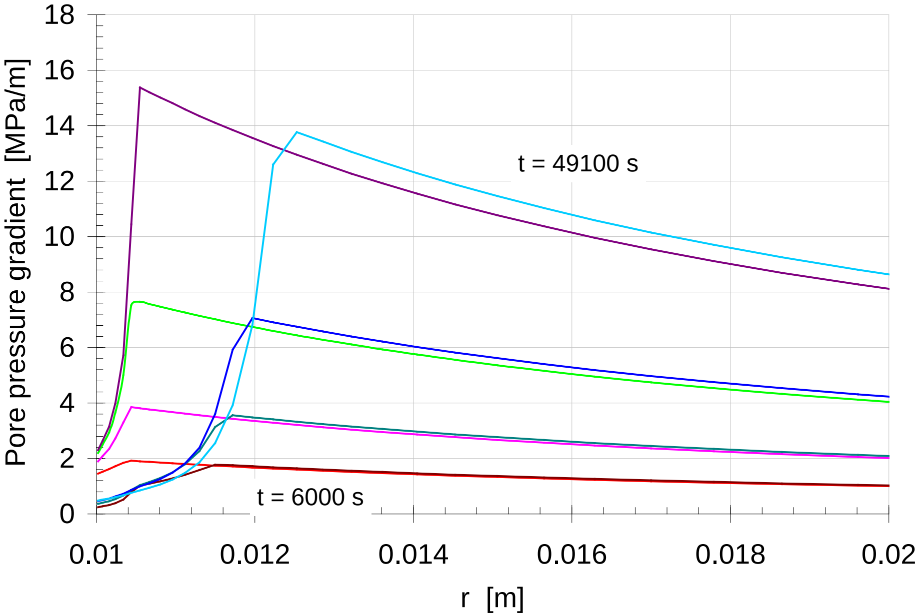

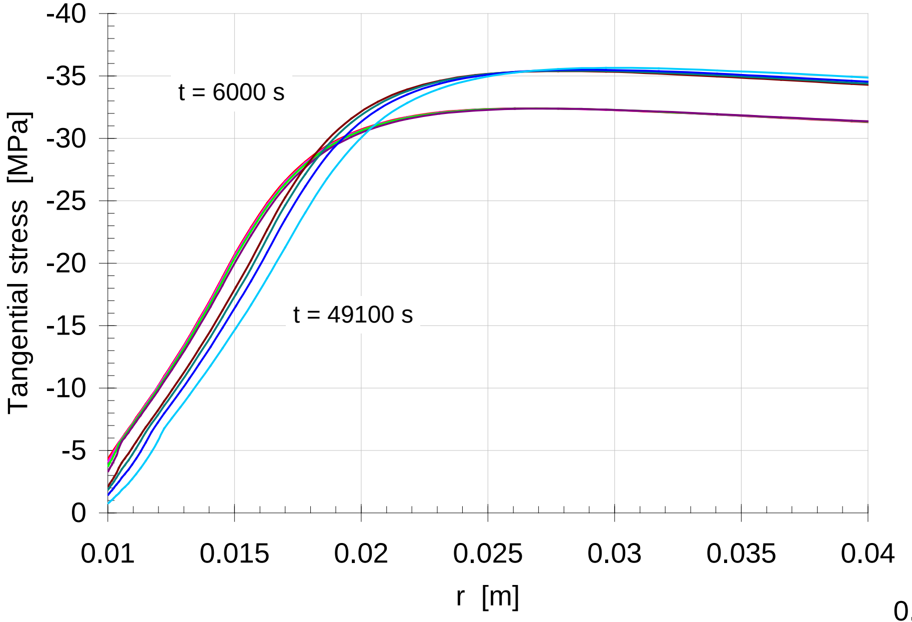

Tangential stress

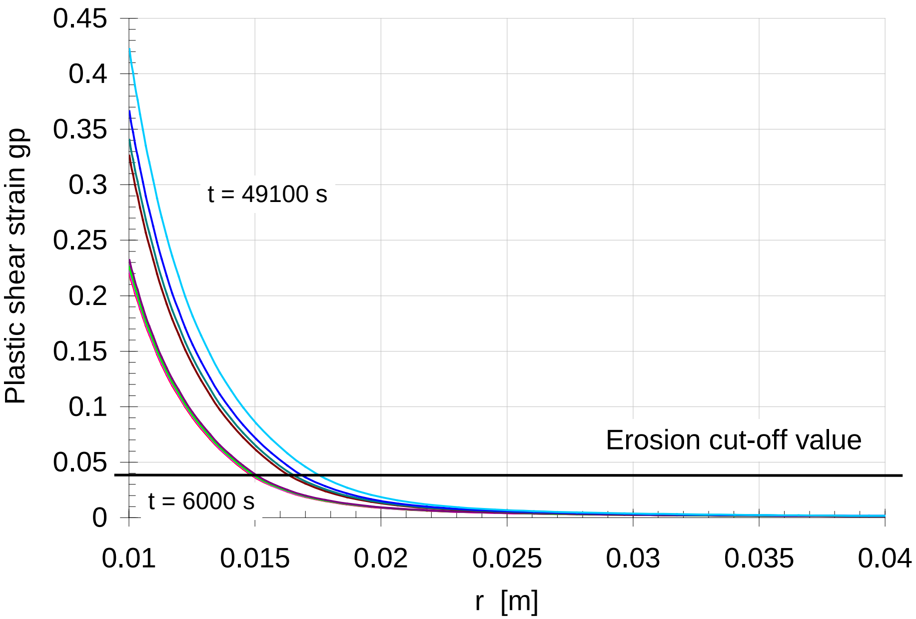

Plastic strain

Sand production in a perforated well

(Wang et al. 2004)

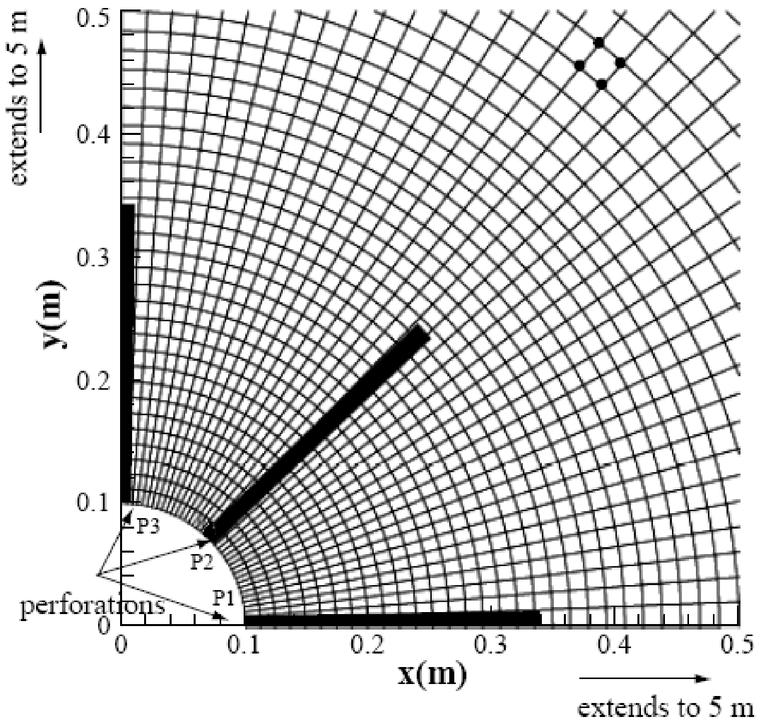

Fig. 3. Mesh layout near wellbore showing perforations.

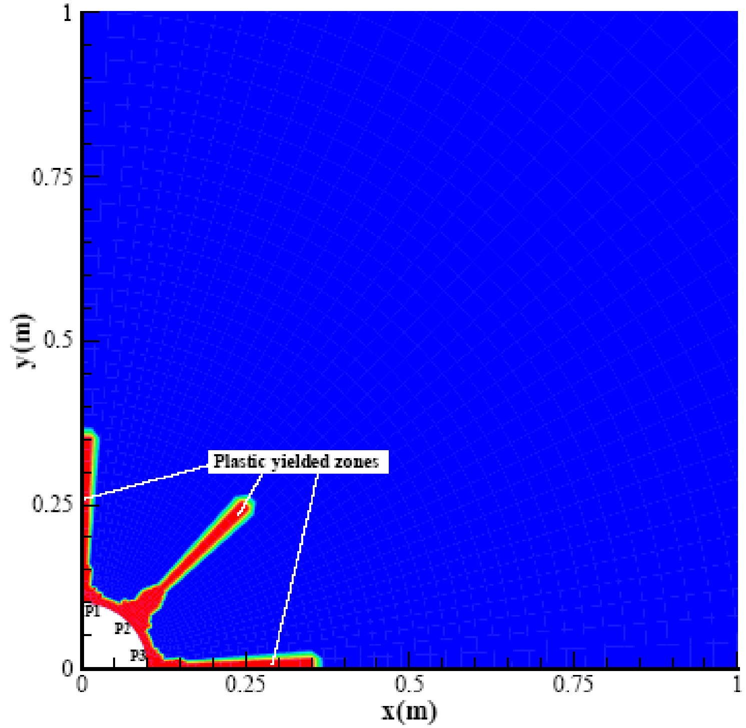

Fig. 4 Plastic yielded zones developed after open-hole completion and perforations (before drawdown).

Fluidized sand

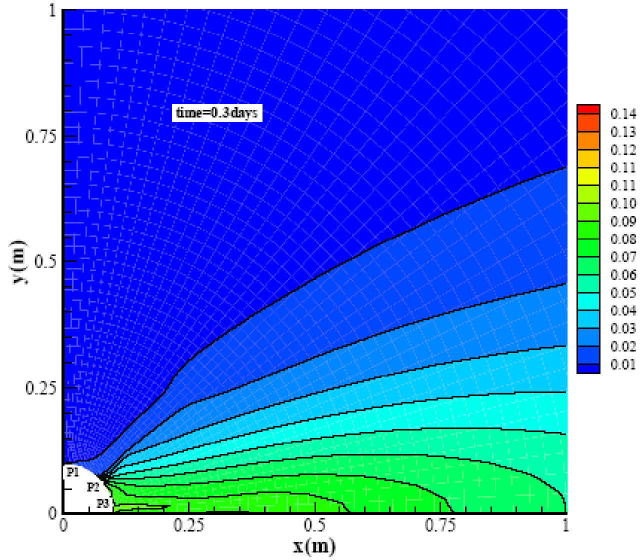

Fig. 5 Fluidized sand saturation profile at time t=0.3 day.

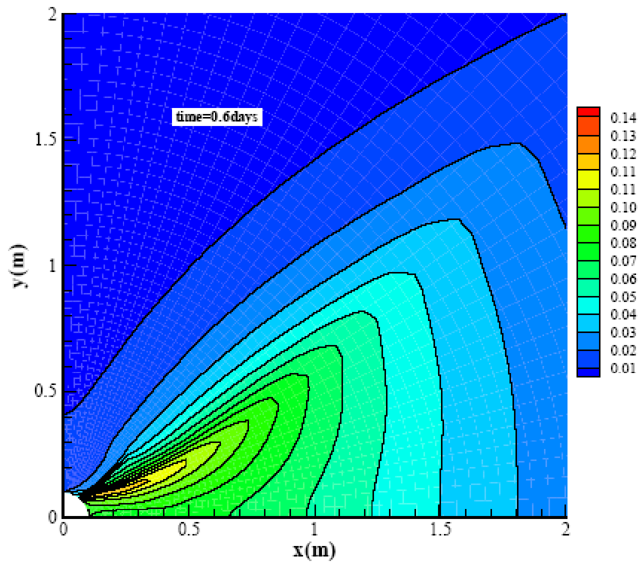

Fig. 6 Fluidized sand saturation profile at time t=0.6 day.

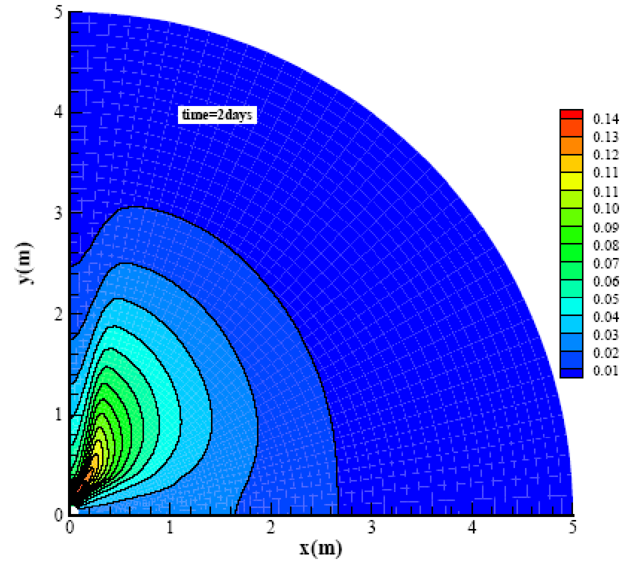

Fig. 7 Fluidized sand saturation profile at time t=2 days.

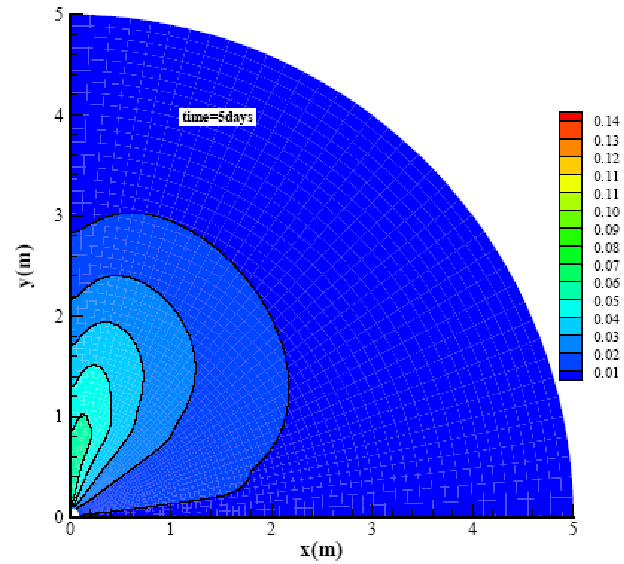

Fig. 8 Fluidized sand saturation profile at time t= 5 days.

Discrete element modeling of sand erosion in the sand production test

- Investigate how **material properties** affect HC failure pattern
- Discrete element simulations with **bonded** particles (*PFC2D*, Itasca)
  - Smaller particles near the hole
  - Different stresses can be applied in the two directions, here $\sigma_v/\sigma_h = 1$
  - Increase stresses and flow rate/pore pressure step-wise
  - Measure produced sand

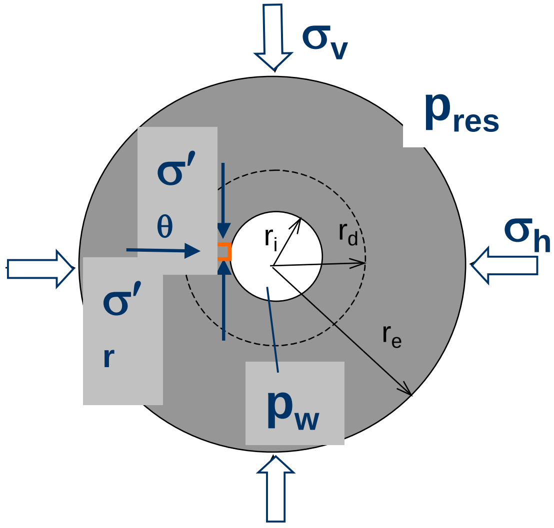

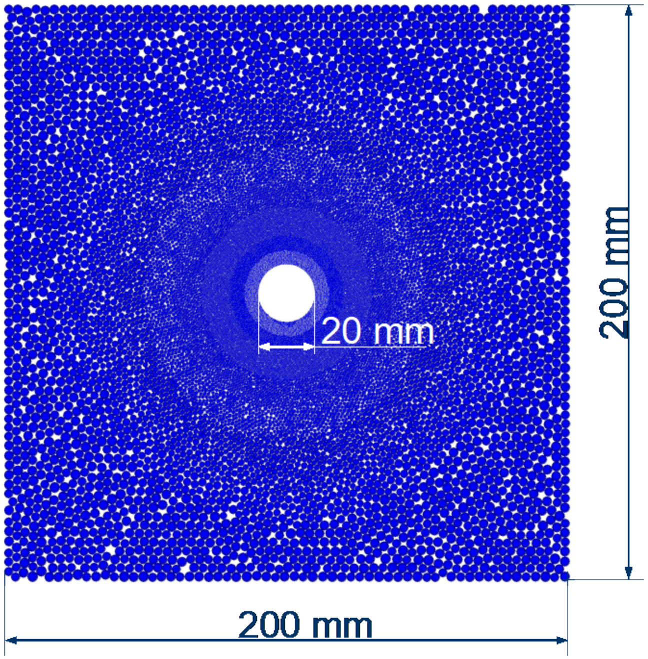

(Li and Papamichos 2006)

Discrete element modeling of sand erosion in the sand production test

- Investigate how **material properties** affect HC failure pattern
- Discrete element simulations with **bonded** particles (*PFC2D*, Itasca)

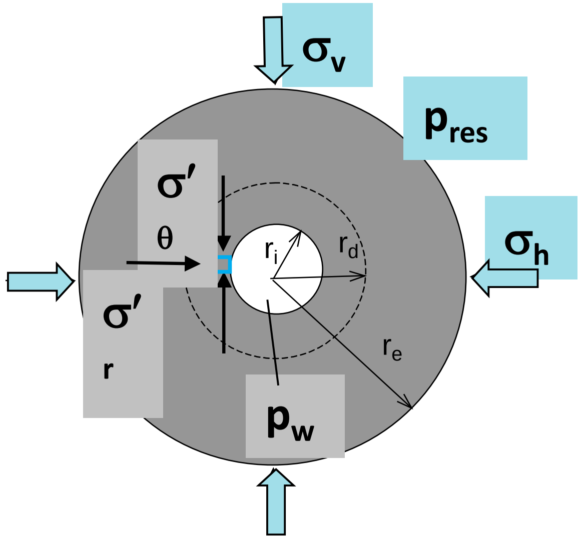

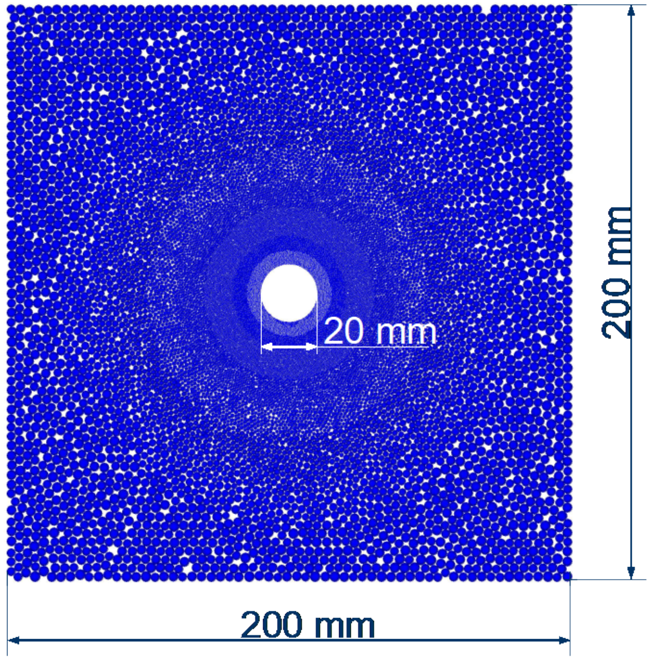

(Li and Papamichos 2006)

Mesh for flow calculation

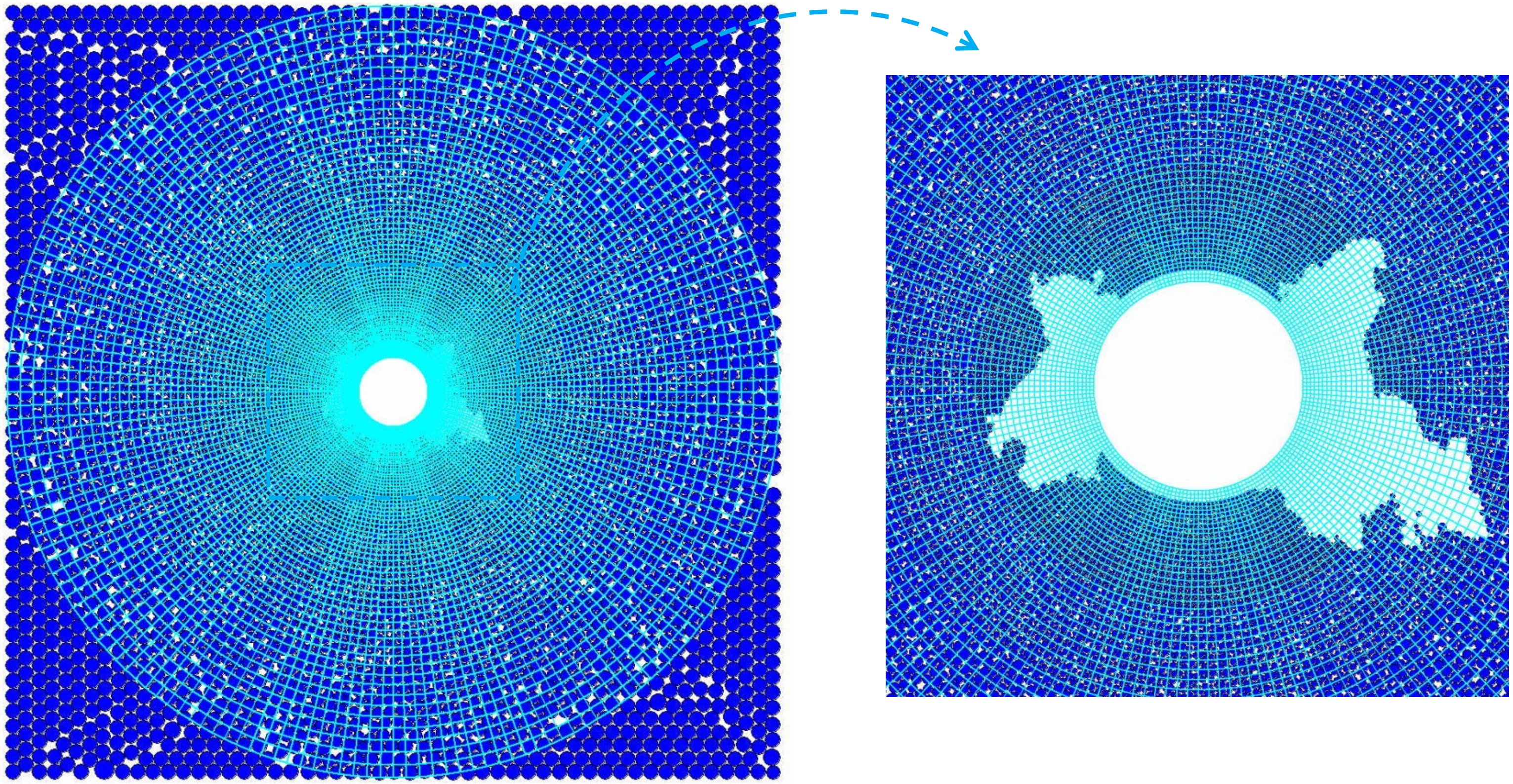

Flow-induced forces to particles

Force on a particle due to fluid pressure and shear drag

$$F_i = \frac{\pi d_g^2 \mu q_i}{6k\left(1-\phi\right)}$$

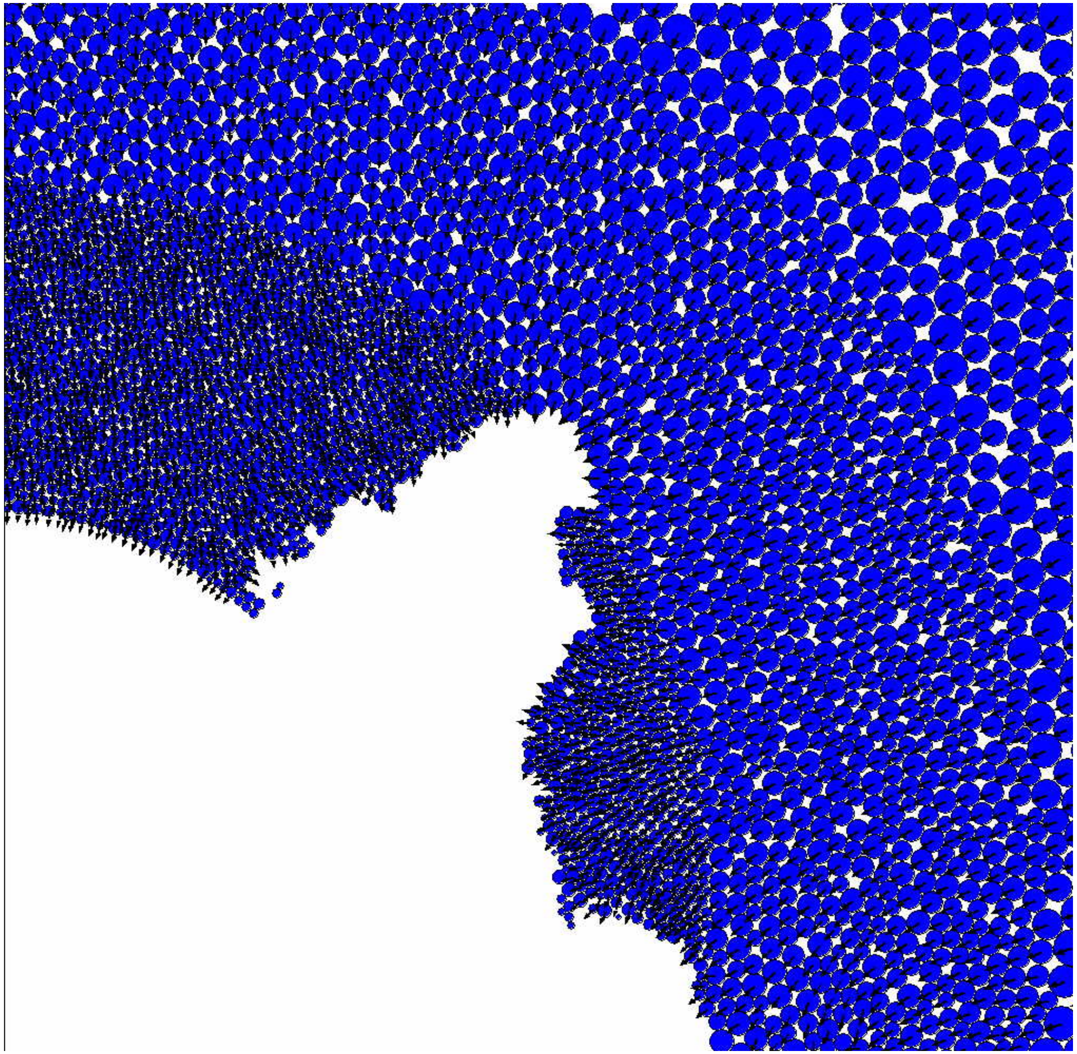

Particle failure criterion

- Particle, depending by the stress in it, fails in
  - Tension
  - Shear
  - Shear-enhanced compaction
  - Compaction (independent of shear stresses; only if normal stress exceeds certain limit)
- Post-failure behavior
  - All particle bonds removed
  - Size of particle is reduced if it simulates rock which is liable to compaction and subject to compaction failure

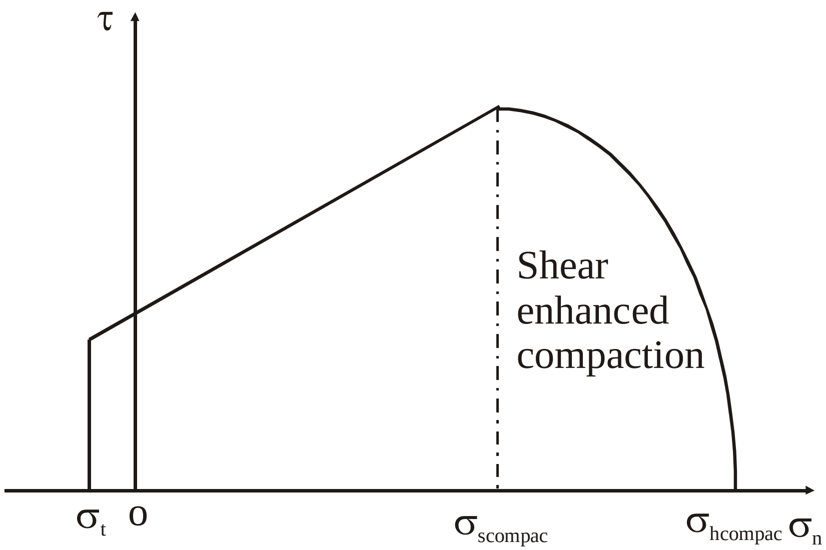

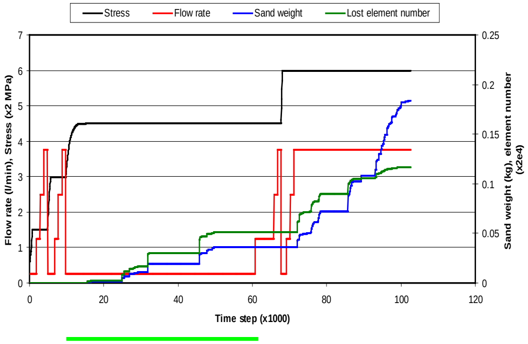

Tensile failure
Movie Sand_I1

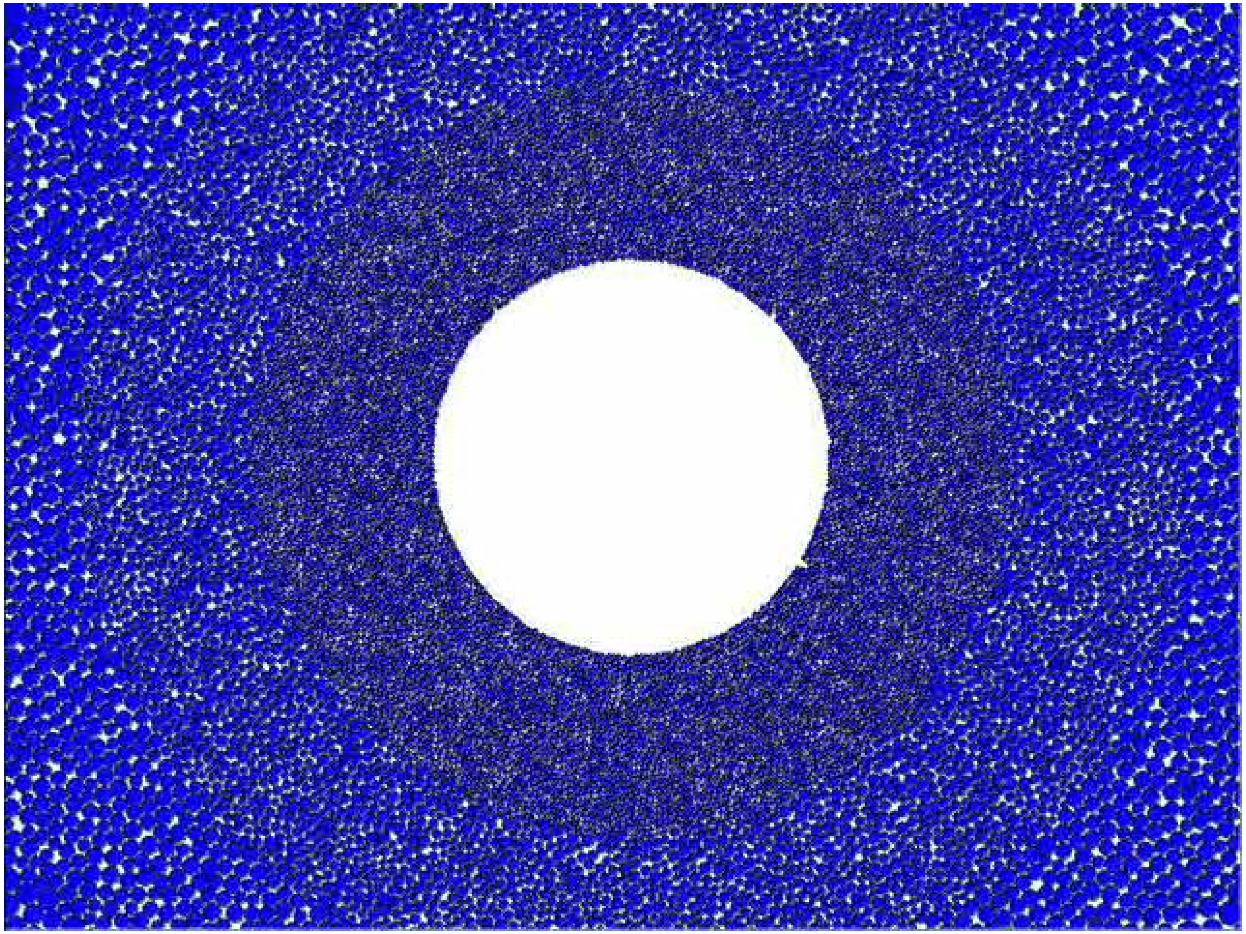

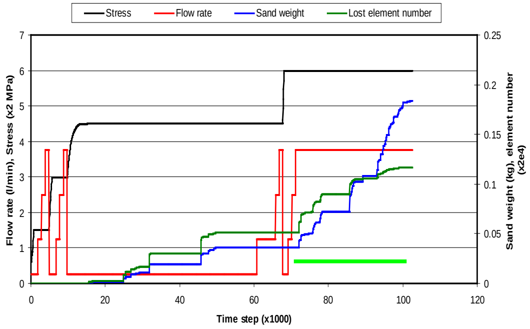

Movie Sand_I2